

Università degli Studi di Milano Bicocca

Dipartimento di Fisica Giuseppe Occhialini

Ph.D. program in Physics and Astronomy, XXXV cycle

Curriculum in Theoretical Physics



Infrared Linear Renormalons in Collider Processes

Giovanni Limatola

Matricola: 854453

Tutor: Prof. Carlo Oleari

Supervisor: Prof. Paolo Nason

Coordinator: Prof. Stefano Ragazzi

Academic year: 2021/2022

Declaration

This thesis is exclusively based on my Ph.D. research projects:

1. *Infrared Renormalons in Kinematic Distributions for Hadron Collider Processes*, S. Ferrario Ravasio, G. Limatola, P. Nason [JHEP 06 \(2021\) 018](#) ([2011.14114 \[hep-ph\]](#))
2. *On linear power corrections in certain collider observables*, F. Caola, S. Ferrario Ravasio, G. Limatola, K. Melnikov, P. Nason [JHEP 01 \(2022\) 093](#) ([2108.08897 \[hep-ph\]](#))
3. *Linear power corrections to e^+e^- shape variables in the three-jet region*, F. Caola, S. Ferrario Ravasio, G. Limatola, K. Melnikov, P. Nason, M. A. Ozcelik ([2204.02247 \[hep-ph\]](#))

I hereby declare that the work reported in this thesis has not been submitted, either in part or full, for the award of any other degree or diploma in this or any other institute or university.

Date: 27th October 2022

Giovanni Limatola

Abstract

Understanding leading non-perturbative corrections, showing up as linear power corrections, is crucial to properly describe observables both at lepton and hadron colliders. Using an abelian model, we examine these effects for the transverse momentum distribution of a Z boson produced in association with a jet in hadronic collisions, that is one of the cleanest LHC observables, where the presence of leading non-perturbative corrections would spoil the chance to reach the current experimental accuracy, even considering higher orders in the perturbative expansion. As we did not find any such corrections exploiting semi-numerical techniques, we looked for a rigorous field-theoretical derivation of them, and explain under which circumstances linear power corrections can arise. We apply our theoretical understanding to the study of event-shape observables in e^+e^- annihilation, focusing in particular on C -parameter and thrust, and obtaining for them an estimate of non-perturbative corrections in the three-jet region for the first time. We also derived a factorisation formula for non-perturbative corrections, with a term describing the change of the shape variable when a soft parton is emitted, and a constant universal factor, proportional to the so-called Milan factor. These observables are routinely used to extract the strong coupling constant α_s and they constitute an environment to test perturbative QCD. It is then extremely important to obtain reliable estimates of non-perturbative corrections in the whole kinematic region relevant for the α_s fits.

Contents

I Infrared Renormalons in the transverse momentum of a Z boson in hadronic collisions	7
1 Details of the computation	11
1.1 On the low transverse momentum of a vector boson	11
1.2 Our computation	12
1.3 The method	13
1.4 Implementation of the method	19
1.5 Computation of the real contribution	21
1.5.1 Region (1)	22
1.6 The $T(\lambda)$ function	22
2 Results	24
2.1 Transverse momentum distribution of the Z boson	24
3 Conclusions	27
II Linear Power Corrections in Shape Variables in the three-jet region	29
4 Generalities on the method	33
4.1 Linear power corrections from real emission	33
4.1.1 Final-final dipole	33
4.1.2 Initial-final dipole	38
4.2 Linear power corrections to shape variables	41
5 Power corrections to the C-parameter in the three-jet region	45
5.1 Direct integration with an explicit energy cut-off	46
5.2 Factorised form of linear power corrections affecting the C -parameter	50
5.3 The observable-independent function F	52
5.3.1 An alternative way to compute F	54
5.4 The observable dependent factor: a general approach	56
5.5 The case of the C -parameter	58
5.6 Connection with the Milan Factor approach	59

6	Applications of the factorised approach	62
6.1	Linear power corrections to thrust in the three-jet region	62
7	Phenomenological predictions in the three-jet region	67
7.1	A semi-analytic method for extracting leading power corrections	67
7.1.1	Comparison with the full large- n_f computation	72
7.2	Non-perturbative correction as a shift in the shape variable	73
7.3	Including radiation from the quark-gluon dipole	74
7.4	Results for the C -parameter and the thrust in the three-jet region and comparison with existing literature	77
8	Conclusions	80
A	Renormalons structure	85
B	Soft integrals	87
C	Full calculation of the shape variables in the large-n_f limit	89
D	On the two-jet limit of C	91
E	The G_i functions	94

Introduction

Despite the great success of the Large Hadron Collider (LHC) since its start up, culminated with the discovery of the Higgs boson in 2012, no clear hint of physics beyond the Standard Model (SM) has been yet detected. As an alternative strategy to investigate new physics signals, one can then increase the accuracy of the measurements and of the theoretical computations, in order to look for modest deviations of the production and decay properties of the SM particles, that can signal the presence of new physics, either as the exchange of virtual particles, or as signals of compositeness. Currently several processes have been computed at the two-loops level in QCD [1–12], and very few at three loops [13–16].

When increasing the loop order one should start to worry about the growth of the size of the coefficients of the perturbative expansion, which will eventually grow factorially. In QCD this growth can manifest itself quite early in the perturbative expansion, due to the large size of the coupling constant α_s , so that the terms of the perturbative expansion will reach a minimum value, and then will start growing. The minimum value thus becomes an inherent limit to the precision of the calculation.

The work presented in this thesis has started with an investigation of the presence of power corrections that are only linearly suppressed in the scale of the process, associated with the factorial growth of the perturbative expansion, in the context of the transverse momentum distribution of the Z boson produced at hadron colliders. This work was based upon a semi-numerical investigation, that showed no evidence for linear power corrections in the Z transverse momentum distribution, with or without rapidity cuts. Subsequently, we looked and found an analytic proof of the absence of linear corrections for this distribution. This analytic proof could also be applied to the production of hadrons in e^+e^- annihilation, and we realized that it had profound implications for the computation of shape variables distributions in this framework. This is the reason why the present work is divided into two parts, one regarding the transverse momentum distribution of the Z boson, and the other regarding shape variables.

In the first part we only illustrate the general framework that we adopt for these kind of calculations, and illustrate our semi-numerical results.

In the second part we present the analytic argument for the computation of shape variables, but also illustrate how the same method can be used to demonstrate the absence of linear corrections in the case of the Z transverse momentum distribution.

Overview on Renormalons

We start by giving a brief introduction to the concept of infrared renormalons, with particular focus on their relation with asymptotic series.

Asymptotic Series

It is well known that, for a generic renormalizable Quantum Field theory, a given observable R can be expressed as a perturbative expansion in the renormalized coupling α

$$R = \sum_{n=0}^{\infty} c_n \alpha^{n+1}. \quad (1)$$

Unfortunately, this series is not convergent, and then, in order to assign a “sum” to it, this needs to be an *asymptotic series*, i.e. such that, for any order N we can find a number K_N in a region \mathcal{C} of the complex α -plane such that

$$\left| R - \sum_{n=0}^{N-1} c_n \alpha^{n+1} \right| < K_N \alpha^{N+1}. \quad (2)$$

In particular, for a factorial growth of the coefficients

$$c_n \simeq a^n \Gamma(1 + b + n), \quad (3)$$

with a and b real and integer numbers, we observe that the series decreases for lower orders, and then it starts to increase, after reaching a minimum value in correspondence of an order N^* such that

$$|c_{N^*-1} \alpha^{N^*}| \simeq |c_{N^*} \alpha^{N^*+1}|, \quad (4)$$

and the expression of N^* assumes the form

$$N^* = \frac{1}{|a|\alpha}. \quad (5)$$

Thus, in order to give a meaning to the sum of the series, we need to truncate it in correspondence of its minimum value, introducing in such a way a truncation error which exponentially decays

$$c_{N^*} \alpha^{N^*+1} \propto \exp\left(-\frac{1}{|a|\alpha}\right). \quad (6)$$

An alternative and very valuable method in order to sum an asymptotic expansion (as the one in eq. (1)) has been introduced by Borel, and consists in defining the Borel sum as [17]

$$B[R](t) = \sum_{n=0}^{\infty} c_n \frac{t^n}{n!}, \quad (7)$$

which can be easily obtained by dividing each coefficient of eq. (1) by $n!$. If $B[R](t)$ is regular for $t > 0$ and does not increase too rapidly for $t \rightarrow \infty$, then it is safe to define its associated *Borel Integral*:

$$R = \int_0^\infty dt e^{-t/\alpha} B[R](t). \quad (8)$$

The last equality stands in the sense that, as far as the integral on the right hand side of eq. (8) converges, it reproduces term by term the perturbative expansion of the observable R .

The Borel method for summing a series is quite valid for alternating sign series, as their associated Borel integral does not contain poles within the integration range.

For what concerns a fixed sign series, the method instead fails. Let us consider a factorially divergent series of the form

$$R = \sum_{n=0}^{\infty} a^n n! \alpha^{n+1}, \quad (9)$$

being $a > 0$; its Borel sum will assume the expression

$$B[R](t) = \sum_{n=0}^{\infty} a^n t^n = \frac{1}{1-at}, \quad (10)$$

such that the associated Borel integral will be

$$R = \int_0^\infty dt e^{-t/\alpha} \frac{1}{1-at}. \quad (11)$$

We can note immediately that, in this case, the Borel integral is not well defined, due to the presence of the pole $t = 1/a$ along the integration path. Nevertheless we can still evaluate the right hand side of eq. (11) by properly specifying a prescription to avoid the pole, on which the final result will depend. Fortunately the ambiguity introduced by this choice is exponentially suppressed. Indeed, by defining

$$R_{\pm} = \int_0^\infty dt e^{-t/\alpha} \frac{1}{1-at \pm i\eta}, \quad (12)$$

then the difference will be proportional to the residue evaluated at the pole $t = 1/a$

$$R_+ - R_- \propto e^{-1/(a\alpha)}. \quad (13)$$

Thus we observed that for a given observable, the factorial growth of the coefficients of its associated perturbative expansion in a generic QFT is related to poles in the Borel plane. This type of divergence for a perturbative series is called a “renormalon”, as it is strictly related to the renormalization group flow of the associated theory. In particular, there are three known sources of factorial growth affecting the perturbative series of a generic QFT: ultraviolet (UV) renormalons, infrared (IR) renormalons and instantons.

In the following we will only focus on IR renormalons in QCD, showing how, due to the asymptotic freedom of the theory, QCD renormalons arising from IR regions are strictly related to power corrections.

Asymptotic Series and QCD Renormalons

It is interesting to investigate the consequences of the argument exposed in the previous section in the QCD case. Let us then consider an $\mathcal{O}(\alpha_s)$ correction to a generic observable, assuming we have already subtracted the UV divergences thanks to the renormalization procedure. Denoting with k the momentum flowing into the gluon propagator, for small k the loop integral takes the form

$$\int^Q dk^p \alpha_s, \quad (14)$$

being Q the scale that characterizes the process and p an integer, process-dependent parameter. If we want to take into account all the perturbative orders, we need to replace

$$\alpha_s \rightarrow \alpha_s(k) = \frac{1}{b_0 \ln(k^2/\Lambda_{\text{QCD}}^2)} = \frac{\alpha_s(Q)}{1 - \alpha_s(Q)b_0 \ln(Q^2/k^2)} \quad (15)$$

where

$$b_0 = \frac{11C_A - 4T_R n_l}{12\pi} \quad (16)$$

is the first coefficient of the QCD β -function, with $T_R = 1/2$, $C_A = N$ for $SU(N)$ (3 for $SU(3)$) and n_l is the number of light flavors in the theory.

The last member of the chain of equalities in eq. (15) can be written as the sum of a geometric series

$$\frac{\alpha_s(Q)}{1 - \alpha_s(Q)b_0 \ln(Q^2/k^2)} = \sum_{n=0}^{\infty} b_0^n \ln^n\left(\frac{Q^2}{k^2}\right) \alpha_s^{n+1}(Q), \quad (17)$$

that can be replaced into eq. (14) to obtain

$$\begin{aligned} & \sum_{n=0}^{\infty} (2b_0)^n \alpha_s^{n+1}(Q) \int_0^Q dk k^{p-1} \ln^n\left(\frac{k}{Q}\right) \\ &= pQ^p \sum_{n=0}^{\infty} (2b_0)^n \alpha_s^{n+1}(Q) \int_0^1 dx x^{p-1} \ln^n x \\ &\propto \sum_{n=0}^{\infty} \left(\frac{2b_0}{p}\right)^n n! \alpha_s^{n+1}(Q), \end{aligned} \quad (18)$$

where, in the second member we implemented the change of variable $k/Q \rightarrow x$.

Thus, by considering higher orders contributions we have obtained a series that diverges factorially. We dubbed this divergence a Infrared (IR) ‘‘Renormalon’’, as it comes from the renormalization group equation for the strong coupling constant α_s , when integrating in the infrared region.

As shown in the previous section, in order to sum the series in eq. (18) we need to truncate it in correspondence of its minimum value $n_{\min} = p/(2b_0\alpha_s(Q))$, introducing in such a way a truncation error scaling as

$$e^{-p/(2b_0\alpha_s(Q))} = e^{\ln(\Lambda_{\text{QCD}}^2/Q^2)^{p b_0/2b_0}} = \left(\frac{\Lambda_{\text{QCD}}}{Q}\right)^p, \quad (19)$$

where p strictly depends upon the considered process.

Thus in QCD, due to asymptotic freedom property, the factorial growth of a perturbative expansion leads to power corrections scaling as $\left(\frac{\Lambda_{\text{QCD}}}{Q}\right)^p$, and we talk about Infrared linear renormalons for $p = 1$.

As we said some lines before, the factorial growth of a perturbative expansion can also lead to UV renormalons, with the same form for n_{min} and p assuming negative integer values starting with -2. In this case we can still use formula eq. (19), replacing p with $|p|$, and the minimal term is, at worse, of order of Λ^2/μ^2 . Furthermore, the perturbative expansion is alternating in sign and then can be easily resummed exploiting the Borel techniques. For what concerns the instantons, they lead to a much stronger power suppression, and then can be safely neglected here.¹

It is clear that IR linear renormalon can easily affect the theoretical expectations at the percent level for hardness scales $Q \sim 100$ GeV and then it becomes crucial to estimate them in a proper and reliable way.

The Large- n_f method

The full renormalon tower in QCD is not known, and there is not yet a solid theoretical framework to estimate NP corrections for any process. In particular, general field theoretical arguments demonstrate the absence of IR linear renormalons for specific quantities.

Indeed, for observables which do not admit an Operator Product Expansion (OPE), a very valuable method to investigate the presence of IR QCD renormalons is the *Large- n_f* limit (see [24]), i.e. one takes the abelian limit of QCD, containing a large and negative number of light flavors n_f , keeping $\alpha_s n_f$ constant. With this approximation, the theory stays asymptotic free, with the gluon self-coupling suppressed by a factor of n_f , and the dominant perturbative corrections are obtained by inserting an arbitrary number of fermionic bubbles along the gluon propagator. The Large- n_f limit then appears quite useful, since it is a fully calculable model theory, where one can explicitly determine the IR renormalons.

The usual way to recover the non-abelian behaviour of the theory consists in restoring the proper expression of b_0 by hand. This method relies upon the argument that the factorial behaviour is strictly related to the running of the coupling constant, and then all the uncalculated diagrams would combine in order to reproduce this ad-hoc manipulation [25]. From a practical point of view, this method consists in replacing, at the end of the all-order computation

$$n_f \rightarrow -\frac{11C_A}{4T_R} + n_l \quad (20)$$

where n_l is the real number of light flavors of the theory, implementing in such a way the *Large- b_0 approximation*.

¹Renormalons have been first discussed in 1970s in references [18–20] and have received renewed attention from a phenomenological perspective since 1992 in refs. [21–23]. A well-known review of this topic is given in [24].

Part I

Infrared Renormalons in the transverse momentum of a Z boson in hadronic collisions

Introduction

The transverse momentum of a Z boson, produced in association with a jet in hadronic collisions, is one of the cleanest and well measured LHC-observables, also providing a useful background for Beyond Standard Model (BSM) research, and for constraining the strong coupling constant α_s and the PDFs at LHC (see for instance ref. [26]). The normalized distributions are indeed measured with a sub-percent level precision, in the low-intermediate values of the transverse momentum [27–30], whilst the uncertainties in theoretical computations are still at the percent level. In particular, the process of Z +jet production in hadronic collisions has been computed at Next-to-Next-to Leading Order (NNLO) in QCD [31–33], and the state of the art is NNLO+N³LL [34], where it is evident the effect of resummation for small values of the transverse momentum of the Z boson, with Non-Perturbative (NP) terms also playing a role [35–37]. The 13 TeV ATLAS measurements [30] show a good agreement with the NNLO+N³LL results for $p_T^Z < 30$ GeV, with some tension observed for larger values of the transverse momentum, where the resummation effects are actually negligible. This tension looks similar in size to the residual scale uncertainty and, furthermore, is not observed in the 8 TeV measurements [38]. Given the high accuracy reached for this observable, it is crucial to investigate whether it is affected by NP corrections arising as Infrared (IR) linear renormalons.

Consider the transverse momentum distribution of the Z boson

$$\frac{d\sigma}{dp_T^2}, \quad \frac{d^2\sigma}{dp_T^2 dy}, \quad (21)$$

where p_T and y are the transverse momentum and rapidity of the Z boson, respectively.

If these distributions were affected by linear NP corrections, their natural size would be Λ_{QCD}/p_T , where Λ_{QCD} is a typical hadronic scale. Thus this ratio could easily reach the percent level, larger than the present experimental errors and the theoretical accuracy.

There are reasons to worry about the presence of linear power corrections in the transverse momentum distribution of a Z boson. In fact, if the Z has a sizable transverse momentum, we are essentially looking at a Z +jet event. Thus, unlike for the case of the inclusive Z cross section or for its rapidity distribution, the associated radiation is not azimuthally symmetric (see fig. 1). If we model non-perturbative corrections as due to the emission of a very soft gluon, with transverse momentum of order Λ_{QCD} , one can reasonably assume that it will also affect the transverse momentum of the Z boson by recoil.

As we explained before, certain kinds of factorial growth of the perturbative expansion in QCD, associated with the so called Infrared (IR) renormalons, lead to power corrections

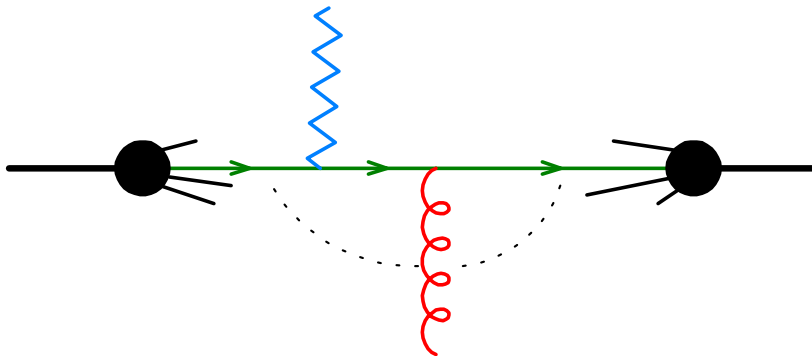


Figure 1: Feynman diagram contributing to the transverse momentum distribution of a Z boson, represented by a zigzag line. The soft-radiation pattern is represented by the dashed line, and is associated with the color dipoles formed by the outgoing gluon (wavy line) and the initial state quarks.

$\mathcal{O}(\Lambda_{\text{QCD}}/Q)^p$. In the following we will be interested into the case $p = 1$, that we dub linear renormalon in this work.

General field-theory arguments assure us that linear renormalons cannot arise for certain quantities. This is the case for observables that admit an Operator Product Expansion (OPE), and are such that there are no operators of dimension higher than one power with respect to the leading contributions. Indeed IR renormalons in hard processes originate from subgraphs with low momenta, and thus, if the process under consideration allows for an OPE, then it will be possible to organize the involved Feynman diagrams in terms of expectation values of local operators [23, 39]. Unfortunately, for processes that do not admit an OPE, one needs to recur to assumptions and approximations in order to get some insight into the problem.

An often used method is the large- b_0 approximation (see [24] and references therein), which consists in considering the Abelian limit of QCD with a large and negative number of fermions n_f . In this limit the terms of order $(\alpha_s n_f)^k$ are fully calculable for each order k and the theory develops IR and UV renormalons. At the end of the computation, in order to restore the proper non-Abelian behaviour of the full theory, one needs to replace the b_0 factor in the Abelian theory (proportional to $-n_f$) with the full QCD one.

In the first part of this work we will investigate the presence of IR linear renormalons in the transverse momentum distribution of a vector boson working within the large- b_0 approximation. The interest in this process also stems from the fact that, as said previously, the soft emission pattern in the production of a vector boson in association with a hard jet is not azimuthally symmetric. Under these circumstances, it is reasonable to assume that soft gluons may induce linear renormalon corrections to the transverse momentum distribution of the vector boson, as they are not emitted according to an azimuthally symmetric pattern.²

²We also stress that, contrary to the common assumptions that leptonic observables should be less affected by NP corrections than the hadronic ones, in ref. [40] we can observe that leptonic observables in top quark production and decay are actually affected by linear renormalons.

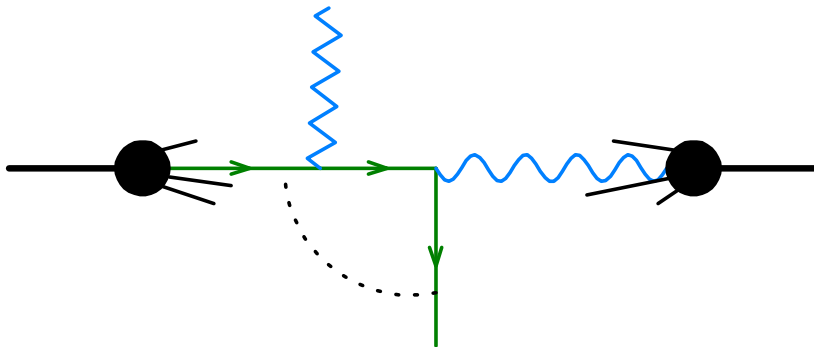


Figure 2: Born diagram for the production of a Z boson in photon-quark collision. The green lines represent the incoming and outgoing quarks, while the photon and the Z are represented by the wavy and zig zag line, respectively. This process has an asymmetric pattern for the soft emission, and looks suitable for probing the presence of IR linear renormalons in the p_T distribution of the Z .

The first part of this thesis is structured as follows. In chapter 1 we investigate the presence of IR linear renormalons in the transverse momentum distribution of a Z boson, produced in association with a jet in hadronic collisions. Even though the realistic parton level process would involve a gluon in the final state (see fig. 1), no Large- n_f computation for a process involving a gluon at the Born level has been ever carried out. Thus, in order to overpass this issue, we consider the process represented in fig. 2 as a proxy for the one represented in fig. 1, involving a photon in the initial state, with associated production of a Z boson plus a quark.

By doing this we are able to perform an all-order computation working in the large- n_f limit, also preserving the azimuthal asymmetry of the soft emission pattern affecting the realistic QCD process.

It is a well known result [24] that the presence of IR linear renormalons in a Large- n_f computation can be probed by simply evaluating the QCD radiative corrections to the process of interest due to the emission or exchange of a massive gluon with mass λ , and looking for linear terms in λ . As we will show later, there is a simple relation between IR linear renormalons and a linear sensitivity with the mass λ of the gluon. Within this framework, we simply evaluated the cross section for the production of a Z boson in association with a jet at NLO in α_s , in a theory in which the gluon has a non vanishing mass λ , and looked for λ terms at the end of the computation.

In this chapter a description of the treatment of the initial state singularities affecting our process, in the DIS scheme, is also given.

Finally in chapter 2 we present our results and in chapter 3 we give our conclusions.

Chapter 1

Details of the computation

In this chapter we are going to show how to practically investigate the presence of an IR linear renormalon affecting the transverse momentum of a Z boson produced in association with a jet in hadronic collisions.

1.1 On the low transverse momentum of a vector boson

The transverse momentum distribution of vector bosons in hadronic collisions has been the subject of an intense theoretical study since the early days of perturbative QCD [35–37], up to nowadays [38, 41–46], also given the high accuracy reached by experimental collaborations in the measure of such observables. Thus this observable can be expressed as a perturbative expansion in QCD, starting with a $\delta^2(p_T)$ at leading order, and receiving singular contributions at higher perturbative orders, due to soft and collinear gluon emissions. It is usual to deal with it resumming the singular contributions to all order in the perturbative expansion. It has been shown [36] that this approach yields (for very large masses) to finite results in the limiting region of zero transverse momentum.

Nevertheless this approach needs a non-perturbative input, as the resummation of soft-collinear gluons must be cut-off at transverse momenta of the order of typical hadronic scales. Furthermore, it is intuitive to assume that the $\delta^2(p_T)$ leading order behaviour (and the higher orders singular terms) can be smeared to a transverse size of order of a Fermi, due to some effects related to Fermi motion.¹

If we consider the smearing due to Fermi motion, we can define with $f(\vec{q}_T)d^2\vec{q}_T$ the primordial transverse momentum distribution of the quarks in a hadron. Assuming that $f(\vec{q}_T)$ is dominated by values of \vec{q}_T of the order of hadronic scales, then we can expand it in moments

$$f(\vec{q}_T) = \delta^2(\vec{q}_T) + \Lambda^2(\vec{\partial}_{q_T})^2\delta^2(\vec{q}_T) + \text{higher derivatives}, \quad (1.1)$$

being Λ a typical hadronic scale. By Fourier transforming eq. (1.1) we get the behaviour

¹These effects are also well described thanks to Transverse Momentum Distributions (TMD) parton densities [47].

$$\tilde{f}(\vec{b}) = \int d^2 q_T e^{i\vec{q}_T \cdot \vec{b}} f(\vec{q}_T) = 1 - \Lambda^2 b^2 + \text{higher orders in } b. \quad (1.2)$$

We can observe the absence of linear terms in ∂_{p_T} (or in b), as long as one does not take into account spin structures in the distribution, and indeed the behaviour in eq. (1.2) has been exposed as early in [36], where the expression $\tilde{f}(b) = \exp(-\Lambda^2 b^2)$ has been proposed. This exponential expression also appears in many subsequent works.² If we convolute eq. (1.2) with some perturbative mechanism which gives rise to the transverse momentum of the vector boson, we will obtain in the end subleading corrections of order Λ^2/p_T^2 . It is possible as well to provide a more intuitive argument in order to explain the absence of leading power corrections within this context. The primordial transverse momentum smearing gives a transverse kick, of the order of typical hadronic scales, to the perturbative distribution. Nevertheless, being azimuthally symmetric, this first-order effect cancels out, leaving only quadratic corrections. One can also observe that these non-perturbative corrections are all that is necessary in order to regularise the ill-behaved perturbative series in the small- p_T region. Nevertheless they cannot be the *only* non-perturbative corrections relevant for the problem, as other arguments are needed when phase space regions, where QCD perturbative expansion is well-behaved, are considered.

For what concerns our computation, we do not deal with the small transverse momentum region, considering in this sense a process which has a well-behaved perturbative expansion in α_s . Furthermore we do not rely on any assumption concerning the arising (or eventually the cancellation) of non-perturbative corrections, only performing the full all-order computation recurring to the large- n_f limit, and looking for renormalon effects in the final result. Our main hypothesis deals with the assumption according to which such linear effects can only arise when considering a process with a soft radiation which is not azimuthally symmetric, and, in order to do that, we chose a process where this asymmetry is realized. Indeed we did not consider a process involving two incoming partons that produce a Z boson plus a photon with large transverse momentum. This process indeed does yield an azimuthally symmetric pattern and thus we do not expect any linear renormalon in this case.

In conclusion we remark that the thrust of a jet actually receives linear power corrections related to IR linear renormalons (as can be seen in eq. (5.56) in [24]). As for our study we consider the Z recoiling against a jet, it seems reasonable to assume that such linear corrections may also affect the Z transverse momentum distribution.

1.2 Our computation

A calculation in the large- b_0 limit of a process like in fig. 1 is too demanding and indeed no large- b_0 computation for processes involving a gluon emission or exchange at Born level has been ever carried out. Such a computation would in fact lead to consider dressed gluon propagator joining into a three-gluon vertex, also including a vertex correction with a quark

²Exhaustive analysis of these NP corrections can be found in [48, 49]. Within the framework of the TMD parton distributions, one can also explain the absence of linear power corrections by exploiting arguments given by the OPE they obey.

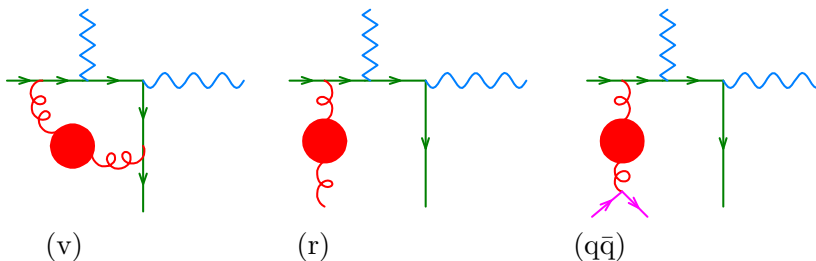


Figure 1.1: Sets of Feynman diagrams to be evaluated in order to compute QCD radiative corrections to the process represented in fig. 2 in the large- b_0 limit.

triangle graph, being such corrections of order $g_s(g_s^2 n_f)$, where g_s is the gauge coupling for the strong interaction. In order to overcome this problem, we will instead compute the process depicted in fig. 2, involving the production of a Z boson in a photon-quark collision. In particular we will assume that only a single quark flavor (that we will call for definiteness a d quark) can couple to the photon, but there is a large number n_f of light quark flavors q that can couple to gluons. With this setup we can then perform the whole computation in the large- n_f limit, restoring the non-Abelian behaviour of the theory by taking the *Large- b_0* limit at the end of the computation. Furthermore, the color pattern for the soft emission for the process in fig. 2 is still affected (as the realistic QCD one) by an azimuthal asymmetry. Thus we can investigate whether IR linear renormalons affect the transverse momentum of the Z boson, due to its recoil against a soft emission. In order to do that, we need to evaluate the relevant radiative QCD corrections in the large- n_f limit, considering for instance the diagrams represented in fig. 1.1. The solid blobs along the gluon propagators stand for the inclusion of the all orders corrections given by a fermion loop in the abelian QCD limit, as shown by the recursive graphic equation

$$\text{gluon blob} = \text{gluon} + \text{gluon} \text{ loop} \text{ gluon blob} . \quad (1.3)$$

The inclusion of all corrections embodied in eq. (1.3) amounts to consider $\alpha_s n_f$ to be of order 1, and because of this it is also necessary to consider the contribution arising from the gluon splitting into a quark-antiquark pair as this contributes, when squared, with a factor $\alpha_s n_f$.

In the following we will discuss in detail the method adopted to perform an all-order computation for our process, borrowing the formalism exposed in [40] and also discussing the method adopted in order to remove the initial state collinear singularity.

1.3 The method

Let us assume to compute a cross section for the process $d\gamma \rightarrow Zd$ with a given set of kinematic cuts, expressed through the use of theta functions defined upon the phase space

$\Theta(\Phi)$, assuming the value 1 when the cuts are satisfied, and zero otherwise. Thus the cross section can be written as (see [50] for more details upon the formalism)

$$\begin{aligned}
 \sigma &= \int d\Phi_B (B(\Phi_B) + V(\Phi_B)) \Theta(\Phi_B) \\
 &+ \int d\Phi_{\oplus} C_{\oplus}(\Phi_{\oplus}) \Theta(\Phi_{\oplus}) \\
 &+ \int d\Phi_{\ominus}^g C_{\ominus}^g(\Phi_{\ominus}^g) \Theta(\Phi_{\ominus}^g) + \int d\Phi_{\ominus}^{q\bar{q}} C_{\ominus}^{q\bar{q}}(\Phi_{\ominus}^{q\bar{q}}) \Theta(\Phi_{\ominus}^{q\bar{q}}) \\
 &+ \int d\Phi_g R_g(\Phi_g) \Theta(\Phi_g) \\
 &+ \int d\Phi_{q\bar{q}} R_{q\bar{q}}(\Phi_{q\bar{q}}) \Theta(\Phi_{q\bar{q}}),
 \end{aligned} \tag{1.4}$$

where B stands for the Born term, V refers to the virtual correction, R_g refers to the process involving $d\gamma \rightarrow Zdg$, and $R_{q\bar{q}}$ to the process $d\gamma \rightarrow Zdq\bar{q}$ (see the diagrams in fig. 1.1). The term involving C_{\oplus} stands for the counterterm to subtract the initial state collinear singularities affecting both R_g and $R_{q\bar{q}}$, arising when the gluon or the light $q\bar{q}$ pair get collinear with the incoming quark. The use of a single C_{\oplus} contribution is justified by the fact that both these singularities are associated with the same underlying Born configuration $d\gamma \rightarrow Zd$. The C_{\ominus}^g and $C_{\ominus}^{q\bar{q}}$ refer to the collinear counterterms associated with the collinear singularities arising from the splitting of the initial state photon into a $d\bar{d}$ pair, contained both in the R_g and $R_{q\bar{q}}$ contributions, respectively. The phase space elements are defined as follows

$$d\Phi_B = dx_{\oplus} dx_{\ominus} d\Phi_B, \tag{1.5}$$

$$d\Phi_B = \frac{d^3\vec{k}_Z}{2k_Z^0(2\pi)^3} \frac{d^3\vec{k}_d}{2k_d^0(2\pi)^3} (2\pi)^4 \delta^{(4)}(p_{\oplus}x_{\oplus} + p_{\ominus}x_{\ominus} - k_Z - k_d), \tag{1.6}$$

where we labeled with p_{\oplus} and p_{\ominus} the momenta of the incoming positive and negative rapidity hadrons respectively, and with x_{\oplus} , x_{\ominus} the momentum fractions carried by the incoming d quark and photon; k_Z and k_d stand for the momenta of the final state Z and d . Furthermore we have

$$B(\Phi_B) = f_d(x_{\oplus}) f_{\gamma}(x_{\ominus}) \mathcal{B}(p_{\oplus}x_{\oplus}, p_{\ominus}x_{\ominus}, k_d, k_Z), \tag{1.7}$$

with \mathcal{B} the Born squared amplitude for the partonic process, divided by the flux factor, and f_d (f_{γ}) the parton distribution function related to the incoming d quark (photon). The phase space elements $d\Phi_g$ and $d\Phi_{q\bar{q}}$, as well as $d\Phi_g$, $d\Phi_{q\bar{q}}$ and R_g , $R_{q\bar{q}}$ are defined along the same lines of eqs. (1.5), (1.6) and (1.7).

For Φ_{\oplus} , Φ_{\ominus} and C_{\oplus} , C_{\ominus} we have

$$d\Phi_{\oplus} = dx_{\oplus} dx_{\ominus} \frac{dz}{z} d\Phi_B, \tag{1.8}$$

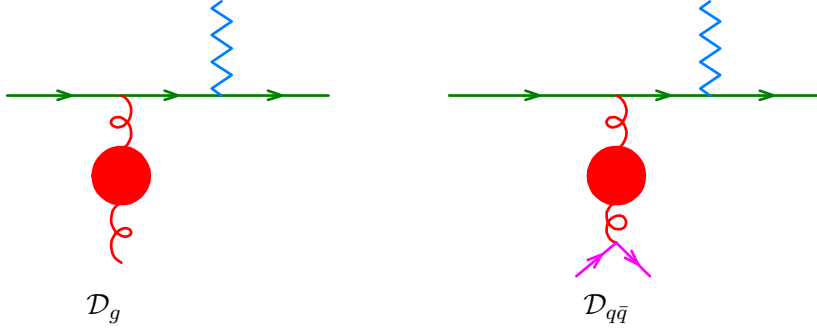


Figure 1.2: Feynman diagrams for the $q\bar{q}$ initiated subprocesses, entering in the factorization formula for initial state collinear singularities, arising as the outgoing quark gets collinear to the initial state photon, contributing respectively to the \mathcal{D}_g and $\mathcal{D}_{q\bar{q}}$ amplitudes.

$$d\Phi_{\ominus}^g = dx_{\oplus} dx_{\ominus} \frac{dz}{z} d\Phi_{\text{D}}^g, \quad (1.9)$$

$$d\Phi_{\ominus}^{q\bar{q}} = dx_{\oplus} dx_{\ominus} \frac{dz}{z} d\Phi_{\text{D}}^{q\bar{q}}, \quad (1.10)$$

with

$$C_{\oplus}(\Phi_{\oplus}) = f_d\left(\frac{x_{\oplus}}{z}\right) f_{\gamma}(x_{\ominus}) C_{dd}(z) \mathcal{B}(p_{\oplus} x_{\oplus}, p_{\ominus} x_{\ominus}, k_Z, k_d), \quad (1.11)$$

$$C_{\ominus}^g(\Phi_{\ominus}^g) = f_d(x_{\oplus}) f_{\gamma}\left(\frac{x_{\ominus}}{z}\right) C_{d\gamma}(z) \mathcal{D}_g(p_{\oplus} x_{\oplus}, p_{\ominus} x_{\ominus}, k_Z, k_g), \quad (1.12)$$

$$C_{\ominus}^{q\bar{q}}(\Phi_{\ominus}^{q\bar{q}}) = f_d(x_{\oplus}) f_{\gamma}\left(\frac{x_{\ominus}}{z}\right) C_{d\gamma}(z) \mathcal{D}_{q\bar{q}}(p_{\oplus} x_{\oplus}, p_{\ominus} x_{\ominus}, k_Z, k_q, k_{\bar{q}}). \quad (1.13)$$

The C_{\ominus} collinear counterterms correspond to the diagrams (g) and (q \bar{q}) depicted in fig. 1.1, when the outgoing quark becomes collinear to the incoming photon. In particular, the \mathcal{D}_g and $\mathcal{D}_{q\bar{q}}$ squared amplitudes refer to the processes $q\bar{q} \rightarrow Zg$ and $q\bar{q} \rightarrow Zq\bar{q}$, respectively, as depicted in fig. 1.2 and obviously Φ_{D}^g and $\Phi_{\text{D}}^{q\bar{q}}$ are the corresponding phase spaces. C_{dd} and $C_{d\gamma}$ are the universal collinear divergent functions for the $d \rightarrow d + X$ and $\gamma \rightarrow d + X$ splitting, respectively. Working in our approximation we do not have any interference from the final state d quark connected to the incoming quark line and the final states quarks arising from the gluon splitting, as this interference term would be suppressed by a factor of n_f . When evaluating the virtual corrections reported in fig. 1.1 we face both UV and IR divergences, that we chose to regulate recurring to conventional dimensional regularization (CDR), introducing a number of dimensions $d = 4 - 2\epsilon$. Nevertheless, it turns out that all the UV divergences cancel, being exclusively associated with vertex and propagator corrections in an Abelian limit. For the C_{\ominus} collinear counterterm, the divergent function $C_{d\gamma}$ is given by

$$C_{d\gamma}(z) = \frac{\alpha C_d^2}{2\pi \epsilon} (z^2 + (1-z)^2), \quad (1.14)$$

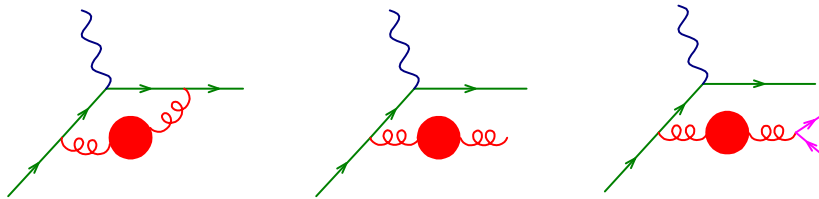


Figure 1.3: Relevant Feynman diagrams contributing to F_2 in the Large- n_f limit.

where α is the electromagnetic coupling and C_d is the electric charge of the d quark. According to the $\overline{\text{MS}}$ prescription, the term in eq. (1.14) must also be accompanied by the replacement $\mu_F^2 \rightarrow \mu_F^2 \exp(-\gamma_E)/(4\pi)$ where μ_F is the factorization scale and γ_E is the Euler-Mascheroni constant. For what concerns the $\overline{\text{MS}}$ subtraction term for the collinear singularity associated with the C_\oplus counterterm, it is not straightforward to compute it, working in an Abelian theory in the Large- n_f limit. Indeed one must include all the $\mathcal{O}(\alpha_s n_f)$ corrections, i.e. all the vacuum polarizations insertions along the emitted gluon line, also considering the gluon splitting into a light $q\bar{q}$ pair. Following the approach of ref. [25] we can avoid this problem, performing our collinear subtraction in the DIS scheme. In order to do that we require that the structure function F_2 has the expression

$$F_2(x, Q^2) = x \sum_i q_i(x, Q^2) C_i^2, \quad (1.15)$$

(C_i is the electric charge of the species i , with i running over all quarks and antiquarks) at all orders in perturbation theory.

With this approach we can simply evaluate $F_2(x, Q^2)$ using the same approximation we recurred for our process, i.e. including all fermion polarizations insertions along gluon propagators, and expressing our cross section in terms of the q_i in the DIS scheme. The relevant Feynman diagrams involved in this computation are depicted in fig. 1.3. It is important to stress that, when translating the DIS cross section into the $\overline{\text{MS}}$ scheme, no new linear renormalon arises. This can be easily explained observing that F_2 obeys an OPE where power corrections are controlled by the twist of the operator, with the dominant power corrections, which correspond to twist 4, that are quadratic.

It can be shown that, considering a process that does not involve a gluon at leading order, an all-order computation performed in the Large- n_f limit can be handled by considering the radiative corrections to the process due to the exchange or emission of a gluon with a non-vanishing mass λ . More specifically, the cross section computed with an all-order computation in an abelian limit takes the expression (borrowed from [40], with the inclusion of the collinear remnants, needed in order to subtract the collinear singularities due to the initial state emission):

$$\sigma = \sigma_B - \frac{1}{b_0 \alpha_s} \int_0^\infty \frac{d\lambda}{\pi} \frac{dT(\lambda)}{d\lambda} \arctan \frac{\pi b_0 \alpha_s}{1 + b_0 \alpha_s \ln^2 \frac{\lambda^2}{\mu_C^2}} \quad (1.16)$$

where $\alpha_s = \alpha_s(\mu)$, $\mu_C = \mu e^{C/2}$, $C = \frac{5}{3}$ and b_0 is the first coefficient of the QCD β -function taken in the abelian limit $n_f \rightarrow -\infty$, i.e. $b_0 = -\frac{T_F}{2\pi}$, where $T_F = n_f T_R$.

Furthermore

$$\sigma_B = \int d\Phi_B B(\Phi_B) \Theta(\Phi_B), \quad (1.17)$$

$$T(\lambda) = T_V(\lambda) + T_{\oplus}(\lambda) + T_{\ominus}(\lambda) + T_{\ominus}^{\Delta}(\lambda) + T_R(\lambda) + T_R^{\Delta}(\lambda), \quad (1.18)$$

$$T_V(\lambda) = \int d\Phi_B V^{(\lambda)}(\Phi_B) \Theta(\Phi_B), \quad (1.19)$$

$$T_{\oplus}(\lambda) = \int d\Phi_{\oplus} f_d\left(\frac{x_{\oplus}}{z}\right) f_{\gamma}(x_{\ominus}) C_{dd}^{(\lambda)}(z) \mathcal{B}(p_{\oplus} x_{\oplus}, p_{\ominus} x_{\ominus}, k_Z, k_d) \Theta(\Phi_{\oplus}), \quad (1.20)$$

$$T_{\ominus}(\lambda) = \int d\Phi_{\ominus}^{g^*} f_d(x_{\oplus}) f_{\gamma}\left(\frac{x_{\ominus}}{z}\right) C_{d\gamma}(z) \mathcal{D}_{g^*}(p_{\oplus} x_{\oplus}, p_{\ominus} x_{\ominus}, k_Z, k_{g^*}) \Theta(\Phi_{\ominus}^{g^*}), \quad (1.21)$$

$$\begin{aligned} T_{\ominus}^{\Delta}(\lambda) &= \int d\Phi_{\ominus}^{q\bar{q}} f_d(x_{\oplus}) f_{\gamma}\left(\frac{x_{\ominus}}{z}\right) C_{d\gamma}(z) \mathcal{D}_{q\bar{q}}(p_{\oplus} x_{\oplus}, p_{\ominus} x_{\ominus}, k_Z, k_q, k_{\bar{q}}) \\ &\times \delta(\lambda^2 - k_{q\bar{q}}^2) \left[\Theta(\Phi_{\ominus}^{q\bar{q}}) - \Theta(\Phi_{\ominus}^{g^*}) \right], \end{aligned} \quad (1.22)$$

$$T_R(\lambda) = \int d\Phi_{g^*} R_{g^*}(\Phi_{g^*}) \Theta(\Phi_{g^*}), \quad (1.23)$$

$$T_R^{\Delta}(\lambda) = \frac{3\pi}{\alpha_s T_F} \lambda^2 \int d\Phi_{q\bar{q}} \delta(\lambda^2 - k_{q\bar{q}}^2) R_{q\bar{q}}(\Phi_{q\bar{q}}) \left[\Theta(\Phi_{q\bar{q}}) - \Theta(\Phi_{g^*}) \right]. \quad (1.24)$$

Where g^* denotes a gluon with mass λ , and with the superscript (λ) applied to previously defined objects we mean that the same object has been evaluated considering a gluon with mass λ . Within this framework, the virtual correction $V^{(\lambda)}$ stands for a usual one-loop correction to the process, with the gluon propagator replaced by a massive gluon propagator with mass λ . Along these lines Φ_{g^*} labels the phase space for the process $d\gamma \rightarrow Z d g^*$, and so on. We also introduced the momentum $k_{q\bar{q}} = k_q + k_{\bar{q}}$ in eqs. (1.22) and (1.24).

Eq. (1.16) is a well-known result (see ref. [24]), as long as one considers the virtual corrections and the inclusive real corrections, but we do not know a reference before [40] where also the $q\bar{q}$ splitting is cast in the same form.

Therefore the fact that a Large- n_f limit computation can be expressed in terms of a simple NLO calculation performed with a massive gluon has been used in [25] to compute the Drell-Yan and DIS process in the Large- n_f limit. The Δ term has been introduced for the first time in ref. [51], where it was shown to be necessary for quantities that are not fully inclusive in the gluon splitting products. As the Δ correction only involves kinematic cuts related to the emission of a gluon that further splits into a $q\bar{q}$ pair, it cannot contribute if we only focus upon the kinematic of the colourless system, i.e. of the Z boson. Our cuts in fact only involve the kinematics of the Z boson, and thus are insensitive to the replacement of the $q\bar{q}$ arising from the gluon splitting with an undecayed massive gluon with the mass equal to the invariant mass of the pair. Within this configuration, the difference of the theta functions in the square bracket of eq. (1.22) and eq. (1.24) are always zero and we can neglect the Δ term for our computation.

The universal collinear divergent factor $C_{dd}^{(\lambda)}(z)$ has been computed in eq. (3.10) of ref. [25] and we have

$$C_{dd}^{(\lambda)}(z) = -f^{(1),\text{real}}\left(z, \frac{\lambda^2}{\mu^2}\right) - \delta(1-z)f^{(1),\text{virtual}}\left(z, \frac{\lambda^2}{\mu^2}\right), \quad (1.25)$$

being μ the hard scale of the process. Denoting $\xi = \lambda^2/\mu^2$ and $\bar{x} = 1-x$, we write $f^{(1),\text{real}}$ as

$$\begin{aligned} f^{(1),\text{real}}(x, \xi) = & \frac{C_F \alpha_s(\mu)}{2\pi} \left\{ \left[-\frac{1+x^2-2\xi x(1+x-\xi x)}{\bar{x}} - 6\xi x^2(2-3\xi x) \right] \ln \frac{\xi x^2}{\bar{x}(1-\xi x)} \right. \\ & + \frac{\bar{x}-\xi x}{\xi x-1} + \frac{(\bar{x}-\xi x)^2}{2\bar{x}^3} - 2(1-\xi)x \frac{\bar{x}-\xi x}{\bar{x}^2} + 3x \frac{(\bar{x}-\xi x)^2}{\bar{x}^2} \\ & \left. - 12\xi x^2 \frac{\bar{x}-\xi x}{\bar{x}} + 6\xi x \bar{x}(1-\xi x) - 6\xi^2 x^3 \right\} \Theta(\bar{x}-\xi x), \end{aligned} \quad (1.26)$$

while the virtual corrections are

$$\begin{aligned} f^{(1),\text{virt}}(x, \xi) = & \frac{C_F \alpha_s(\mu)}{2\pi} \delta(1-z) \left\{ 2(1-\xi)^2 \left[\text{Li}_2(\xi) - \frac{1}{2} \ln^2 \xi + \ln \xi \ln(1-\xi) - \frac{\pi^2}{3} \right] \right. \\ & \left. - 3 \ln \xi - \frac{7}{2} + 2\xi \ln \xi + 2\xi \right\}. \end{aligned} \quad (1.27)$$

Furthermore the z variable in the real contribution is limited as

$$z < z_{\text{max}} \equiv \frac{1}{1 + \frac{\lambda^2}{\mu^2}}. \quad (1.28)$$

From the Adler sum rule we have

$$\int_0^1 dz C_{dd}^{(\lambda)}(z) = - \int_0^{z_{\text{max}}} dz f^{(1),\text{real}}\left(z, \frac{\lambda^2}{\mu^2}\right) - f^{(1),\text{virt}}\left(\frac{\lambda^2}{\mu^2}\right). \quad (1.29)$$

As we have said previously, eq. (1.16) relates an all-order computation performed in the Large- n_f limit to a NLO computation performed with a gluon with non-vanishing mass λ . In particular, the integrand in eq. (1.16) is formally a power expansion in $b_0 \alpha_s$ with factorially growing coefficients. The function $T(\lambda)$ is finite as $\lambda \rightarrow 0$ and it can be expanded in λ as

$$T(\lambda) = T(0) + T'(0)\lambda + \mathcal{O}(\lambda^2), \quad (1.30)$$

where possible logarithmic enhancements in the quadratic remainder could be present. The presence of a linear renormalon is strictly related to the linear coefficient in the above equation. In fact if $T'(0) \neq 0$ then the perturbative expansion is affected by a linear renormalon, as it is explained in detail in appendix A.

The computation of the collinear subtraction associated with the collinear splitting of the incoming photon is a standard NLO subtraction, and can be handled by the standard means already coded in the POWHEG BOX package [52]. However we stress that no linear renormalon correction to the Z boson transverse-momentum distribution is expected from this collinear

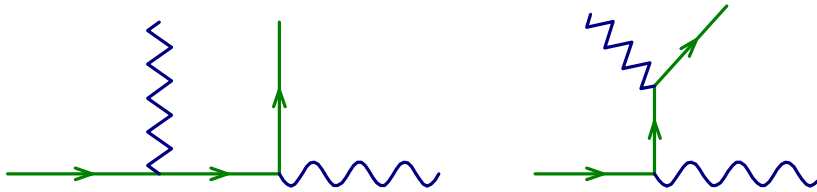


Figure 1.4: Feynman diagrams contributing to the process $d\gamma \rightarrow Zd$ at the Born level. The zigzag line represents the Z boson, while the wavy line represents the incoming photon.

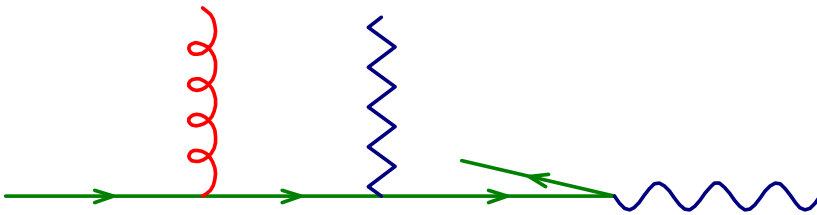


Figure 1.5: Feynman diagram describing the collinear singularities due to the splitting of the photon into a $d\bar{d}$ pair, in the process $d\gamma \rightarrow Zd$ process.

region. Indeed, as mentioned previously, the $T_{\ominus}^{\Delta}(\lambda)$ term does not contribute, and if the final state quark gets collinear to the initial state photon, the transverse momentum of the Z must be balanced by the massive gluon. Since we are only considering phase space regions where the Z boson has a sizable transverse momentum, the massive gluon will have a large transverse momentum as well, and thus the mass correction to the process turns out to be quadratic in λ .

1.4 Implementation of the method

In the previous sections we have shown that, in order to probe the presence of IR linear renormalon for a generic cross section, we can perform the same computation in an Abelian limit with a massive gluon. In fig. 1.4 we have reported the Born diagrams contributing to our process, where we have chosen, for sake of simplicity, a Z boson which is only vectorially coupled and stable. The Born and Virtual amplitudes have been evaluated at fixed external momenta; in particular, all the amplitudes have been analytically computed recurring to the symbolic manipulation program MAXIMA [53]. The Virtual contribution has been dealt with by first decomposing the amplitude in terms of a set of scalar integrals, thanks to the Passarino-Veltman algorithm [54], and then evaluating them using the COLLIER library [55]. Due to the presence of a massive gluon, the virtual corrections are infrared finite, as the gluon mass acts as an IR regulator. Nevertheless each contribution is affected by UV divergences, that have been extracted by performing the whole computation in CDR ($d = 4 - 2\epsilon$), in order to preserve gauge invariance at each step. Summing up all the contributions we obtain a UV finite result, and then one can safely take the $\epsilon \rightarrow 0$ limit. For what concerns the integration

over the external momenta, we will show that for the Born and the Virtual terms we need to require a lower bound on the Z transverse momentum in order to get a finite result.

On the other hand the real corrections are not infrared finite even if one requires a finite transverse momentum for the Z -boson, because of the collinear singularities arising from the incoming photon splitting into two massless quarks, as we show in fig. 1.5. This singularity also needs to be first regulated in CDR, and then subtracted in the $\overline{\text{MS}}$ scheme, as required by the factorization formalism.

Furthermore, the singularities associated with the soft or collinear emitted gluon are automatically regulated by the gluon mass. These configurations are illustrated in fig. 1.6 and correspond to an initial and a final state collinear singularity, associated with a soft one. Thus the real contributions behave as $\ln^2 \lambda$ in the $\lambda \rightarrow 0$ limit. An equal $\ln^2 \lambda$ term also arises from the virtual contributions, with the opposite sign, that cancels the one coming from the real term. After this cancellation, a $\ln \lambda$ singularity remains, which will be canceled thanks to an opposite contribution in the collinear counterterm (see eq. (1.20)). At this point, after these cancellations, we get a finite result as $\lambda \rightarrow 0$: the cross section goes to a constant, and our goal is to understand whether this constant is approached with a linear slope in λ .

We have described a computation involving massive cancellations among the various terms, and then in order to get a reliable numeric evidence of the small λ behaviour, the numerical integration must be performed using a proper importance sampling in the neighbourhood of regions that are singular in the $\lambda \rightarrow 0$ limit. Furthermore, we also need a direct calculation in the full theory, i.e. for $\lambda = 0$, in order to obtain a point with negligible error, that would be difficult to obtain considering small values of λ . In order to perform the computation we chose to separate the real contribution into three terms

$$R = R^{(1)} + R^{(2)} + R^{(3)}, \quad (1.31)$$

$$R^{(1)} = \frac{\frac{1}{p_{T,d}^2}}{\frac{1}{p_{T,d}^2} + \frac{1}{m_{T,g}^2} + \frac{(E_d+E_g)^2}{E_d E_g m_{d,g}^2}} R, \quad (1.32)$$

$$R^{(2)} = \frac{\frac{1}{m_{T,g}^2}}{\frac{1}{p_{T,d}^2} + \frac{1}{m_{T,g}^2} + \frac{(E_d+E_g)^2}{E_d E_g m_{d,g}^2}} R, \quad (1.33)$$

$$R^{(3)} = \frac{\frac{(E_d+E_g)^2}{E_d E_g m_{d,g}^2}}{\frac{1}{p_{T,d}^2} + \frac{1}{m_{T,g}^2} + \frac{(E_d+E_g)^2}{E_d E_g m_{d,g}^2}} R, \quad (1.34)$$

where $p_{T,d}$ stands for the transverse momentum of the final-state d quark, $m_{T,g}$ is the transverse mass of the final-state gluon, defined as

$$m_{T,g}^2 = p_{T,g}^2 + \lambda^2, \quad (1.35)$$

and m_{dg} is the invariant mass of the quark-gluon final-state system, with E_d and E_g the energies of the outgoing quark and gluon respectively, taken in the partonic center of mass frame.



Figure 1.6: On the left (right) the Feynman diagram contributing to the collinear initial (final) state singularity, and to a soft singularity.

In eqs. (1.32), (1.33), (1.34) we introduced the superscripts (1), (2) and (3) to label the three regions where each of the three contributions is singular. For instance region (1) is singular when the final state quark gets collinear to the incoming photon; region (2) becomes relevant when the gluon is collinear to the incoming quark, and region (3) contributes when the emitted gluon gets collinear to the outgoing quark.

The contributions due to regions (2) and (3) have been computed independently, parameterising the phase space in a proper way for each of them. For the region (2) the phase space has been factorized as the product of the two-body phase space formed by the final state gluon recoiling against the quark- Z system, and the two-body phase space for the quark- Z system itself. In the case of the region (3) we factorized the phase space in terms of the two-body phase space for the system comprising the Z , and the quark-gluon system which recoils against it, with the quark-gluon system itself parameterized as a two-body phase space. It is important to notice that Born, real and virtual contributions are also singular when the transverse momentum of the Z boson goes to zero. Nevertheless, as we are interested into the transverse momentum distribution of the Z for transverse momentum comparable to the Z mass, in the integration stage we can safely suppress this region, introducing a suppression factor proportional to the Z transverse momentum itself. Thus we introduce

$$F_{\text{supp}} = \frac{p_{T,Z}^4}{p_{T,Z}^4 + p_{T,\text{cut}}^4}, \quad (1.36)$$

with $p_{T,\text{cut}}$ a parameter chosen close to the transverse momentum cut that we want to apply to our cross section. Thus the adaptive Monte Carlo integration is performed in a very standard way, by multiplying the Born, virtual and real contributions by the suppression factor in eq. (1.36), in order to get a finite result. Nevertheless, as we always require a transverse momentum for the Z boson larger than a given cut, this suppression factor never vanishes in the region of our interest and can be divided out at the analysis stage, when computing the cross section with cuts.

1.5 Computation of the real contribution

In this section we are going to describe in detail how we did integrate the real contribution reported in eq. (1.31), after separating it into three regions, as shown in eqs. (1.32), (1.33) and (1.34).

1.5.1 Region (1)

As this region is associated with the collinear splitting of the incoming photon into a $d\bar{d}$ pair, we can handle this singularity recurring to the POWHEG-BOX [52] framework, considering the real process $d\gamma \rightarrow Zd g$ and the Born process $d\bar{d} \rightarrow Zg$. The Born contribution by itself is absent, as we only consider a quark-photon system in the initial state. Nevertheless it enters in the collinear subtraction, automatically performed by the POWHEG-BOX, in order to implement the factorization of collinear singularities, as well as in the collinear remnant, also computed within the POWHEG-BOX framework. Actually we do not expect that an IR linear renormalon could arise from region (1), as the phase space region dominated by soft and collinear gluons is highly suppressed here. In fact, the collinear and soft-collinear regions associated with an ISR gluon is suppressed by a $m_{T,g}^2$ factor (eq. (1.33)). In this limit, for small λ , $R^{(1)}$ behaves like

$$\frac{d\theta_g}{\theta_g} \frac{dE_g}{E_g} m_{T,g}^2 \simeq \frac{d\theta_g}{\theta_g} \frac{dE_g}{E_g} \theta_g^2 E_g^2 \simeq dE_g^2 d\theta_g^2, \quad (1.37)$$

where E_g is the gluon energy and θ_g is its angle with respect to the incoming (outgoing) quark direction. As the gluon mass λ acts as a natural cutoff on the integrations over E_g and θ_g , we can safely conclude that no linear term in λ can arise from eq. (1.37).

1.6 The $T(\lambda)$ function

Here we are going to expose in detail all the steps for the complete evaluation of the $T(\lambda)$ function present in the integrand of eq. (1.16), also considering the case for $\lambda = 0$, which is crucial in order to get a point with negligible error.

- The $\lambda = 0$ term can be computed working within the POWHEG BOX framework, computing the contributions of regions (2) and (3) together. These are affected by initial and final state singularities, arising as the gluon gets soft or collinear to the initial or final state quark. The subtraction of the initial state singularity has been performed, for consistency, in the DIS scheme, and then one needs to take care of properly modifying the POWHEG BOX code in order to comply with this request. We chose the factorization scale, which is equal to the Q scale of the DIS subtraction scheme, equal to the mass of the Z boson. Furthermore we also took into account the virtual corrections for the process $d\gamma \rightarrow Zd$ process, directly computed for $\lambda = 0$ and working in dimensional regularization. The infrared divergences associated with soft and collinear gluons are automatically cancelled in the POWHEG BOX framework in a fully general way, and thus no further work is required.
- The contribution coming from the regions (2) and (3) for $\lambda \neq 0$ cannot be implemented within the POWHEG BOX framework, as this was not designed to handle singularities regulated by a mass. For this reason we performed the computation using a dedicated Fortran code, choosing a proper phase space parameterisation for the real term, that

could be suitable to handle each region with an adequate importance sampling. Furthermore, in order to manage the collinear subtraction, we made use of the relation (1.29) to implement a local cancellation of the associated soft divergence, rather than computing separately the virtual and real contributions of the collinear subtractions.

- For the region (1), either for $\lambda = 0$ or $\lambda \neq 0$ we performed the computation exploiting the POWHEG BOX framework. The singular region is the one associated with the final state quark getting collinear to the incoming photon. The underlying Born process to deal with this singularity is the one involving $d\bar{d} \rightarrow Zg$, with a gluon g with mass λ . The collinear singularity is treated working in the $\overline{\text{MS}}$ scheme, and the collinear remnant is automatically provided by the POWHEG BOX.

Chapter 2

Results

In this chapter we will show the results we obtained for the transverse momentum distribution of the Z boson, first applying cuts only over its transverse momentum and evaluating the $T(\lambda)$ function defined in eq. (1.18) for different values of the gluon mass λ . Then we will also perform a more exclusive analysis, also applying kinematic cuts over the rapidity of the Z . As our setup we have considered two colliding particles with a center-of-mass (CM) energy equal to 300 GeV. We also considered the positive rapidity incoming particle (labelled as (1)) with a parton density consisting only of down quarks, whilst the negative rapidity particle (labelled as (2)) with a parton density consisting only of photons, distributed as

$$f_d^{(1)}(x = x_{\oplus}) = f_{\gamma}^{(2)}(x = x_{\ominus}) = \frac{(1-x)^3}{x}. \quad (2.1)$$

This totally arbitrary choice is only dictated by simplicity and is adequate for our purposes. We computed the cross section for the production of a stable Z boson with mass $M_Z = 91.188$ GeV (only vectorially coupled). The couplings of both the Z and γ are equal to $g_{Z,\gamma}^2 = 4\pi$ and the down quark is taken to have an electric charge of $-1/3$.¹ The color factor has been taken into account for the Born diagrams (where it assumes the value 1), and for the real and virtual as well, for which it is equal to $C_F = 4/3$. In conclusion we have chosen the factorization scale $\mu_F = M_Z$, while the renormalization scale is completely irrelevant for $T(\lambda)$. Indeed, by looking at eq. (1.16), we observe that the α_s in the denominator in front of the integral is simplified by the α_s contained in $T(\lambda)$ and thus the resummed result does not depend on the renormalization scale.

2.1 Transverse momentum distribution of the Z boson

We first computed the full function $T(\lambda)$ for different values of the gluon mass λ , taking a Z boson with a transverse momentum larger than 20 GeV (see fig. 2.1 on the left) and 40 GeV (see fig. 2.1 on the right). In order to extract the slope around $\lambda = 0$, responsible for the

¹We stress that the actual values of the couplings are completely irrelevant for our purposes, and have the only scope to give a well-defined meaning to our conclusions.

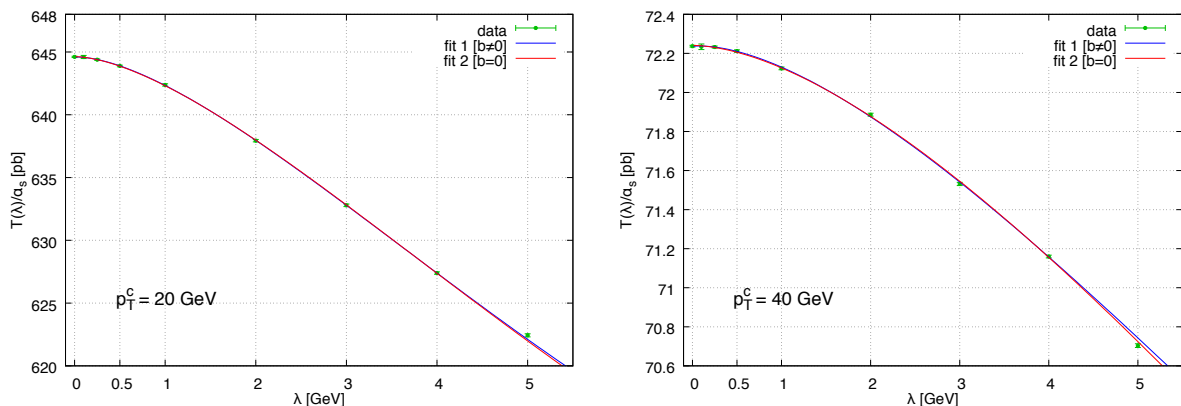


Figure 2.1: $T(\lambda)$ function (as defined in eq. (1.18)) as a function of the gluon mass λ for the cross section of a Z boson with a transverse momentum $p_{T,Z} > p_T^c$, with $p_T^c = 20$ GeV (left) and $p_T^c = 40$ GeV (right). The green points have been obtained by computing $T(\lambda)$ for different values of λ . The curves for fit 1 and 2 have been derived from the fit function in eq. (2.2), where for fit 1 we considered all the fit parameters, and in fit 2 we fixed the linear coefficient b to 0. We did not consider the point $\lambda = 5$ GeV in the fitting procedure.

presence of linear renormalons (see eq. (1.30) and also appendix A) we fitted $T(\lambda)$ with the function

$$f(\lambda) = a \left[1 + b \left(\frac{\lambda}{p_T^c} \right) + c \left(\frac{\lambda}{p_T^c} \right)^2 \ln^2 \left(\frac{\lambda}{p_T^c} \right) + d \left(\frac{\lambda}{p_T^c} \right)^2 \ln \left(\frac{\lambda}{p_T^c} \right) \right], \quad (2.2)$$

where the presence of single and double logarithmic terms is motivated by the findings for the Drell-Yan case [25, 56]. We did not take into account the point for $\lambda = 5$ GeV for our fitting procedure, in order to increase the reliability of the fit in the neighbourhood of $\lambda = 0$. The results of the fit are listed in table 2.1, where we reported the results obtained including the linear coefficient b as a fit parameter, and then fixing it to 0, in order to assess its actual impact on $T(\lambda)$. We can observe that the linear coefficient has a negligible impact on the fitting function, as its size is at least an order of magnitude smaller than the dominant quadratic coefficient, and then its value is consistent with zero. Thus we can safely conclude that we do not find any evidence of the presence of a IR linear renormalon affecting the transverse momentum distribution of the Z boson, and furthermore we found that the size of the corresponding coefficient is much smaller than the coefficients of the quadratic terms.

We also performed a more exclusive analysis, adding an additional cut over the rapidity of the Z boson y_Z , besides the one over the transverse momentum. The results are shown in fig. 2.2 and in table 2.2. Once again we do not find any numerical evidence of a linear sensitivity to λ , concluding that the doubly differential distribution in rapidity and transverse momentum is free from linear renormalons.

By looking at the coefficients in tables 2.1 and 2.2 we observe that, when considering $p_T^c = 40$ GeV instead of 20 GeV we face larger errors in the determination of the fit parameters c and d , observing that they look less important as the cuts are increased.

$p_T^c = 20 \text{ GeV}$		$p_T^c = 40 \text{ GeV}$	
fit 1	fit 2	fit 1	fit 2
$a = 644.60 \pm 0.02$	$a = 644.63 \pm 0.02$	$a = 72.237 \pm 0.005$	$a = 72.241 \pm 0.004$
$b = 0.009 \pm 0.004$	$b = 0$	$b = 0.024 \pm 0.017$	$b = 0$
$c = -0.063 \pm 0.008$	$c = -0.047 \pm 0.004$	$c = -0.11 \pm 0.06$	$c = -0.028 \pm 0.021$
$d = 0.341 \pm 0.005$	$d = 0.341 \pm 0.007$	$d = 0.50 \pm 0.08$	$d = 0.59 \pm 0.05$
$\chi^2/\text{ndf} = 0.12$	$\chi^2/\text{ndf} = 0.23$	$\chi^2/\text{ndf} = 1.13$	$\chi^2/\text{ndf} = 1.36$

Table 2.1: Results of the fit of the $T(\lambda)$ function, defined in eq. (1.18) and illustrated in fig. 2.1. The fit function is given in eq. (2.2). In the first fit, corresponding to the blue lines in the figures, b is unconstrained, while in the second fit, corresponding to the red lines, b has been set to 0. The last line corresponds to the associated reduced χ^2 .

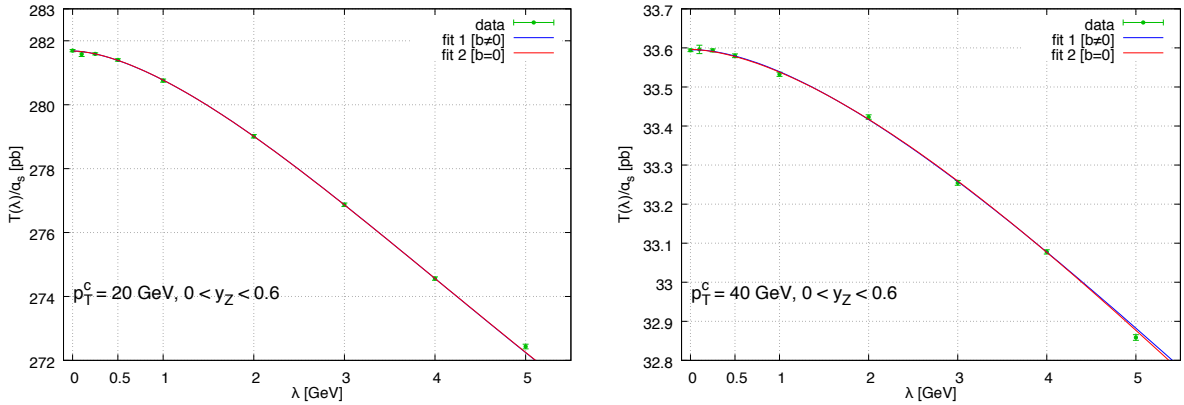


Figure 2.2: The same as in fig. 2.1, with the further cut over the rapidity of the Z : $0 < y_Z < y_c$, where $y_c = 0.6$.

$p_T^c = 20 \text{ GeV}$		$p_T^c = 40 \text{ GeV}$	
fit 1	fit 2	fit 1	fit 2
$a = 281.68 \pm 0.02$	$a = 281.68 \pm 0.01$	$a = 33.595 \pm 0.003$	$a = 33.596 \pm 0.002$
$b = -0.001 \pm 0.009$	$b = 0$	$b = 0.015 \pm 0.025$	$b = 0$
$c = -0.026 \pm 0.018$	$c = -0.028 \pm 0.006$	$c = -0.11 \pm 0.09$	$c = -0.06 \pm 0.03$
$d = 0.35 \pm 0.01$	$d = 0.35 \pm 0.01$	$d = 0.49 \pm 0.11$	$d = 0.54 \pm 0.06$
$\chi^2/\text{ndf} = 0.39$	$\chi^2/\text{ndf} = 0.32$	$\chi^2/\text{ndf} = 0.89$	$\chi^2/\text{ndf} = 0.77$

Table 2.2: Results of the fit of the $T(\lambda)$ function defined in eq. (1.18) illustrated in fig. 2.2. The fit function is given in eq. (2.2). The first fit corresponds to the blue lines, while in the second fit the linear coefficient has been set to 0 and corresponds to the red lines. The last line corresponds to the associated reduced χ^2 .

Chapter 3

Conclusions

The high precision reached by LHC has pushed the theoretical efforts towards an unprecedented accuracy, beyond next-to-leading order and, in some cases, even beyond next-to-next-to-leading order. With this level of precision, it is crucial to properly estimate contributions arising from non-perturbative regime, which manifest as power corrections, suppressed by the hard scale of the process and that can sometimes be comparable or even larger in size than the current theoretical uncertainties. Nevertheless, we are not yet able to formulate a general theory of even the most relevant non-perturbative corrections, unlike for other frameworks, where the existence of an Operator Product Expansion constitutes a safe guideline in order to classify and parameterise non-perturbative effects.

Renormalon effects have been estimated in the past recurring to an Abelian limit of QCD, in the so called large- b_0 approximation, that proved a way to explore the structure of non-perturbative corrections affecting collider processes. These models have been used to probe the presence of renormalons in Drell-Yan processes [25, 56] and have been also used recently in order to get some insights on issues regarding precision top mass measurements [40]. The presence of linear renormalon effects has also been studied using related methods, within the context of jet physics (see [24] and references therein).

In the first part of this thesis we have shown how the large- b_0 approximation is a useful method in order to understand whether linear renormalon effects can yield linear power corrections to the inclusive differential distribution for the production of a vector boson at LHC, probing the phase space region where the transverse momentum is safely in the perturbative region, and where resummation effects are safely negligible. This process is sufficiently complex, as it involves the presence of gluon radiation either from initial or final state, and develops single and double logarithmic singularities, which cancel out when combining real and virtual contributions with the factorization of initial state collinear singularities. Furthermore we have chosen a process that mimics the Z production in an Abelian model, but with the preservation of an azimuthally asymmetry in the soft radiation pattern, as in the full QCD case, which, on intuitive ground, may be associated with non-perturbative recoil effects, linearly affecting the Z transverse momentum. We found no numerical evidence of a linear renormalon, observing instead how the renormalon structure is well represented by quadratic terms associated with some logarithmic enhancements.

A numerical evidence gives a useful indication, but, by its own nature, cannot be considered as a solid proof for the absence of infrared renormalons. Nevertheless, as we found that the linear coefficient is way much smaller than the quadratic one, we can conjecture that these specific observables are free from linear renormalon effects. In the second part of this thesis we prove that in fact this is the case in an analytic fashion.

Currently it seems that, in all collider processes considered so far that involve massless flavours, no linear renormalon is present, from a large- b_0 computation, for observables that are fully inclusive with respect to production of colored particles. This assessment is no longer valid when considering massive quarks, as reported in ref [40].

Part II

Linear Power Corrections in Shape Variables in the three-jet region

Introduction

The study presented in the following chapters is based on a result which can be formulated as follows: an observable which is inclusive with respect to soft QCD radiation does not exhibit linear power corrections. Leaving a detailed explanation of this result in the next sections, we emphasise that it has important implications for the computation of shape variables in e^+e^- collisions. Indeed this result implies that no linear power corrections arise from the recoil of hard partons due to the emission of a soft parton. Furthermore, this conclusion also provides an analytic explanation on our findings described in part I, about the absence of IR linear renormalons in the transverse momentum distribution of a massive gauge boson, produced in association with a jet in hadronic collisions. We will elaborate more on this in section 4.1.2.

Shape variables in e^+e^- annihilation

The purpose of this part of the thesis is to investigate non-perturbative power-suppressed corrections affecting shape variable distributions in e^+e^- annihilation into hadrons in the three-jet region and beyond. This study is interesting for a twofold reason, as the three-jet production in e^+e^- collision is sensitive to the strong coupling constant α_s , and thus is a very relevant process for its determination. Furthermore, even though other methods look more promising for this purpose (see ref. [57]), studying three-jet production in e^+e^- collisions still remains relevant from a theoretical perspective. Indeed it constitutes a very valuable environment in order to explore the interplay between perturbative and non-perturbative effects in jet-production processes in the simplest possible setting and, hopefully, understand how to extend such studies to the more complex case of hadronic collisions.

Leading power-suppressed corrections to shape variables are usually linear, i.e. they are of the order of Λ_{QCD}/Q , where Λ_{QCD} is a hadronic scale and Q is the hard scale of the process under consideration. For typical e^+e^- collider energies, these corrections can reach even the percent level, and thus it is crucial to properly include them in the analysis of shape variables distributions. In the recent past power corrections have been estimated either using Monte Carlo event generators [58–60] or recurring to analytic models [61–68]. Nevertheless, even if more practical, the Monte Carlo approach has been widely criticized, as it is very difficult to justify it theoretically in a convincing way. Analytic models are conceptually more appealing, since they make contact with certain features that the full theory should have, such as infrared renormalons. Unfortunately, analytic estimates of non-perturbative corrections are usually performed in the two-jet region [51, 69–83] and then extrapolated to the three-jet region. The

estimates of the strong coupling constant obtained from the application of these methods lead to values of α_s that differ of several standard deviations from the world average value, $\alpha_s(M_Z) = 0.1179(1)$ [57]. A possible explanation for this discrepancy can rely upon significant ambiguities in the extraction of the leading power corrections from the two- to the three-jet region [84].

In this work we will examine power corrections affecting shape variables in an Abelian limit of QCD, due to the emission of a soft massive gluon, in order to obtain a fully analytic expression for them in the three-jet region, also considering the $g^* \rightarrow q\bar{q}$ splitting and using the quark and anti-quark momenta to compute changes in the shape variable. The presence of analytical results is very helpful for obtaining solid phenomenological predictions in a very efficient way since they do not require a numerical extrapolations to small gluon masses, as done in part I. Moreover, we will show that the analytic computation allows us to uncover peculiar structures in our results, which can be interesting to examine in a field-theoretic framework.

We start by computing the linear renormalon contributions to the C -parameter, considering the process $\gamma^* \rightarrow q\bar{q}\gamma + (g^* \rightarrow q\bar{q})$.¹ Then we compute the linear power corrections to the C -parameter by integrating over the soft gluon energy. This direct calculation is quite complex, as it involves elliptic integrals, but the final result looks very simple, suggesting the existence of an alternative and simpler way to compute it. In this sense we will explain how to perform the computation in a more feasible way, in order to directly get a simple final result. We show that linear power corrections affecting the C -parameter can be cast in a factorised expression, where one factor depends on the properties of the shape variable and the kinematics of soft partons, and the second factor turns to be a universal constant that only depends on the radiation dynamics. The important point to subtle is that this factorisation property also applies to a large class of shape variables, besides the C -parameter, with the same constant term for all of them.

We formulate the conditions an observable must satisfy for this factorisation to happen, and demonstrate its power and generality by computing linear power corrections to the thrust distribution in the three-jet region, in addition to the C -parameter. These results can also be extended to the more general case where N jets are produced in e^+e^- annihilation. Although a study of C -parameter and thrust in the N -jet region for $N > 3$ has limited scope, they can still be useful for phenomenological analyses [58, 85, 86].

Our method can also be applied to the computation of shape variables in the two-jet region, and, doing so, we obtain the same result as in refs. [76, 77], and find that the universal constant factor that we identified within the context of the three-jet calculations is related to the so called “Milan Factor” of refs. [76, 77]. In the literature the constant “Milan factor” has often been presented as a correction term to be applied to shape variables calculations performed with massive gluons, but neglecting the gluon splitting into $q\bar{q}$ pairs and also the impact of the splitting on the observable itself. This way of describing it, though justified by historical reasons, looks slightly misleading, as the computation of power corrections to shape variables considering the emission or the exchange of a massive gluon leads to wrong

¹As in the case of the Z transverse momentum, we cannot address directly the $\gamma^* \rightarrow q\bar{q}g + (g^* \rightarrow q\bar{q})$, since the large n_f calculation becomes too complex if applied to processes with a hard gluon.

answers. Indeed the weakness of this approach is also due to the fact that the final results strictly depend upon ambiguities in the definition of shape variables when final state massive partons are present.² Nevertheless these ambiguities are not present if the universal factor is attached to corrections to shape variables caused by an emission of a massless soft parton in a particular kinematic, as we will see in the following.³

The remainder of this part is organized as follows. In chapter 4 we set up the notation we are going to use, focusing on the real emission contribution for two different configurations for the emitting dipole, namely the “final-final” and the “initial-final” ones. The main result of this chapter is that, for observables that are fully inclusive with respect to QCD radiation, no linear power corrections can arise.

In chapter 5 we study linear power corrections to the C -parameter in the three-jet region. In section 5.1 we begin to compute these corrections by a direct analytic integration, with a cut-off on the energy of the virtual gluon. This approach leads to the arising of elliptic integrals and it is highly non-trivial, but in principle it can be performed exploiting the formalism of elliptic polylogarithms [87–92]. It turns out, however, that the whole calculation can be performed without resorting to this technology, as we will explain in the remaining part of the chapter.

As we mentioned earlier, the computation of power-corrections affecting C -parameter in the three-jet region is quite demanding, but its result is so simple that it needs a detailed explanation, that can be found in section 5.2, where we show how linear power corrections naturally factorise into a process-dependent part and a universal factor, that can be easily computed.

In section 5.4 we formulate the general conditions that an observable must satisfy for this factorisation to happen, and in section 5.5 we show in detail how they are satisfied in the case of the C -parameter. In section 5.6 we discuss the differences between our approach and the one of refs. [76,77], where the Milan factor was originally introduced.

In chapter 6 we show that the factorisation property of power corrections valid for the C -parameter also applies for a broader class of observables and compute linear power corrections affecting the thrust distribution in the three-jet region.

Given the high relevance of this study for phenomenological purposes dealing with extraction of α_s , in chapter 7 we perform preliminary phenomenological studies of the power corrections in the three-jet region, first validating the analytic results against the ones obtained from a numerical computation. Then we conjecture how to generalise our results, which are only valid for a $q\bar{q}\gamma$ final state, to the realistic QCD scenario. In section 7.4 we present phenomenological predictions for the C -parameter and the thrust distributions in the three-jet region, comparing our results for the C -parameter with the ones in ref. [84].

Finally, in chapter 8 we give our conclusions.

² For a further analysis on this issue, see eq. (5.56) in ref. [24].

³We want to emphasize that the definition of the Milan factor for the two-jet and symmetric three-jet limit given in ref. [77] is fully consistent with ours, as our claims only deal with the factorisation in a generic three-jet configuration. In our treatment, the Milan factor rigorously arises in a computation performed within the large- n_f framework, where it is evident that a final state with a massive gluon cannot contribute to power corrections.

Chapter 4

Generalities on the method

In this chapter we will briefly introduce the notation and formalism we are going to use in order to study non-perturbative corrections affecting a shape variable in e^+e^- collisions, working in the large- n_f limit.

4.1 Linear power corrections from real emission

In this section we want to demonstrate that if one considers an observable that is fully inclusive with respect to soft QCD radiation, the real squared amplitude cannot contribute any $\mathcal{O}(\lambda)$ correction, in an Abelian theory involving a gluon with non-zero mass λ .

Furthermore, by considering a process only involving massless particles, the one loop contribution cannot provide power corrections. The main point is that the Passarino-Veltman reduction, in conjunction with the formula for the evaluation of scalar integrals, makes it obvious that the virtual corrections only admit an expansion in powers of λ^2 , with eventual logarithmic enhancements. Furthermore, we observe that the Passarino-Veltman reduction algorithm remains valid when considering more complex processes, only involving more complicated scalar integrals.

We will consider two different cases for the QCD emitting dipole: the “final-final” configuration, with both the partons in the final state, and the “initial-final” configuration. The former is indeed suitable in order to investigate the presence of linear power corrections affecting shape variables in e^+e^- annihilation. The latter instead suits for analytically explaining the result obtained for the transverse momentum distribution of the Z -boson produced in hadronic collisions.

4.1.1 Final-final dipole

Let us consider the contribution due to the real radiation. Specifically, we consider a generic process $I \rightarrow F$, being I and F short-hand notations for the collection of initial and final state particles, respectively, and the real correction $I \rightarrow F + g$, where g is a gluon with mass λ . For sake of simplicity we imagine that there are two and only two massless QCD charged partons. We do not consider cases when one of these partons is a gluon, and, on the other

hand, we allow for an arbitrary number of (massless or massive) QCD-neutral particles. In order to keep the contact with the kinematic configuration we will further describe in the following sections, we will take both the QCD partons in the final state (“final-final” dipole). For definiteness, the momenta of the partons forming the dipole will be denoted by p_1 and p_2 .

Let us consider a process where colorless particles with a total momentum p_I produce final state particles with momenta $p_1, p_2, p_3, \dots, p_N$

$$p_I \rightarrow p_1 + p_2 + p_3 + \dots + p_N, \quad (4.1)$$

where the particles $p_{1,2}$ have QCD charges and all other particles are colorless. For our treatment we consider cases where the QCD dipole is formed by massless particles, $p_1^2 = p_2^2 = 0$, and, for ease of notation, in this section we will also assume that the colorless particles satisfy the mass-shell condition $p_{3,\dots,N}^2 = 0$. In order to investigate the presence of linear power corrections we consider the emission of a massive gluon with momentum k and mass λ . From momentum conservation we have

$$p_I \rightarrow p_1 + p_2 + p_3 + \dots + p_N + k. \quad (4.2)$$

With this situation, as there is only one gluon involved, we are insensitive to the non-Abelian behaviour of the QCD, and the Ward identities are trivially satisfied.

In order to study soft-gluon emission it may be useful to introduce mappings of hard final state particles

$$p_i \rightarrow \tilde{p}_i = \tilde{p}_i(\{p_j\}, k), \quad i = 1, \dots, N, \quad (4.3)$$

that preserve both the on-shell conditions $\tilde{p}_i^2 = p_i^2$, $i = 1, \dots, N$ and the momentum conservation constraint. In the following we will refer to the \tilde{p}_i momenta as the *underlying Born momenta*, denoting with $\{\tilde{p}\}$ the set $\{\tilde{p}_1, \tilde{p}_2, \tilde{p}_3\}$. We will also use the notation $\{p\}$ to denote $\{p_1, p_2, p_3\}$. From momentum conservation we get

$$p_I = \sum_{i=1}^N \tilde{p}_i = \sum_{i=1}^N p_i + k. \quad (4.4)$$

As we are interested only in linear power corrections, we only require these mappings to first order in the gluon momentum k . Although for our purposes we need to determine a specific mapping, we will take the discussion as general as possible, also to show the flexibility of our conclusions. We first require that the mappings behave as

$$p_i^\mu = \tilde{p}_i^\mu + R_{i,\nu}^\mu(\{\tilde{p}\})k^\nu + \mathcal{O}(k_0^2), \quad (4.5)$$

for small gluon momentum, where the tensors $R_{i,\nu}^\mu$ depend on the momenta \tilde{p}_i and the metric tensor. Momentum conservation in eq. (4.4) implies

$$\sum \tilde{p}_i = \sum p_i^\mu + k^\mu \rightarrow \sum R_{i,\nu}^\mu k^\nu = -k^\mu. \quad (4.6)$$

We also require our mapping to satisfy the on-shell condition through the relation

$$p_i^2 = (1 + \lambda_i)\tilde{p}_i^2, \quad (4.7)$$

where we have introduced the analytic functions λ_i , depending upon the momenta. Using eq. (4.5) we get

$$2\tilde{p}_{i,\mu}K_i^{\mu\nu}k_\nu = \lambda_i\tilde{p}_i^2, \quad (4.8)$$

with $\lambda_i \sim \mathcal{O}(k)$.

At this point we are able to express the phase-space element for the final state particles in terms of the underlying Born momenta \tilde{p}_i . We write

$$\begin{aligned} \text{dLips}(p_I; p_1, \dots, p_N, k) &= \left[\prod_{i=1}^N \frac{d^4 p_i}{(2\pi)^3} \delta_+(p_i^2) \right] [dk] (2\pi)^4 \delta^{(4)} \left(p_I - \sum_{i=1}^N p_i - k \right) \\ &= \left[\prod_{i=1}^N \frac{d^4 \tilde{p}_i}{(2\pi)^3} \delta_+(\tilde{p}_i^2 (1 + \lambda_i)) \right] [dk] \frac{\partial(p_1, \dots, p_N)}{\partial(\tilde{p}_1, \dots, \tilde{p}_N)} (2\pi)^4 \delta^{(4)} \left(p_I - \sum_{i=1}^N \tilde{p}_i \right), \end{aligned} \quad (4.9)$$

with $[dk] = d^4 k / (2\pi)^3 \delta_+(k^2 - \lambda^2)$. Since we are interested to extract only the $\mathcal{O}(k)$ terms from this expression, we recur to a relation between the determinant and the trace of a matrix connected with the identity matrix, and to the fact that $\lambda_i \sim k$, obtaining

$$\text{dLips}(p_I; p_1, \dots, p_N, k) \approx \text{dLips}(p_I; \tilde{p}_1, \dots, \tilde{p}_N) \frac{d^4 k}{(2\pi)^3} \delta_+(k^2 - \lambda^2) J \quad (4.10)$$

where

$$J = 1 - \sum_{i=1}^N \lambda_i + \sum_{i=1}^N \frac{\partial R_i^{\mu\nu}}{\partial \tilde{p}_i^\mu} k_\nu. \quad (4.11)$$

To proceed further we need to specify the mapping explicitly, and in order to do that, we will focus on the so-called dipole-local mappings, i.e. those mappings such that the recoil due to the emission is absorbed only by the particles forming the emitting dipole, with the other particles left unchanged. By assumption, in our case the dipole is formed by the final state particles with momenta $p_{1,2}$ and thus we impose $R_i = 0$ for $i = 3, \dots, N$. Furthermore, we want to construct the tensors $R_{1,2}^{\mu\nu}$ using only $\tilde{p}_{1,2}$ and the metric tensor. Under these assumptions, the most general form for the tensors $R_{1,2}^{\mu\nu}$ reads

$$R_i^{\mu\nu} = (a_i \tilde{p}_1^\mu \tilde{p}_1^\nu + b_i \tilde{p}_2^\mu \tilde{p}_2^\nu + c_i \tilde{p}_1^\mu \tilde{p}_2^\nu + d_i \tilde{p}_2^\mu \tilde{p}_1^\nu) + e_i g^{\mu\nu}. \quad (4.12)$$

Using eq. (4.6), together with the fact that the coefficients in eq. (4.12) do not depend on k , we can impose the following constraints equations

$$a_1 + a_2 = 0, \quad b_1 + b_2 = 0, \quad c_1 + c_2 = 0, \quad d_1 + d_2 = 0, \quad e_1 + e_2 = -1. \quad (4.13)$$

Exploiting the fact that it must be $\tilde{p}_{i,\mu} R_i^{\mu\nu} k_\nu \propto \tilde{p}_i^2$, we yield the following set of equations for the coefficients in eq. (4.12)

$$\begin{aligned} a_1 \tilde{p}_1^2 + d_1 (\tilde{p}_1 \tilde{p}_2) + e_1 &\propto \tilde{p}_1^2, & b_1 (\tilde{p}_1 \tilde{p}_2) + c_1 \tilde{p}_1^2 &\propto \tilde{p}_1^2, \\ b_2 \tilde{p}_2^2 + c_2 (\tilde{p}_1 \tilde{p}_2) + e_2 &\propto \tilde{p}_2^2, & a_2 (\tilde{p}_1 \tilde{p}_2) + d_2 \tilde{p}_2^2 &\propto \tilde{p}_2^2. \end{aligned} \quad (4.14)$$

We can see that eq. (4.13), in conjunction with eq. (4.14) provide a set of nine equations for a total of ten unknowns a_i, b_i, c_i, d_i, e_i . Thus we can express our solution in terms of one of them, say e_i , obtaining

$$a_{1,2} = b_{1,2} = 0, \quad c_2 = -c_1 = \frac{1 + e_1}{(\tilde{p}_1 \tilde{p}_2)}, \quad d_2 = -d_1 = \frac{e_1}{(\tilde{p}_1 \tilde{p}_2)}, \quad e_2 = -1 - e_1. \quad (4.15)$$

Renaming $e_1 = -\alpha$, we finally get the quite simple expressions

$$\begin{aligned} R_1^{\mu\nu} &= -\alpha g^{\mu\nu} - \frac{(1 - \alpha) \tilde{p}_1^\mu \tilde{p}_2^\nu - \alpha \tilde{p}_2^\mu \tilde{p}_1^\nu}{(\tilde{p}_1 \tilde{p}_2)}, \\ R_2^{\mu\nu} &= -(1 - \alpha) g^{\mu\nu} + \frac{(1 - \alpha) \tilde{p}_1^\mu \tilde{p}_2^\nu - \alpha \tilde{p}_2^\mu \tilde{p}_1^\nu}{(\tilde{p}_1 \tilde{p}_2)}. \end{aligned} \quad (4.16)$$

Now it is straightforward to implement the phase space transformation, in such way

$$\begin{aligned} \lambda_1 &= -2(1 - \alpha) \frac{(\tilde{p}_2 k)}{(\tilde{p}_1 \tilde{p}_2)}, \quad \lambda_2 = -2\alpha \frac{(\tilde{p}_1 k)}{(\tilde{p}_1 \tilde{p}_2)}, \\ \frac{\partial K_1^{\mu\nu}}{\partial \tilde{p}_1^\mu} &= -(3 - 4\alpha) \frac{\tilde{p}_2^\nu}{(\tilde{p}_1 \tilde{p}_2)}, \quad \frac{\partial K_2^{\mu\nu}}{\partial \tilde{p}_2^\mu} = (1 - 4\alpha) \frac{\tilde{p}_1^\nu}{(\tilde{p}_1 \tilde{p}_2)}. \end{aligned} \quad (4.17)$$

Thanks to these equations, we can easily rewrite the Jacobian of the transformation J in eq. (4.11) in the more compact form

$$J = 1 + (1 - 2\alpha) \frac{(\tilde{p}_1 k - \tilde{p}_2 k)}{(\tilde{p}_1 \tilde{p}_2)}. \quad (4.18)$$

For sake of generality, in the rest of this section we will keep α to be fully arbitrary. Furthermore we observe that, writing $q = \tilde{p}_1 + \tilde{p}_2$, and using momentum conservation $p_1 + p_2 = q - k$, we obtain an upper bound on the possible values of the gluon momentum k , from the condition $(q - k)^2 > 0$. We also want to emphasize that the mappings defined in eq. (4.16) automatically satisfy nice infrared conditions. The soft limit is trivially satisfied, as for $k \rightarrow 0$ one gets $p_i = \tilde{p}_i$ by construction. For what concerns the collinear limit, if we consider k collinear to p_1 for instance, we need to replace $k = \eta p_1$, finding $p_1 = (1 - \eta) \tilde{p}_1$ and $p_2 = \tilde{p}_2$, that is precisely what we expect from a collinear-safe mapping. An analogous result holds if we consider $k \rightarrow \eta p_2$ case.¹

¹Although for our purposes it is fully sufficient to consider mappings of the form eq. (4.16), we observe that in principle we could have also employed mappings with a weaker smoothness condition. For instance, let us assume that the tensors $R_{1,2}^{\mu\nu}$ could be written as

$$R_i^{\mu\nu} = R_{i,\parallel}^{\mu\nu} + R_{i,\perp}^{\mu\nu},$$

with $R_{i,\parallel}$ and $R_{i,\perp}$ satisfying the conditions

$$R_{i,\parallel}^{\mu\nu} \left(g_{\mu\alpha} - \frac{\tilde{p}_{1,\mu} \tilde{p}_{2,\alpha} + \tilde{p}_{1,\alpha} \tilde{p}_{2,\mu}}{(\tilde{p}_1 \tilde{p}_2)} \right) = 0, \quad R_{i,\perp}^{\mu\nu} \tilde{p}_{1,\nu} = R_{i,\perp}^{\mu\nu} \tilde{p}_{2,\nu} = 0.$$

Even though the transverse term $R_{i,\perp}^{\mu\nu}$ could depend in a non trivial way on $(\tilde{p}_{1,2} k)$, one can easily observe that this term leads to an odd linear dependence upon the transverse momentum component of k , that cancels out after azimuthal integration. By virtue of this it is possible to show that all the arguments exposed in this section also apply to this more general case, with no significant modifications.

At this point, after studying the phase-space transformation, we can move on to discuss the matrix element and its integration as well. As we only have one QCD dipole, the squared amplitude for the real emission, summed over quarks and gluon polarizations, reads as

$$|\mathcal{M}|^2(\{p_i\}, k) = \frac{A(\{p_i\}, k)}{(p_1 + k)^2(p_2 + k)^2} + \frac{B_1(\{p_i\}, k)}{[(p_1 + k)^2]^2} + \frac{B_2(\{p_i\}, k)}{[(p_2 + k)^2]^2}. \quad (4.19)$$

Where the functions $A, B_{1,2}$ are polynomials in k , and describe the interference term, the emission from the first leg, and the emission from the second leg, respectively. The limiting behaviour of A follows from the usual soft approximation, from which we obtain

$$A(\{p_i\}, k) = a_0(\{p_i\}) + a_1^\mu(\{p_i\})k_\mu + \mathcal{O}(k^2), \quad (4.20)$$

where $a_1^\mu(\{p_i\})$ is a four-vector depending, in principle, on all vectors p_i . For what concerns the $B_{1,2}$ diagrams, as they can arise only from squares of diagrams involving a gluon that is emitted and absorbed by the same fermion line, they can be expressed as (taking B_1 as example)

$$\frac{B_1(\{p_i\}, k)}{[(p_1 + k)^2]^2} \propto -g^{\mu\nu} \frac{1}{[(p_1 + k)^2]^2} \text{Tr} \left[(\not{p}_1 + \not{p}_2) \gamma_\mu \not{p}_1 \gamma_\nu (\not{p}_1 + \not{k}) \dots \right], \quad (4.21)$$

where we have used $\sum \epsilon_\mu \epsilon_\nu^* = -g_{\mu\nu}$ to sum over gluon polarizations.² After some algebra from eq. (4.21) we obtain (and analogously for B_2)

$$B_1(\{p_i\}, k) = \lambda^2 [b_{10}(\{p_i\}) + b_{11}^\mu(\{p_i\})k_\mu] - (p_1 + k)^2 b_{11}^\mu(\{p_i\})k_\mu. \quad (4.22)$$

The terms proportional to $(p_1 + k)^2$ in eq. (4.22) remove the double pole in eq. (4.19). Finally, from a power counting argument, we can show that the contributions of the form $\lambda^2/[(p_i + k)^2]^2$ can be neglected, as, because of the λ^2 suppression, the small- k region in these integrals only provide $\mathcal{O}(\lambda^2)$ terms.

At this point we need to integrate the squared amplitude, expanded at first order in the gluon momentum k , over the gluon phase space, after performing the transformation $p_i \rightarrow \tilde{p}_i$. Eq. (4.19) is used to remap the matrix element squared, discarding the double poles for the reasons explained before. By virtue of the mapping transformation we can rewrite the propagators as

$$(p_{1,2} + k)^2 = 2(\tilde{p}_i k) \pm (1 - 2\alpha)\lambda^2 \mp 2(1 - 2\alpha) \frac{(\tilde{p}_1 k)(\tilde{p}_2 k)}{(\tilde{p}_1 \tilde{p}_2)}, \quad (4.23)$$

and, expanding them to next-to-leading order in $k \sim \lambda$, we get

$$\frac{1}{(p_{1,2} + k)^2} = \frac{1}{(2\tilde{p}_i k)} \left(1 \mp (1 - 2\alpha) \frac{\lambda^2}{2(\tilde{p}_i k)} \pm (1 - 2\alpha) \frac{(\tilde{p}_1 k)(\tilde{p}_2 k)}{(\tilde{p}_i k)(\tilde{p}_1 \tilde{p}_2)} \right). \quad (4.24)$$

Now we consider the theoretical predictions for an IR-safe observable that is inclusive with respect to QCD radiation. By virtue of this, it follows that

$$\mathcal{O}(p_1, p_2, p_3, \dots, p_N; k) = \mathcal{O}(\tilde{p}_1, \tilde{p}_2, \dots, \tilde{p}_N). \quad (4.25)$$

²In presence of massive gluons, the sum over polarizations leads to a term $k_\mu k_\nu / k^2$. Anyway this term can be dropped by virtue of the Ward identity, which still stands in the (Abelian) problem.

For this species of observable one can write its expectation value as

$$\begin{aligned}
 & \int d\sigma \mathcal{O}(p_1, \dots, p_N; k) \\
 &= \int d\text{Lips}(\tilde{p}_1, \dots, \tilde{p}_N) \mathcal{O}(\tilde{p}_1, \dots, \tilde{p}_N) g_s^2 C_F |\mathcal{M}_o(\{\tilde{p}_i\})|^2 \int \frac{d^4 k}{(2\pi)^3} \delta_+(k^2 - \lambda^2) \theta[(q - k)^2] \\
 & \times \frac{2(\tilde{p}_1 \tilde{p}_2)}{(\tilde{p}_1 k)(\tilde{p}_2 k)} \left[1 + v^\mu k_\mu - (1 - 2\alpha) \left(\frac{\lambda^2}{2(\tilde{p}_1 k)} - \frac{\lambda^2}{2(\tilde{p}_2 k)} \right) \right], \tag{4.26}
 \end{aligned}$$

where the vector v^μ is a function of the momenta \tilde{p}_i , whose exact form is completely irrelevant for our purposes. We also note that an upper bound on the k integration follows from the presence of the constraint $\theta[(q - k)^2]$. In principle, as the expression in eq. (4.26) refers to an expansion performed around the soft region $k \sim \lambda$, we could have restricted the integration over k accordingly. Nevertheless, as our aim is to investigate the presence of $\mathcal{O}(\lambda)$ terms arising in the differential cross section, we can safely extend the integration path to the full phase space for k , since the regions where k is hard cannot contribute linear $\mathcal{O}(\lambda)$ terms. In appendix B we give a discussion on the integrals appearing in eq. (4.26), also showing that they can be written as a power series in λ^2 .

The main conclusion of this section is that arbitrary differential cross sections that are *inclusive* with respect to QCD radiation are free from linear power corrections, related to IR linear renormalons. On the other hand, linear sensitivity on λ can arise when one considers observables that are sensitive to gluon momenta.

4.1.2 Initial-final dipole

At this point we are able to generalize the arguments exposed in section 4.1.1, considering a configuration where one of the radiating partons is in the initial state, and the other one is in the final state. As we said previously, this scenario is relevant in order to better describe the production of a vector boson with a non-vanishing transverse momentum, in hadronic collisions. Thus, keeping the same notation as in section 4.1.1 for the emitting QCD dipole momenta, we consider at the Born level

$$p_1 + p_3 \rightarrow p_2 + p_F \tag{4.27}$$

where p_F stands for the momenta of the colorless particles. Since we are not able to perform a large- n_f computation for a process involving a gluon at the Born level, we use the same strategy as in part I, considering a quark-photon collision

$$q(p_1) + \gamma(p_3) \rightarrow q(p_2) + X(p_F), \tag{4.28}$$

where X stands for a generic colorless system.

At this point we need to construct a local dipole mapping, involving the partons p_1 and p_2 , and that could be used to probe linear power corrections in this process. At variance with the case described in section 4.1.1, when constructing the mapping for the initial-state parton we impose that the direction of its momentum stays unchanged. Then, writing the p_1 transformation as

$$p_1^\mu = \tilde{p}_1^\mu + (\kappa_1 k) \tilde{p}_1^\mu, \tag{4.29}$$

and using momentum conservation

$$p_1 - p_2 - k = \tilde{p}_1 - \tilde{p}_2, \quad (4.30)$$

we obtain the transformation law for p_2

$$p_2^\mu = \tilde{p}_2^\mu + (\kappa_1 k) \tilde{p}_1^\mu - k^\mu. \quad (4.31)$$

In this case also we require that the on-shell conditions are not affected by the mapping. This is obvious for eq. (4.29), that implies

$$p_1^2 = (1 + 2(\kappa_1 k) + \mathcal{O}(k^2)) \tilde{p}_1^2, \quad (4.32)$$

for a generic κ_1 . The equation for p_2^2 gives more information. Indeed we write

$$p_2^2 = \tilde{p}_2^2 + 2(\tilde{p}_1 \tilde{p}_2)(\kappa_1 k) - 2(\tilde{p}_2 k) + \mathcal{O}(k^2). \quad (4.33)$$

Hence, to satisfy the condition $p_2^2 \propto \tilde{p}_2^2$, we require

$$2[(\tilde{p}_1 \tilde{p}_2) \kappa_1^\mu - \tilde{p}_2^\mu] k_\mu = 0. \quad (4.34)$$

Since κ_1 does not depend on the gluon momentum k , it follows that

$$\kappa_1^\mu = \frac{\tilde{p}_2^\mu}{(\tilde{p}_1 \tilde{p}_2)}. \quad (4.35)$$

In conclusion, the final form of the mapping for an initial-final dipole is

$$p_1^\mu = \left(1 + \frac{(\tilde{p}_2 k)}{(\tilde{p}_1 \tilde{p}_2)}\right) \tilde{p}_1^\mu, \quad p_2^\mu = \tilde{p}_2^\mu + \frac{(\tilde{p}_2 k)}{(\tilde{p}_1 \tilde{p}_2)} \tilde{p}_1^\mu - k^\mu. \quad (4.36)$$

In this case as well it is easy to check that the mapping implemented in eq. (4.36) is well-behaved in the soft and collinear limits. In fact, in the soft limit $k \rightarrow 0$ one has, by construction, $p_i \rightarrow \tilde{p}_i$. For k getting collinear to p_1 for instance, we need to replace k with ηp_1 , obtaining $p_1 = (1 + \eta) \tilde{p}_1$, $p_2 = \tilde{p}_2$. Similarly, for $k = \eta p_2$, we get $p_1 = \tilde{p}_1$ and $p_2 = (1 - \eta) \tilde{p}_2$.

At this point we need to study the phase space transformation, proceeding exactly in the same way as done in section 4.1.1 for a final-final dipole, except that for the current case we only need to integrate over p_2 . The parameter λ_2 introduced in the previous section can be set to zero, since $p_2^2 = \tilde{p}_2^2$. Furthermore, exploiting the result for the Jacobian

$$\frac{\partial p_2}{\partial \tilde{p}_2} = 1 + \frac{(\tilde{p}_1 k)}{(\tilde{p}_1 \tilde{p}_2)}, \quad (4.37)$$

and the momentum conservation, we obtain

$$d\text{Lips}(p_1, p_3; p_2, p_F, k) = d\text{Lips}(\tilde{p}_1, \tilde{p}_3; \tilde{p}_2, \tilde{p}_F) \frac{d^4 k}{(2\pi)^3} \delta_+(k^2 - \lambda^2) \left(1 + \frac{(\tilde{p}_1 k)}{(\tilde{p}_1 \tilde{p}_2)}\right), \quad (4.38)$$

where $p_3 = \tilde{p}_3$, as we are considering a dipole local mapping. Furthermore, in eq. (4.38) the integral over the gluon momentum is assumed to be constrained by the requirement $(q - k)^2 < 0$, being $q = \tilde{p}_1 - \tilde{p}_2$.

As we are considering a parton in the initial state, in order to compute the cross section, we must convolute the partonic phase space and the squared matrix element with parton distribution functions. Thus we have

$$\begin{aligned} d\sigma_R &= \int dx_1 dx_3 f_q(x_1) f_\gamma(x_3) \\ &\times \text{dLips}(x_1 P_1, x_3 P_3; p_2, p_F, k) \frac{|\mathcal{M}(x_1 P_1, x_3 P_3, p_2, \dots, k)|^2}{2s_{\text{hadr}} x_1 x_3}, \end{aligned} \quad (4.39)$$

where $P_{1,3}$ are the momenta of the incoming hadrons, $s_{\text{hadr}} = 2(P_1 P_3)$ is the hadronic center-of-mass energy squared and $f_{q,\gamma}$ are the quark and photon parton distribution functions, respectively. We observe that eq. (4.36) can also be interpreted as a transformation rule for x_1 . Indeed, given that $p_1 = x_1 P_1$ and $\tilde{p}_1 = \tilde{x}_1 P_1$ we find, through linear order in k

$$x_1 = \tilde{x}_1 + \frac{(\tilde{p}_2 k)}{(\tilde{p}_2 P_1)} = \tilde{x}_1 + \xi(k, \tilde{p}_2). \quad (4.40)$$

Thanks to the phase space transformation we can easily rewrite eq. (4.39) as

$$\begin{aligned} d\sigma_R &= \int d\tilde{x}_1 dx_3 f_q(\tilde{x}_1 + \xi(k, \tilde{p}_2)) f_\gamma(x_3) \text{dLips}(\tilde{x}_1 P_1, x_3 P_3; \tilde{p}_2, p_F) \\ &\times \frac{d^4 k}{(2\pi)^4} \delta_+(k^2 - \lambda^2) \left(1 + \frac{(P_1 k)}{(P_1 \tilde{p}_2)}\right) \frac{|\mathcal{M}((\tilde{x}_1 + \xi) P_1, x_3 P_3; \tilde{p}_2, \dots, k)|^2}{2s_{\text{hadr}}(\tilde{x}_1 + \xi(k, \tilde{p}_2)) x_3}. \end{aligned} \quad (4.41)$$

Assuming x_1 is a regular point, we can expand the above equation in ξ ; since ξ also appears in the argument of the quark distribution function f_q , we write

$$f_q(\tilde{x}_1 + \xi) = f_q(\tilde{x}_1) + f'_q(\tilde{x}_1) \xi + \mathcal{O}(k^2). \quad (4.42)$$

Along the same lines of section 4.1.1 we can also expand the real squared amplitude up to next-to-eikonal term, taking care of the different forms of the two singular propagators, that now read

$$\begin{aligned} \frac{1}{(p_1 - k)^2} &= -\frac{1}{2(\tilde{p}_1 k)} \left(1 - \frac{(\tilde{p}_2 k)}{(\tilde{p}_1 \tilde{p}_2)} + \frac{\lambda^2}{2(p_1 k)}\right) + \mathcal{O}(\lambda), \\ \frac{1}{(p_2 + k)^2} &= \frac{1}{2(\tilde{p}_2 k)} \left(1 - \frac{(\tilde{p}_1 k)}{(\tilde{p}_1 \tilde{p}_2)} + \frac{\lambda^2}{2(\tilde{p}_2 k)}\right) + \mathcal{O}(\lambda). \end{aligned} \quad (4.43)$$

Combining these results we find that we need to consider integrals of the same species as the ones for the final-final case. All these integrals are discussed in appendix B where we show that they admit an expansion in powers of λ^2 . Thus we can conclude that also in this case there are no linear power corrections affecting kinematic distributions of final-state QCD-neutral particles.

This result provides a solid analytic proof of the numerical evidence found in part I of this thesis, concerning the transverse momentum distribution of a Z boson in hadronic collisions. Here in fact we proved that this observable cannot manifest leading non-perturbative corrections, even if rapidity cuts are applied, at least in our simplified ‘‘hadron-photon’’ setup.

4.2 Linear power corrections to shape variables

As we have already mentioned in part I of this thesis, the large- n_f prediction for a generic observable (in a process that does not involve a gluon at leading order) can be rigorously computed by considering the NLO QCD corrections to its expectation value, considering the exchange and emission of a gluon with mass λ , and looking for $\mathcal{O}(\lambda)$ corrections. For our purposes we are interested in linear power corrections affecting the cumulative distribution Σ for a generic shape variable V in e^+e^- collisions in the three-jet region, considering the process $\gamma^* \rightarrow q + \bar{q} + \gamma + (g^* \rightarrow q + \bar{q})$. We define the cumulant as

$$\Sigma(v) = \sum_F \int d\sigma_F \theta(V(\Phi_F) - v), \quad (4.44)$$

where F stands for a particular final state, Φ_F denotes the phase-space point of the state F and $V(\Phi_F)$ is the value of the shape variable V evaluated at the point Φ_F . In our treatment we always assume that the shape variable is defined such that it vanishes in the two-jet limit.³ We observe that in eq. (4.44) we have defined the cumulant as the cross section for producing a final state with the value of the shape variable V larger than a constant value v , while it is common in literature to define it as the cross section for $V < v$. Our choice is motivated by the fact that the total cross section is free from IR renormalons, and, doing so, we can avoid contributions from the two-jet region, as we are only interested in the three-jet region.

Following the notation introduced in section 1.3 and based on ref. [40], power corrections to eq. (4.44) are obtained by computing

$$\begin{aligned} \Sigma(v; \lambda) = & \int d\Phi_b \left[\frac{d\sigma^b(\Phi_b)}{d\Phi_b} + \frac{d\sigma^v(\Phi_b)}{d\Phi_b} \right] \theta(V(\Phi_b) - v) + \int d\Phi_{g^*} \frac{d\sigma^{g^*}(\Phi_{g^*}^\lambda)}{d\Phi_{g^*}^\lambda} \theta(V(\Phi_{g^*}^\lambda) - v) \\ & - \frac{\lambda^2}{b_{0,f}\alpha_s} \int d\Phi_{q\bar{q}} \frac{d\sigma^{q\bar{q}}(\Phi_{q\bar{q}})}{d\sigma_{q\bar{q}}} \delta(m_{q\bar{q}}^2 - \lambda^2) \left[\theta(V(\Phi_{q\bar{q}}) - v) - \theta(V(\Phi_{g^*}^\lambda) - v) \right], \end{aligned} \quad (4.45)$$

where Φ_b is the Born phase space (i.e. the $q\bar{q}\gamma$ phase space for our case), and σ^b is the corresponding cross section. σ^v describes the correction to the cross section due to the exchange of a virtual massive gluon with mass λ ; $\Phi_{g^*}^\lambda$ stands for the phase space for the emission of such a gluon, with σ^{g^*} the corresponding cross section. Finally, $\Phi_{q\bar{q}}$ is the phase space element that contains a $q\bar{q}$ pair with invariant mass $m_{q\bar{q}}$, and $\sigma^{q\bar{q}}$ the corresponding cross section. In eq. (4.45) we have also defined the QCD beta function in the large- n_f limit

$$b_{0,f} = -\frac{n_f T_R}{3\pi}. \quad (4.46)$$

We will label by p_1, p_2, p_3 the momenta of the primary quarks and of the photon, respectively, and by l, \bar{l} the momenta of the $q\bar{q}$ pair arising from the splitting of the gluon g^* , such that $l + \bar{l} = k$, being k the gluon momentum.

³ For the C -parameter this feature follows from its definition. For the thrust T we need to consider $\bar{T} = 1 - T$ in order to ensure it.

Introducing the more compact notation for the invariant phase space element

$$[dp] = \frac{d^3p}{2p^0(2\pi)^3}, \quad (4.47)$$

we can define the phase space elements in eq. (4.45) as follows

$$d\Phi_b = [dp_1][dp_2][dp_3](2\pi)^4\delta^{(4)}(p_1 + p_2 + p_3 - q), \quad (4.48)$$

$$d\Phi_{g^*}^\lambda = [dp_1][dp_2][dp_3][dk](2\pi)^4\delta^{(4)}(p_1 + p_2 + p_3 + k - q), \quad (4.49)$$

$$d\Phi_{q\bar{q}} = [dp_1][dp_2][dp_3][dl][d\bar{l}](2\pi)^4\delta^{(4)}(p_1 + p_2 + p_3 + l + \bar{l} - q), \quad (4.50)$$

where q is the total momentum of the e^+e^- pair, and all the momenta are light-like except for k , for which we have $k^2 = \lambda^2$. The normalisation factor in the third term on the right hand side of eq. (4.45) is such that

$$-\frac{\lambda^2}{b_{0,f}\alpha_s} \int [dl][d\bar{l}] \frac{d\sigma^{q\bar{q}}(\Phi_{q\bar{q}})}{d\Phi_{q\bar{q}}} (2\pi)^4\delta^{(4)}(l + \bar{l} - k) = 2\pi \frac{d\sigma^{g^*}(\Phi_{g^*}^\lambda)}{d\Phi_{g^*}}. \quad (4.51)$$

We know that linear terms in λ arising from eq. (4.45) are associated with infrared renormalons and thus lead to linear power corrections $\mathcal{O}(\Lambda_{\text{QCD}}/Q)$. Furthermore, looking at eq. (4.51) we observe that the contribution proportional to $\theta(V(\Phi_{g^*}^\lambda) - v)$ cancels in eq. (4.45) among the second and third terms. Thus we can assume that linear contributions in λ can only be generated by the terms proportional to $\theta(V(\Phi_{q\bar{q}}^\lambda) - v)$, and, as we have seen in section 4.1, for a certain class of observables that are inclusive with respect to soft QCD radiation, these power corrections can be extracted by studying the emission of a soft $q\bar{q}$ pair.

In section 4.1 we have shown in details how to construct a suitable mapping from the full phase space to the underlying Born phase space, also showing that it is possible to realize different mappings, all ensuring the condition in eq. (4.5), as well as soft and collinear-safety. We stress that we choose to work with this class of mappings because they significantly simplify the investigation of linear power corrections.

In order to extract linear power corrections in λ , we introduce an operator \mathcal{T}_λ , that extracts the $\mathcal{O}(\lambda)$ contributions from the expression it acts upon. Then by defining

$$|M(\{p\}, l, \bar{l})|^2 \equiv -\frac{\lambda^2}{2\pi b_{0,f}\alpha_s} \frac{d\sigma^{q\bar{q}}(\Phi_{q\bar{q}})}{d\Phi_{q\bar{q}}}, \quad (4.52)$$

we get

$$\mathcal{T}_\lambda[\Sigma(v; \lambda)] = \mathcal{T}_\lambda \left[\int d\Phi_{q\bar{q}} 2\pi\delta(m_{q\bar{q}}^2 - \lambda^2) |M(\{p\}, l, \bar{l})|^2 \theta(V(\{p\}, l, \bar{l}) - v) \right]. \quad (4.53)$$

In the soft limit we can expand the θ function around $V(\{p\}, l, \bar{l}) = V(\{\tilde{p}\})$ (being $\{\tilde{p}\}$ the underlying Born momenta), obtaining

$$\mathcal{T}_\lambda[\Sigma(v; \lambda)] = \mathcal{T}_\lambda \left[\int d\Phi_{q\bar{q}} 2\pi\delta(m_{q\bar{q}}^2 - \lambda^2) |M(\{p\}, l, \bar{l})|^2 \theta(V(\{\tilde{p}\}) - v) \right]$$

$$+ \left[\int d\Phi_{q\bar{q}} 2\pi \delta(m_{q\bar{q}}^2 - \lambda^2) |M(\{p\}, l, \bar{l})|^2 \delta(V(\{\tilde{p}\}) - v) [V(\{p\}, l, \bar{l}) - V(\{\tilde{p}\})] \right]. \quad (4.54)$$

In section 4.1 we also demonstrated that if the mapping in eq. (4.3) satisfies the condition in eq. (4.5), no $\mathcal{O}(\lambda)$ terms can arise from an inclusive integration performed at fixed underlying Born momenta. This implies that the first term in eq. (4.54) cannot contribute a linear term in λ , and thus the \mathcal{T}_λ operator projects this term to zero. As the second term in the right-hand side of eq. (4.54) does not involve an inclusive integration over the radiation phase space, it can, in principle, provide leading terms in λ . Furthermore we can observe that this term also contains a factor $V(\{p\}, l, \bar{l}) - V(\{\tilde{p}\})$, that vanishes in the collinear and soft limit as long as V is IR-safe. By virtue of this behaviour, one can take into account the infrared-singular part of $|M|^2$ in order to probe the presence of linear terms in λ . Thus we are allowed to consider the leading soft approximation, replacing

$$|M(\{p\}, l, \bar{l})|^2 \rightarrow \mathcal{N} \frac{d\sigma^b(\tilde{\Phi}_b)}{d\tilde{\Phi}_b} \frac{J^\mu J^\nu}{\lambda^2} \text{Tr} [l\gamma^\mu \bar{l}\gamma^\nu], \quad (4.55)$$

where we have introduced the underlying Born phase space $d\tilde{\Phi}_b$

$$d\tilde{\Phi}_b = [d\tilde{p}_1][d\tilde{p}_2][d\tilde{p}_3](2\pi)^4 \delta^{(4)}(\tilde{p}_1 + \tilde{p}_2 + \tilde{p}_3 - q), \quad (4.56)$$

and J^μ is the eikonal current for the emission of a soft gluon with momentum k

$$J^\mu = \frac{\tilde{p}_1^\mu}{(\tilde{p}_1 k)} - \frac{\tilde{p}_2^\mu}{(\tilde{p}_2 k)}, \quad (4.57)$$

and the trace arises from the inclusion of the gluon splitting into a quark-antiquark pair. The normalisation factor \mathcal{N} in eq. (4.55) reads as

$$\mathcal{N} = \left[-\frac{1}{2b_{0,f}\alpha_s} \right] \times g_s^2 C_F \times g_s^2 T_R n_f = 24\pi^2 \alpha_s C_F. \quad (4.58)$$

At this point we can factorize the phase-space in the soft limit, obtaining

$$\begin{aligned} \mathcal{T}_\lambda[\Sigma(v; \lambda)] &= \int d\tilde{\Phi}_b \frac{d\sigma^b(\tilde{\Phi}_b)}{d\tilde{\Phi}_b} \delta(V(\{\tilde{p}\}) - v) \times \mathcal{T}_\lambda \left[\mathcal{N} \int [dk] \frac{J^\mu J^\nu}{\lambda^2} \theta\left(\omega_{\max} - \frac{kq}{\sqrt{q^2}}\right) \right. \\ &\quad \left. \times \int [dl][d\bar{l}] (2\pi)^4 \delta^{(4)}(k - l - \bar{l}) \text{Tr}[l\gamma^\mu \bar{l}\gamma^\nu] [V(\{p\}, l, \bar{l}) - V(\{\tilde{p}\})] \right]. \end{aligned} \quad (4.59)$$

In eq. (4.59) we have implicitly defined a cut-off ω_{\max} on the energy of the intermediate gluon, in the rest frame of q , in order to regularise the UV divergences of the eikonal integral, and make eq. (4.59) finite. Linear power corrections will not depend on ω_{\max} . In order to further simplify eq. (4.59), we observe that it is possible to separately study the change of the shape variable due to the emission of two soft partons and to recoil effects, as follows

$$V(\{p\}, l, \bar{l}) - V(\{\tilde{p}\}) = [V(\{\tilde{p}\}, l, \bar{l}) - V(\{\tilde{p}\})] + [V(\{p\}) - V(\{\tilde{p}\})] + \mathcal{O}(k_0^2). \quad (4.60)$$

In the next sections we will elaborate more in details on this point; for this moment we just observe that both the C -parameter and the Thrust satisfy this condition. If the separation as in eq. (4.60) is allowed, one can make use of eq. (4.5) to expand the second term on the r.h.s. in k . In section 4.1 we demonstrated how linear power corrections cannot arise from an integration performed at fixed underlying Born kinematics, even if we multiply the cross section by an expression that is linear in λ . Thus, inserting eq. (4.60) into eq. (4.59), the second term cannot lead to any linear power correction, and eq. (4.59) can be further simplified as follows

$$V(\{p\}, l, \bar{l}) - V(\{\tilde{p}\}) \rightarrow V(\{\tilde{p}\}, l, \bar{l}) - V(\{\tilde{p}\}). \quad (4.61)$$

Thus we obtain

$$\mathcal{T}_\lambda[\Sigma(v; \lambda)] = \int d\sigma^b(\tilde{\Phi}_b) \delta(V(\{\tilde{p}\}) - v) \times \left[\mathcal{N} \mathcal{T}_\lambda[I_V(\{\tilde{p}\}, \lambda)] \right], \quad (4.62)$$

where we have introduced

$$\begin{aligned} I_V(\{\tilde{p}\}, \lambda) &= \int [dk] \frac{J^\mu J^\nu}{\lambda^2} \theta\left(\omega_{\max} - \frac{(kq)}{\sqrt{q^2}}\right) \int [dl][d\bar{l}] (2\pi)^4 \delta^{(4)}(k - l - \bar{l}) \\ &\quad \times \text{Tr}[l\gamma^\mu \bar{l}\gamma^\nu] [V(\{\tilde{p}\}, l, \bar{l}) - V(\{\tilde{p}\})]. \end{aligned} \quad (4.63)$$

The two eqs. (4.62, 4.63) constitute the starting point in order to perform the analytic investigations reported in the next chapters.

Chapter 5

Power corrections to the C -parameter in the three-jet region

In this chapter we show how to obtain an analytic result for linear power corrections affecting the C -parameter in the three-jet region, considering the process

$$\gamma^*(q) \rightarrow q(p_1) + \bar{q}(p_2) + \gamma(p_3), \quad (5.1)$$

with all final-state particles resolved. If we consider a process involving N massless final-state particles with momenta p_1, \dots, p_N , then the C -parameter is defined as

$$C = 3 - 3 \sum_{j < i} \frac{(p_i p_j)^2}{(p_i q)(p_j q)}, \quad (5.2)$$

where $q = \sum_{i=1}^N p_i$ is the momentum of the decaying virtual photon. We want to apply eq. (5.2) to the case $N = 5$, labelling $p_4 = l$ and $p_5 = \bar{l}$, being l and \bar{l} the momenta of the $q\bar{q}$ pair produced by the splitting of the gluon. Looking at eq. (5.2) we can immediately conclude that the C -parameter satisfies the condition shown in eq. (4.60). Thus, in order to compute linear power corrections to the cumulant, we can use eqs. (4.62, 4.63).

As we mentioned in the introduction, we can implement the computation in two ways. Indeed we can directly integrate eq. (4.62), also obtaining a robust benchmark for the following investigations. The direct integration technique of eq. (4.62) is quite interesting from a technical point of view, as it involves elliptic structures and it is highly non trivial, though leading to very simple results. Indeed it turns out that the complexity of the computation strictly depends on the regularization procedure of the integral over virtual-gluon energy (cf. eq. (4.62)). In the following we will see how the use of the ω_{\max} regulator in eq. (4.62) is not optimal. We will also show that it is possible to perform the whole calculation in a fully factorised approach, that strongly simplifies it and also allows us to generalise our results to a wide class of observables. Furthermore, in the following we will study this factorisation in detail, and also comment on the connection between our results and the ones obtained within the Milan factor approach [76, 77], for computations performed in the two-jet and in the symmetric three-jet limits.

5.1 Direct integration with an explicit energy cut-off

We want to analytically integrate the function $I_V(\{\tilde{p}\}, \lambda)$, introduced in eq. (4.63), for $V = C$. For ease of notation, from now on we will replace $\tilde{p}_i \rightarrow p_i$ in all the expressions, as the p_i momenta ($i = 1, 2, 3$) do not appear in the following calculation.

First we consider the integration over the phase space of the emitted quarks, keeping the gluon momentum k and q fixed. For sake of convenience we perform this integration in the rest frame of the decaying gluon. Then we integrate over the direction of the vector \vec{k} in the rest frame of q , keeping $p_{1,2,3}$ fixed and leaving the integration over the gluon energy at the end. We observe that, since the gluon mass acts as a cut-off for both the soft and collinear divergences, the angular integrations become straightforward. Thus we can directly write

$$I_C(p_1, p_2, p_3, \lambda) = -\frac{3\lambda}{4\pi^3 q} \sum_{i=1}^5 I_i(x, y, \lambda), \quad (5.3)$$

where

$$I_i(x, y, \lambda) = \int_0^{\beta_{\max}} d\beta G_i(\beta, x, y). \quad (5.4)$$

In eq. (5.3) we have $q = \sqrt{q^2}$, β is the velocity of the massive gluon in the q rest frame, and $\beta_{\max} = \sqrt{1 - \lambda^2/\omega_{\max}^2}$; the two variables x and y parameterise the kinematics of the three-jet configuration. They allow us to express the scalar products qp_i , $i = 1, 2, 3$ as follows

$$qp_i = \frac{q^2}{2}(1 - z_i), \quad (5.5)$$

such that $\sum_{i=1}^3 z_i = 1$. Thus we can parameterise $z_{1,2,3}$ as $z_1 = xy$, $z_2 = x(1 - y)$, $z_3 = 1 - x$. The explicit expressions for the G_i functions are rather lengthy, and we chose to report them in appendix E. By looking at these functions we can observe that their integration is not straightforward. Indeed, when taken separately, the G_i functions exhibit strong singularities for $\beta = 0$ and moderately strong singularities for $\beta = 1$. The first ones, for $\beta = 0$ are unphysical, and cancel in the sum. The $\beta = 1$ singularities instead are physical and are due to the fact that the integral in eq. (4.63) diverges for large values of gluon energy (this is the reason for the presence of the cut-off ω_{\max} or β_{\max}). Furthermore, the integrand exhibits an *elliptic* structure. Indeed, a glance at $G_{3,5}$ shows the arising of square roots of a degree-four polynomial, $\sqrt{(1 - \beta^2)(1 - c_{12}^2 \beta^2)}$, being $c_{12}^2 = 1 - s_{12}^2 = \cos^2(\theta_{12}/2)$ and θ_{12} is the angle between the three-momenta \vec{p}_1 and \vec{p}_2 in the q rest frame. It is a well known result that the integration of square roots of degree-four polynomials leads to elliptic integrals. Although it is possible to integrate over β systematically, a similar integration would involve the presence of both generalised and elliptic polylogarithms, making the whole computation very complicated.

It turns out, however, that one can integrate over β bypassing entirely the arising of elliptic polylogarithms, and we can illustrate this point by considering the G_5 function for sake of example, that also allows us to expose all the key features of the method, keeping the discussion relatively short.

The explicit expression of G_5 reads

$$\begin{aligned}
 G_5 = & \frac{\sqrt{1-\beta^2} \ln\left(\frac{1+\beta}{1-\beta}\right) \ln\left(\frac{\sqrt{1-\beta^2 c_{12}^2 + \beta s_{12}}}{\sqrt{1-\beta^2 c_{12}^2 - \beta s_{12}}}\right)}{64\beta^8 s_{12} x(x(y-1)+1)(xy-1)\sqrt{1-\beta^2 c_{12}^2}} \\
 & \times \left(\beta^6 x[x^2(y-1)y + x(-4y^2 + 4y - 5) + 5] + \beta^4 [x^2(54y^2 - 54y - 17) \right. \\
 & - 21x^3(y-1)y + 55x - 38] + 5\beta^2 [x^2(-24y^2 + 24y + 5) \\
 & \left. + 11x^3(y-1)y - 17x + 12] - 35(x-2)(x^2(y-1)y + x - 1) \right). \quad (5.6)
 \end{aligned}$$

We observe that G_5 is integrable at $\beta = 1$ but not at $\beta = 0$. Thus we set $\beta_{\max} = 1$ in I_5 , but we need to define the following integral

$$I_5^{\text{reg}} = \int_{\beta_{\min}}^1 d\beta G_5(\beta, x, y). \quad (5.7)$$

In the following we will drop the superscript ‘‘reg’’.

The G_5 function contains two logarithms of β , two β -dependent square roots and a rational function of β . In order to integrate over β it is convenient to consider an integral representation of the two logarithms contained in eq. (5.6). Thus we write

$$\begin{aligned}
 \ln \frac{1+\beta}{1-\beta} &= 2\beta \int_0^1 \frac{dr}{1-r^2\beta^2}, \\
 \ln \left(\frac{\sqrt{1-\beta^2 c_{12}^2 + \beta s_{12}}}{\sqrt{1-\beta^2 c_{12}^2 - \beta s_{12}}} \right) &= 2\beta s_{12} \sqrt{1-\beta^2 c_{12}^2} \int_0^1 \frac{d\xi}{1-\beta^2 \Delta^2}, \quad (5.8)
 \end{aligned}$$

where Δ is a function of ξ , $\Delta = \sqrt{c_{12}^2 + s_{12}^2 \xi^2}$. After this substitution, eq. (5.7) takes the form

$$I_5 = \int_0^1 dr d\xi \int_{\beta_{\min}}^1 d\beta \sqrt{1-\beta^2} R(\beta^2, r^2, \xi^2), \quad (5.9)$$

being $R(\beta^2, r^2, \xi^2)$ a rational function of its arguments, whose dependence on x and y has been suppressed. Thanks to the integral representations in eq. (5.8), one of the two β -dependent square roots has disappeared from the integrand in eq. (5.9). At this point in order to also remove the second root, we change variables $\beta = \sin \varphi$, obtaining

$$I_5 = \int_0^1 dr d\xi \int_{\varphi_{\min}}^{\pi/2} d\varphi \cos^2(\varphi) R(\sin^2(\varphi), r^2, \xi^2), \quad (5.10)$$

where $\varphi_{\min} = \arcsin(\beta_{\min})$.

At this point, noting that the integral depends on squares of $\cos \varphi$ and $\sin \varphi$, it is convenient to change variables once again, writing $\varphi = \varphi_1/2$, such that $0 < \varphi_1 < \pi$, $\cos^2(\varphi_1/2) = (1 + \cos \varphi_1)/2$, $\sin^2(\varphi_1/2) = (1 - \cos \varphi_1)/2$. Thus we get

$$I_5 = \frac{1}{2} \int_0^1 dr d\xi \int_{2\varphi_{\min}}^{\pi} d\varphi_1 R_1(\cos \varphi_1, r^2, \xi^2), \quad (5.11)$$

where R_1 is another rational function of its arguments. To proceed further we perform a partial fractioning of R_1 with respect to $\cos \varphi_1$, obtaining

$$R_1 = \sum_{i=-3}^{-1} \frac{P_i(r^2, \xi^2)}{(1 - \cos \varphi_1)^i} + \frac{1}{\Delta^2 - r^2} \left[\frac{P_\Delta(r^2, \xi^2)}{(2 - \Delta^2 + \Delta^2 \cos \varphi_1)} + \frac{P_r(r^2, \xi^2)}{(2 - r^2 + r^2 \cos \varphi_1)} \right], \quad (5.12)$$

where $P_{-3,-2,-1}(r^2, \xi^2)$ and $P_{\Delta,r}(r^2, \xi^2)$ are polynomials in r^2 and ξ^2 . As it can be seen in eq. (5.12), these polynomials only contain even powers of r and ξ , and this property will be exploited in the following.

It is straightforward to integrate over φ_1 for all of the five terms in eq. (5.12); in particular, for what concerns the first three terms, we can perform a trivial integration over φ_1 , and then expand in β_{\min} . The resulting expressions can then be integrated over ξ and r very easily. As the treatment of the first three terms in eq. (5.12) is very straightforward, we prefer to focus on the last two terms, studying

$$I_5^{45} = \frac{1}{2} \int_0^1 dr d\xi \int_{2\varphi_{\min}}^{\pi} \frac{d\varphi_1}{\Delta^2 - r^2} \left[\frac{P_\Delta(r^2, \xi^2)}{2 - \Delta^2 + \Delta^2 \cos \varphi_1} + \frac{P_r(r^2, \xi^2)}{2 - r^2 + r^2 \cos \varphi_1} \right]. \quad (5.13)$$

As both the terms in eq. (5.13) are integrable at $\varphi = 0$, corresponding to $\beta = 0$, we can safely set $\varphi_{\min} \rightarrow 0$. Using the identity

$$\int_0^{\pi} \frac{d\varphi}{a - b \cos \varphi} = \frac{\pi}{\sqrt{a^2 - b^2}}, \quad (5.14)$$

we obtain the following result

$$I_5^{45} = \frac{\pi}{4} \int_0^1 \frac{dr d\xi}{\Delta^2 - r^2} \left[\frac{P_\Delta(r^2, \xi^2)}{\sqrt{1 - \Delta^2}} + \frac{P_r(r^2, \xi^2)}{\sqrt{1 - r^2}} \right]. \quad (5.15)$$

Looking at eq. (5.15) we note the presence of a singularity at $\Delta = r$. Nevertheless, using the explicit form of the two polynomials $P_\Delta(r^2, \xi^2)$ and $P_r(r^2, \xi^2)$ one can check that the expression in the square brackets in eq. (5.15) vanishes when $\Delta = r$.

Even though the singularity at $\Delta = r$ and the way we regulated it in eq. (5.15) seem to suggest that the two terms in eq. (5.15) must be integrated at once, it turns out to be convenient to integrate them separately. In order to do this we need to introduce a regulator, by moving the pole at $\Delta = r$ away from the real axis, i.e. we take $1/(\Delta^2 - r^2) \rightarrow 1/(\Delta^2 - r^2 + i0)$. At this point one can deal with the two terms in eq. (5.15) separately. Let us consider the first term, changing variables $\xi = \text{th}(u)$, $r = \text{th}(w)$, we obtain

$$\int_0^1 \frac{dr d\xi}{\Delta^2 - r^2 + i0} \frac{P_\Delta(r^2, \xi^2)}{\sqrt{1 - \Delta^2}} = \frac{1}{s_{12}} \int_0^\infty \frac{du dw \text{ch}(u) P_\Delta(\text{th}^2(u), \text{th}^2(w))}{\text{ch}^2(u) - s_{12}^2 \text{ch}^2(w) + i0}, \quad (5.16)$$

where the integrand in the above equation is an even function of u . Thus we can extend the u -integration to the whole real axis and, changing variable $u \rightarrow z = \text{sh}(u)$ we get an integral that can be evaluated using Cauchy's residue theorem. Now we are left with a one-dimensional integral in w . For the second term in eq. (5.15) we can proceed in a similar

way, by first integrating over w using the residue theorem, and then facing a one-dimensional integral in u .

Thus we map the integration ranges of the two remaining one-dimensional integrals in the interval $[s_{12}, 1]$, introducing the change of variable $t = 1/\text{ch}(w)$ for the first term of eq. (5.15) and $t = 1/\text{ch}(u)$ for the second one. By combining the two terms we arrive at the following result for I_5^{45}

$$I_5^{45} = \int_{s_{12}}^1 \frac{dt t^2}{\sqrt{1-t^2}\sqrt{t^2-s_{12}^2}} [\alpha(x, y) + \beta(x, y)t^2 + \gamma(x, y)t^4 + \delta(x, y)t^6], \quad (5.17)$$

where we have restored the dependence on x and y , to subtle that I_5^{45} depends non-trivially on the underlying Born kinematics. A straightforward integration over t in eq. (5.17) leads to a result that can be expressed through the two complete elliptic integrals

$$K(z) = \int_0^1 \frac{dt}{\sqrt{(1-t^2)(1-zt^2)}}, \quad E(z) = \int_0^1 \frac{dt\sqrt{1-zt^2}}{\sqrt{1-t^2}}. \quad (5.18)$$

To summarise, we were able to get this relatively simple result by *a*) introducing an integral representation for the logarithms in eq. (5.8), that also removes one of the square roots; *b*) choosing a proper change of variables to linearise the square root in eq. (5.8); *c*) using a different integration strategy for the two terms in eq. (5.15), that required the presence of a regulator at intermediate stages.

So far we only considered the I_5 contribution, as all the other I_i terms of eq. (5.4) can be obtained along similar lines. Furthermore, we observe that elliptic integrals only arise in I_5 . When we put all the different contributions together, we get a rather cumbersome result for I_C , depending on the underlying Born kinematics and on β_{max} . We find that, for a generic three-jet configuration, we are left only with the terms that contain elliptic integrals, and the result takes the remarkably simple form

$$\mathcal{T}_\lambda[I_C] = \frac{15}{128\pi} \frac{s_{12}^3}{1-z_3} \left(\frac{\lambda}{q} \right) \left[\frac{(1+z_3)}{2} K(c_{12}^2) - (1-z_1 z_2) E(c_{12}^2) \right], \quad (5.19)$$

where we switched back to the z_i variables defined in eq. (5.5), and used

$$s_{12}^2 = \frac{z_3}{(1-z_1)(1-z_2)}. \quad (5.20)$$

Turning back to eq. (4.62) we can immediately translate this result into the expression for the non-perturbative shift in the cumulative distribution for a generic three-jet configuration, for the C -parameter

$$\begin{aligned} \mathcal{T}_\lambda[\Sigma(c; \lambda)] &= \int d\sigma^b(\Phi_b) \delta(C(\Phi_b) - c) \times \\ &\alpha_s C_F \frac{45\pi}{16} \frac{s_{12}^3}{1-z_3} \left[\frac{(1+z_3)}{2} K(c_{12}^2) - (1-z_1 z_2) E(c_{12}^2) \right] \left(\frac{\lambda}{q} \right). \end{aligned} \quad (5.21)$$

At this point we can study the behaviour of eq. (5.21) in the two- and three-jet symmetric points, in order to compare our results with the ones reported in the literature. In the two-jet limit we take $c_{12} = 0$, $z_2 \rightarrow 0$ and $z_1 + z_3 \rightarrow 1$ (or, equivalently $z_1 \rightarrow 0$ and $z_2 + z_3 \rightarrow 1$), and we obtain the well-known result of refs [93, 94]

$$\frac{\mathcal{T}_\lambda[\Sigma(0; \lambda)]}{d\sigma/dC|_{c=0}} = -\frac{15}{16}\pi^2 \left(\frac{\lambda}{q}\right) \alpha_s. \quad (5.22)$$

In correspondence of the three-jet symmetric point, the three jet share all the same energy fraction, with $z_i = 1/3$ for each i and $c_{12} = 1/2$. Thus we obtain

$$\frac{\mathcal{T}_\lambda[\Sigma(3/4; \lambda)]}{d\sigma/dC|_{c=3/4}} = \frac{15}{32}\sqrt{3}\pi[3K(1/4) - 4E(1/4)] \left(\frac{\lambda}{q}\right) \alpha_s, \quad (5.23)$$

in agreement with the results of ref. [84], that we adapted to our process $\gamma^* \rightarrow q + \bar{q} + \gamma$, corrected for the $n_f \rightarrow \infty$ limit. In the above equations we also made use of the relation

$$\int d\sigma \delta(V - v) = \frac{d\sigma}{dV}. \quad (5.24)$$

We conclude this section by observing that in ref. [84] the whole computation has been carried out in the so-called Milan factor approach, consisting in multiplying the result of a simplified computation only involving the emission of a single massless gluon by a universal factor, in order to correct for the gluon splitting. The approach we described along this section cannot show neither the simplicity of the final result, nor its relation to the Milan factor approach. In order to clarify these issues, it is necessary to change the way of approaching the integration of eq. (4.62), and we discuss about this in what follows.

5.2 Factorised form of linear power corrections affecting the C -parameter

In order to get a simple and factorised form of power corrections for the C -parameter we start from eq. (4.63), taking $V = C$. As for this approach we do not need to introduce a cut off on the gluon energy, we remove the θ -function that implements this constraint. Thus we simply consider

$$I_C^{\text{unreg}}(\{\tilde{p}\}, \lambda) = \int [dk] \frac{J^\mu J^\nu}{\lambda^2} \int [dl][d\bar{l}] (2\pi)^4 \delta^{(4)}(k - l - \bar{l}) \\ \times \text{Tr}[l\gamma^\mu \bar{l}\gamma^\nu][C(\{\tilde{p}\}, l, \bar{l}) - C(\{\tilde{p}\})]. \quad (5.25)$$

In the following we will replace $\tilde{p}_i \rightarrow p_i$ as there is no room for any ambiguity. Furthermore, after removing the gluon energy cut-off, the integral in eq. (5.25) is ill-defined; thus we need to introduce a proper regularisation in order to get a finite integral, and that also allows for its straightforward computation.

However, we start by first simplifying eq. (5.25), by computing the trace in the square bracket, and inserting the definition of the C -parameter. Thus we get

$$I_C^{\text{unreg}} = -24 \int [dk] \frac{J_\mu J_\nu}{\lambda^2} \int [dl][d\bar{l}] (2\pi)^4 \delta^{(4)}(k - l - \bar{l}) \tilde{C}^{\alpha\beta} \frac{l_\alpha l_\beta}{(lq)} \left[-2l^\mu l^\nu - g^{\mu\nu} \frac{\lambda^2}{2} \right], \quad (5.26)$$

where the arguments of I_C^{unreg} have been dropped only for sake of notations, and the relation $\bar{l} = k - l$ has been used, in conjunction with $k_\mu J^\mu = 0$, to discard terms proportional to k , that originate from the trace. We have also introduced the rank-two tensor $\tilde{C}_{\alpha\beta}$, defined as

$$\tilde{C}^{\alpha\beta} = \sum_{i=1}^3 \frac{p_i^\alpha p_i^\beta}{(p_i q)}, \quad (5.27)$$

accounting for the fact that the quark and the antiquark contribute in the same way to the C -parameter.

To proceed further we choose to use the $p_{1,2}$ vectors as a basis, in order to employ the Sudakov parametrisation for l as

$$l^\mu = l_t e^\eta \frac{p_1^\mu}{\sqrt{s}} + l_t e^{-\eta} \frac{p_2^\mu}{\sqrt{s}} + l_\perp^\mu, \quad [dl] = \frac{d\eta d^2 \vec{l}_\perp}{2(2\pi)^3}, \quad (5.28)$$

where $s = 2(p_1 p_2)$, $l_t = |l_\perp|$ and η is the rapidity of the quark l . Thanks to these variables, we can rewrite the quark-antiquark phase space as

$$[dl][d\bar{l}] (2\pi)^4 \delta^{(4)}(k - l - \bar{l}) = 2\pi [dl] \delta_+((k - l)^2) = \frac{1}{8\pi^2} d\eta l_t dl_t d\varphi \delta(\lambda^2 - 2(kl)), \quad (5.29)$$

with φ the azimuthal angle of \vec{l}_\perp . As an integration over the absolute value of the quark transverse momentum l_t is straightforward, we can easily remove the δ -function from eq. (5.29). With this goal we introduce the rescaled vector

$$\tilde{l}^\mu = \frac{l^\mu}{l_t} = \frac{p_1^\mu}{\sqrt{s}} e^\eta + \frac{p_2^\mu}{\sqrt{s}} e^{-\eta} + n^\mu, \quad (5.30)$$

where $n^\mu = l_\perp^\mu / l_t$, and find

$$[dl][d\bar{l}] (2\pi)^4 \delta^{(4)}(k - l - \bar{l}) = \frac{1}{8\pi^2} d\eta d\varphi \frac{\lambda^2}{(2k\tilde{l})^2}, \quad l_t = \frac{\lambda^2}{2(k\tilde{l})}. \quad (5.31)$$

Thanks to eq. (5.31) we can write the function I_C in eq. (5.26) as

$$I_C^{\text{unreg}} = W_C \times \lambda F(p_1, p_2, \tilde{l}), \quad (5.32)$$

with

$$W_C = -3 \int \frac{d\eta d\varphi}{2(2\pi)^3} \tilde{C}_{\alpha\beta} \frac{\tilde{l}^\alpha \tilde{l}^\beta}{(\tilde{l}q)}, \quad (5.33)$$

and

$$F(p_1, p_2, \tilde{l}) = 16\pi \int [dk] \frac{J_\mu J_\nu}{\lambda^3} \left\{ -2\tilde{l}^\mu \tilde{l}^\nu \frac{\lambda^8}{(2k\tilde{l})^5} - \frac{g^{\mu\nu} \lambda^6}{2(2k\tilde{l})^3} \right\}. \quad (5.34)$$

Thus the function I_C can be factorised in the product of two terms: one term, namely F does not depend on the observable, and only involves an integration over the gluon momentum k ; the second term instead involves an integration over the rapidity and azimuthal angle of the emitted quark with momentum l and also contains the dependence on the observable. In the next sections we will show how, even though eq. (5.34) can depend upon p_1, p_2 and \tilde{l} , it is actually a constant.

Furthermore, we would like to stress that eqs. (5.32, 5.34) are ill-defined. Nevertheless, as we will show below, it is possible to exploit a regularisation scheme that allows us to evaluate both F and I_C in a quite simple way. We will also show that the *observable-independent* constant term F can be easily related to the Milan factor of refs. [76, 77].

5.3 The observable-independent function F

In this section we will compute explicitly the function F defined in eq. (5.34). We start by introducing a Sudakov parameterisation for the gluon momentum k

$$k^\mu = m_t e^{\eta_k} \frac{p_1^\mu}{\sqrt{s}} + m_t e^{-\eta_k} \frac{p_2^\mu}{\sqrt{s}} + k_\perp^\mu, \quad (5.35)$$

where, as done for the quark momentum in eq. (5.30) we have introduced $k_t = |k_\perp|$ and also $m_t = \sqrt{k_t^2 + \lambda^2}$. Recurring to eqs. (5.30) and eq. (5.35) it is easy to obtain

$$\begin{aligned} k_\mu \tilde{l}^\mu &= m_t \operatorname{ch}(\eta_{kl}) - k_t \cos(\varphi_{kl}), \\ J_\mu J^\mu &= -\frac{2(p_1 p_2)}{(p_1 k)(p_2 k)} = -\frac{4}{m_t^2}, \quad (J_\mu \tilde{l}^\mu)^2 = \frac{4 \operatorname{sh}^2(\eta_{kl})}{m_t^2}, \end{aligned} \quad (5.36)$$

where we have introduced $\eta_{kl} = \eta_k - \eta$, $\varphi_{kl} = \varphi_k - \varphi$. Recurring to these relations we can write the function F defined in eq. (5.34) as follows

$$\begin{aligned} F &= \frac{\lambda^3}{4\pi^2} \int dk_t k_t \mathcal{I}_M, \\ \mathcal{I}_M &= \int \frac{d\eta_k d\varphi_k}{m_t^2} \left\{ -\frac{\lambda^2 \operatorname{sh}^2(\eta_{kl})}{[m_t \operatorname{ch}(\eta_{kl}) - k_t \cos(\varphi_{kl})]^5} + \frac{1}{[m_t \operatorname{ch}(\eta_{kl}) - k_t \cos(\varphi_{kl})]^3} \right\}. \end{aligned} \quad (5.37)$$

In order to proceed in the computation of F we need to regularise it. A good choice consists in multiplying the integrand by the factor $k_t^{2\epsilon}$, writing

$$F = \frac{\lambda^3}{4\pi^2} \int_0^\infty dk_t k_t^{1+2\epsilon} \mathcal{I}_M. \quad (5.38)$$

For now we just assume that this choice does regulate all the divergences present in eq. (5.37), and at the end of this section we will also explain why one can choose this regularisation.

Furthermore we note that the integrand in eq. (5.37) only depends on the difference of two azimuthal angles φ_{kl} and on the difference of two rapidities η_{kl} . By virtue of this, since we integrate over all possible gluon rapidities and over all azimuthal angles, F must be independent on \tilde{l} . Hence, as pointed out previously, F must be a constant.

When computing F we perform the change variables $\eta_k \rightarrow \eta_{kl} = x$ and $\varphi_k \rightarrow \varphi_{kl}$, such that the azimuthal integration over φ_{kl} becomes straightforward. Thus it is convenient recur to the integral in eq. (5.14) and compute an appropriate number of derivatives with respect to a , to obtain an expression for the integrals of $1/(a - b \cos \varphi)^5$ and $1/(a - b \cos \varphi)^3$. Thus we find the following result

$$F = \frac{\lambda^{2\epsilon}}{128\pi} \int_{-\infty}^{\infty} dx \int_0^{\infty} d\xi \frac{\xi^\epsilon f(\xi, x)}{(\xi + 1)[(\xi + 1)\text{ch}^2 x - \xi]^{9/2}} \quad (5.39)$$

where $\xi = k_t^2/\lambda^2$ and the function $f(\xi, x)$ reads

$$\begin{aligned} f(\xi, x) = & \xi(\xi + 1)^2 \text{ch}(6x) + 4(1 - 2\xi)(\xi + 1)\text{ch}(4x) \\ & - (9\xi^3 + 8\xi^2 - 23\xi - 16)\text{ch}(2x) + 2(4\xi^3 + 7\xi^2 + 14\xi + 6). \end{aligned} \quad (5.40)$$

In order to integrate over ξ , we change variables $\xi \rightarrow r$, with $\xi = [r - \text{ch}^2(x)]/[\text{ch}^2(x) - 1]$, finding

$$F = \frac{\lambda^{2\epsilon}}{256\pi} \int_{-\infty}^{\infty} \frac{dx}{\text{sh}^{2+2\epsilon}(x)} \int_{\text{ch}^2(x)}^{\infty} dr \frac{(r - \text{ch}^2(x))^\epsilon \tilde{f}(x, r)}{(r - 1)r^{9/2}}, \quad (5.41)$$

where

$$\begin{aligned} \tilde{f}(x, r) = & (-8r^2 + 40r - 35)\text{ch}(4x) + 4(8r^3 - 44r^2 + 70r - 35)\text{ch}(2x) \\ & + 64r^3 - 192r^2 + 240r - 105. \end{aligned} \quad (5.42)$$

At this point the integration over r can be performed in a straightforward way, and one can express the result in terms of hypergeometric functions. Thus we get

$$\begin{aligned} F = & \frac{\lambda^{2\epsilon}}{1890\pi^{3/2}} \Gamma\left(\frac{3}{2} - \epsilon\right) \Gamma(\epsilon + 1) \int_0^{\infty} \frac{dx}{\text{sh}^{2+2\epsilon}(x) \text{ch}^{5-2\epsilon}(x)} \left\{ \right. \\ & 630 \text{ch}^2(x) (\text{ch}(2x) + 2) F_{21}\left(1, \frac{3}{2} - \epsilon, \frac{5}{2}; \frac{1}{\text{ch}^2(x)}\right) + \frac{63}{8} (2\epsilon - 3) \left[\right. \\ & (16\epsilon^2 + 8(2\epsilon + 3)\text{ch}(2x) + 3\text{ch}(4x) + 21) F_{21}\left(1, \frac{5}{2} - \epsilon; \frac{7}{2}, \frac{1}{\text{ch}^2(x)}\right) \\ & \left. \left. + 4\text{sh}^2(x) (4\epsilon + \text{ch}(2x) + 3) F_{21}\left(2, \frac{5}{2} - \epsilon; \frac{7}{2}, \frac{1}{\text{ch}^2(x)}\right)\right] \right\}, \end{aligned} \quad (5.43)$$

where we exploit the symmetry of the integrand with respect to $x = 0$ to restrict the integration region to the positive real axis.

The residual integral in eq. (5.43) has a quadratic singularity in correspondence of $x = 0$, that needs to be extracted before integrating over x . In order to do this we consider a suitable limiting form of the integrand in the $x \rightarrow 0$ limit, computed for finite ϵ , that will be subtracted

from the integrand, and then added back. In such a way the difference gets integrable and an expansion in ϵ can be performed, while the subtracted term is simple enough to be integrated for arbitrary ϵ . Thus along these lines we can write F as the sum of two contributions

$$F = F^{(a)} + F^{(b)}. \quad (5.44)$$

$F^{(a)}$ is the subtraction term, which can be obtained by taking the $\text{ch}(x) \rightarrow 1$ limit in eq. (5.41), keeping the $1/\text{sh}^{2+2\epsilon}(x)$ term as it is, and finding

$$\begin{aligned} F^{(a)} &\equiv \frac{\lambda^{2\epsilon}}{256\pi} \int_{-\infty}^{\infty} \frac{dx}{\text{sh}^{2+2\epsilon}(x)} \int_1^{\infty} dr \frac{(r-1)^{\epsilon-1} \tilde{f}(0, r)}{r^{9/2}} \\ &= \frac{\lambda^{2\epsilon} \Gamma(1+\epsilon) \Gamma(\frac{3}{2}-\epsilon)}{6\pi^{3/2}} [3 - \epsilon(1-2\epsilon)] \int_0^{\infty} \frac{dx}{\text{sh}^{2+2\epsilon}(x)}. \end{aligned} \quad (5.45)$$

The regular piece $F^{(b)}$ is given by the difference between F in eq. (5.43) and $F^{(a)}$. As the difference is integrable at $x = 0$, we can expand it in ϵ . Furthermore, we change the integration variables from x to $t = e^x$, $1 < t < \infty$. We get

$$\begin{aligned} F^{(b)} &= \frac{1}{\pi} \int_1^{\infty} dt \left[-\frac{(3+t^2)(1+3t^2)}{32t^3} \ln \frac{t+1}{t-1} + \frac{(3+6t+14t^2+6t^3+3t^4)}{16t^2(1+t)^2} \right] \\ &= \frac{1}{\pi} \left(-\frac{5\pi^2}{64} + \frac{1}{4} \right). \end{aligned} \quad (5.46)$$

Now it remains to compute $F^{(a)}$. In order to do that we perform the change of variables $x = \ln t$, and find

$$\int_0^{\infty} \frac{dx}{\text{sh}^{2+2\epsilon}(x)} = 2^{2+2\epsilon} \int_1^{\infty} \frac{dtt^{1+2\epsilon}}{(t^2-1)^{2+2\epsilon}} = 2^{1+2\epsilon} \frac{\Gamma(-1-2\epsilon)\Gamma(1+\epsilon)}{\Gamma(-\epsilon)}. \quad (5.47)$$

We observe that, although the original integral is ill-defined for $\epsilon = 0$, this result has a smooth $\epsilon \rightarrow 0$ limit. Thus we use eq. (5.47) in the expression for $F^{(a)}$ given in eq. (5.45), take the $\epsilon \rightarrow 0$ limit and obtain

$$F^{(a)} = -\frac{1}{4\pi}. \quad (5.48)$$

By combining the result for $F^{(a)}$ and $F^{(b)}$ in eq. (5.46) and eq. (5.48) we obtain the final result for the universal factor F

$$F = -\frac{5\pi}{64}. \quad (5.49)$$

5.3.1 An alternative way to compute F

Now we will expose an alternative procedure to evaluate F , that, besides showing that F is actually a constant, allows us to express it in terms of a convergent integral, amenable to a direct numerical integration, that we carry out as a further check of the analytic result in eq. (5.49).

Looking at \mathcal{I}_M in eq. (5.34) we can observe that for small values of λ the two terms in the square bracket diverge as η_{kl} and φ_{kl} get small at the same time. This singularity is in fact due to the collinear divergence arising when the quark and the gluon momenta become parallel to each other, in the small λ limit.

Assuming $\eta_{kl} \approx 0$ the following equation holds

$$\frac{1}{m_t \text{ch}(\eta_{kl}) - k_t \cos \varphi_{kl}} = \frac{2}{m_t} \times \frac{1 + \mathcal{O}(\eta_{kl}^2, \varphi_{kl}^2)}{\frac{2(m_t - k_t)}{m_t} + \frac{k_t}{m_t} \varphi_{kl}^2 + \eta_{kl}^2}. \quad (5.50)$$

As the integral in eq. (5.34) is dominated by the region where both η_{kl} and φ_{kl} are of order λ/m_t , for large k_t we can safely substitute in the integrand

$$\frac{1}{m_t \text{ch}(\eta_{kl}) - k_t \cos \varphi_{kl}} \rightarrow \left(\frac{2}{k_t}\right) \times \frac{1}{\lambda^2/k_t^2 + \varphi_{kl}^2 + \eta_{kl}^2}, \quad (5.51)$$

with the neglecting terms that can only lead to $\mathcal{O}(\lambda^2/k_t^2)$ contributions. With eq. (5.51) and using a polar coordinate system $\{\eta_{kl}, \varphi_{kl}\} \rightarrow \{r_{\eta\varphi} \cos \theta_{\eta\varphi}, r_{\eta\varphi} \sin \theta_{\eta\varphi}\}$, we can write

$$\mathcal{I}_M \approx \int dr_{\eta\varphi} d\theta_{\eta\varphi} r_{\eta\varphi} \left[-32 \left(\frac{\lambda^2}{k_t^7}\right) \frac{r_{\eta\varphi}^2 \cos^2 \theta_{\eta\varphi}}{(\lambda^2/k_t^2 + r_{\eta\varphi}^2)^5} + \frac{8/k_t^5}{(\lambda^2/k_t^2 + r_{\eta\varphi}^2)^3} \right] = \frac{8\pi}{3\lambda^4} \times \frac{1}{k_t} + \mathcal{O}(\lambda^2/k_t^2). \quad (5.52)$$

Thus the expression

$$F^{\text{reg}} = \frac{\lambda^3}{4\pi^2} \int_0^\infty dk_t \left(k_t \mathcal{I}_M - \frac{8\pi}{3\lambda^4} \right), \quad (5.53)$$

yields a convergent k_t -integration. In fact the integral in eq. (5.53) can be computed recurring to numerical techniques, verifying the analytic result in eq. (5.49).

Now we can provide an argument to justify the use of a regulator in the evaluation of eq. (5.38). In fact, as the integral in F^{reg} is convergent, we can safely introduce a regulator $k_t^{2\epsilon}$ in the integrand of eq. (5.53) treating the two terms separately. The subtraction term goes to zero thanks to the properties of the analytic regulator

$$\int_0^\infty dk_t k_t^{1+2\epsilon} = 0, \quad (5.54)$$

and the first term in eq. (5.53) leads to an analytically-regulated expression, as in eq. (5.38), that has been used in this section in order to evaluate the constant universal factor F .

To proceed further, we need to compute the observable-dependent part W_C defined in eq. (5.32). It is possible to perform the computation by introducing a proper regulator to the integrand in W_C and proceeding along the same lines as for the computation of the constant F . Nevertheless, in the next section we will perform the computation using a more general approach, also identifying the properties an observable must obey for this factorisation approach to be applicable.

5.4 The observable dependent factor: a general approach

In section 5.2 we have focused exclusively on the C -parameter case, but it is obvious that the arguments we are going to expose in this section are applicable to a wider class of observables. In what follows we will identify the main properties a shape variable must satisfy in order to factorise the non-perturbative contribution as in eq. (5.32).

We will show as well that this general approach bears striking similarities to the Milan factor approach of refs. [76, 77], that has been successfully applied to study non-perturbative corrections near singular kinematic configurations. In order to check our results, we will explore the connections between our formalism and the one used in refs [76, 77].

We start by studying in more detail the contribution due to the recoil effects on shape variables. As shown in section 4.2, we can compute linear power corrections to a generic IR-safe observable V by considering the difference $V(\{p\}, l, \bar{l}) - V(\{\tilde{p}\})$, that we now examine including the recoil effects. Following the arguments exposed in section 4.2, we find, in the small- k limit

$$\begin{aligned}
 V(\{p\}, l, \bar{l}) - V(\{\tilde{p}\}) &= V(\{\tilde{p}\}, l, \bar{l}) - V(\{\tilde{p}\}) + \frac{\partial V(\{\tilde{p}\})}{\partial \tilde{p}_i^\mu} R_{i,\nu}^\mu(\{\tilde{p}\}) k^\nu \\
 &+ \left\{ \frac{\partial V(\{\tilde{p}\}, l, \bar{l})}{\partial \tilde{p}_i^\mu} - \frac{\partial V(\{\tilde{p}\})}{\partial \tilde{p}_i^\mu} \right\} R_{i,\nu}^\mu(\{\tilde{p}\}) k^\nu + \mathcal{O}(k_0^2), \quad (5.55)
 \end{aligned}$$

where we assume summation over repeated indices. The term in the curly bracket on the right-hand side of eq. (5.55) is suppressed in the soft limit and, being multiplied by k^ν , can be dropped. For observables that are linear with respect to soft emissions we have¹

$$\begin{aligned}
 V(\{\tilde{p}\}, l, \bar{l}) - V(\{\tilde{p}\}) &= V(\{\tilde{p}\}, l, \bar{l}) - V(\{\tilde{p}\}, l) + V(\{\tilde{p}\}, l) - V(\{\tilde{p}\}) \\
 &\approx V(\{\tilde{p}\}, \bar{l}) - V(\{\tilde{p}\}) + V(\{\tilde{p}\}, l) - V(\{\tilde{p}\}), \quad (5.56)
 \end{aligned}$$

leading to

$$\begin{aligned}
 V(\{p\}, l, \bar{l}) - V(\{\tilde{p}\}) &\approx V(\{\tilde{p}\}, l) - V(\{\tilde{p}\}) + \frac{\partial V(\{\tilde{p}\})}{\partial \tilde{p}_i^\mu} R_{i,\nu}^\mu(\{\tilde{p}\}) l^\nu \\
 &+ V(\{\tilde{p}\}, \bar{l}) - V(\{\tilde{p}\}) + \frac{\partial V(\{\tilde{p}\})}{\partial \tilde{p}_i^\mu} R_{i,\nu}^\mu(\{\tilde{p}\}) \bar{l}^\nu, \quad (5.57)
 \end{aligned}$$

where we have used $k = l + \bar{l}$, and we have neglected terms of higher order in l . As long as the observable V and the mapping satisfy the linearity condition of eq. (5.57), the effect of the emission of two soft massless partons (arising from the decay of a virtual gluon) can be written as the sum of two equivalent contributions, each contributing with a soft massless parton, and each recoil effect is computed as if only one parton was emitted. For our treatment we assume that our observable V satisfies these requirements, and this strongly simplifies the computation, as it allows us to focus on modifications of the shape variables due to the emission of a single massless parton. We label by l the momentum of the emitted soft massless parton, with φ , η , l_\perp its azimuthal angle, rapidity and transverse momentum, taken

¹The definition on linearity means that $V(\{\tilde{p}\}, l, \bar{l}) = V(\{p\}) + V_2^\mu(\{p\}, l) l_\mu + V_3^\mu(\{p\}, \bar{l}) \bar{l}_\mu$.

in the dipole rest frame, respectively. We expect that the shape variable modification can be described by the following equation at small $l_t = |l_\perp|$

$$V(\{p\}, l) - V(\{\tilde{p}\}) = \frac{l_t}{q} h_V(\eta, \varphi), \quad (5.58)$$

that obviously vanishes in the soft limit. In order for it to vanish also in the collinear limit, we need the function h_V to be bounded for large η and arbitrary φ . This because, being the rapidity limited by a logarithm of Q/l_t , an exponential behaviour in η would lead to powers of Q/l_t (where Q is the hard scale of the process), canceling the l_t suppression. Nevertheless, this requirement is not enough for our purposes. Indeed we work under the assumption that hard-collinear regions cannot contribute to linear power corrections. For this reason h_V must also be suppressed for large η .² For an emission from a $q\bar{q}$ dipole, the collinear divergence does not depend upon the azimuth of the emitted parton, such that we can rely on the weaker condition that $\int d\varphi h_V(\eta, \varphi)$ vanishes for large η . When we generalise our result to the realistic QCD scenario of an emission from a qg ($\bar{q}g$) dipole, we may have to worry also about the azimuthal-dependent collinear divergences, arising from terms proportional to $l_\perp^\mu l_\perp^\nu$ in the splitting function. However these terms are even in φ , i.e. they are invariant under the parity transformation $\varphi \rightarrow \pi - \varphi$. Thus we require that $h_V(\eta, \varphi) - h_V(\eta, \pi - \varphi)$ must be integrable for $-\infty < \eta < \infty$. Thus we can obtain an expression for linear power corrections similar to eq. (5.32). We write

$$I_V^{\text{unreg}} = W_V \times \lambda F, \quad (5.59)$$

where

$$W_V = \int \frac{d\eta d\varphi}{2(2\pi)^3} \frac{h_V(\eta, \varphi)}{q}, \quad (5.60)$$

with h_V defined in eq. (5.58). In section 5.3 we have shown that the singularities in F can be handled either introducing an analytic regulator or by subtraction. Under the assumptions listed above, the integral in W_V of eq. (5.60) is automatically convergent and no further regularisation is needed. Using eq. (4.62) we get our final formula for the linear power corrections affecting the cumulant

$$\begin{aligned} \mathcal{T}_\lambda[\Sigma(v; \lambda)] &= \int d\sigma^b(\tilde{\Phi}_b) \delta(V(\tilde{\Phi}_b) - v) \frac{\lambda}{q} [\mathcal{N}F(qW_V)] \\ &= \int d\sigma^b(\tilde{\Phi}_b) \delta(V(\tilde{\Phi}_b) - v) \frac{\lambda}{q} \left[-\frac{15}{64} \alpha_s \pi C_F \int d\eta \frac{d\varphi}{2\pi} h_V(\eta, \varphi) \right]. \end{aligned} \quad (5.61)$$

Now we note that rather than using the full expression for the shape variable, also including recoil effects, we can simply consider

$$V(\{\tilde{p}\}, l) - V(\{\tilde{p}\}) \equiv \frac{l_t}{q} \hat{h}(\eta, \varphi). \quad (5.62)$$

We know indeed that $l_t \hat{h}$ must differ from $l_t h$ by terms linear in the components of l , i.e. we must have

$$\hat{h}(\eta, \varphi) - h(\eta, \varphi) = Ae^\eta + Be^{-\eta} + C \cos \varphi + D \sin \varphi, \quad (5.63)$$

²We subtle that not all shape variables satisfy this requirement. The jet-broadening, for instance, does not.

where A and B are the same for all acceptable mappings, and C and D do not contribute. Now we can move to complete the computation of the shape variable contribution by replacing

$$\hat{h}(\eta, \varphi) \rightarrow \frac{1}{2} \left[\hat{h}(\eta, \varphi) + \hat{h}(\eta, \pi - \varphi) - Ae^\eta - Be^{-\eta} \right], \quad (5.64)$$

with A and B chosen in order to remove the $\eta \rightarrow \infty$ and $\eta \rightarrow -\infty$ behaviour of the first term.

We want to conclude this section by observing that underlying Born mappings that do not satisfy the condition in eq. (4.5), and that are such that the non-linear term has the form $k_\perp g(\eta)$ (e.g. the Catani-Seymour dipole scheme [95]), still have the same feature as linear schemes, as far the absence of linear power corrections is concerned. Nevertheless these schemes do not satisfy the linearity condition in eq. (5.57) and thus cannot be used for a fully analytic treatment. Therefore this does not imply that such schemes are pathological in any sense, and in fact we used them for our numerical checks.

5.5 The case of the C -parameter

We are going to show an application of the arguments exposed before to the case of the C -parameter, explicitly computing the h_V function (for $V = C$). The variation in the C -parameter due to the emission of a single soft massless parton is given by

$$\delta C = -3 \sum_{i>j=1}^3 \frac{(p_i p_j)^2}{(p_i q)(p_j q)} + 3 \sum_{i>j=1}^3 \frac{(\tilde{p}_i \tilde{p}_j)^2}{(\tilde{p}_i q)(\tilde{p}_j q)} - 3 \sum_{j=1}^3 \frac{(\tilde{p}_j l)^2}{(\tilde{p}_j q)(l q)} + \mathcal{O}(l_0^2), \quad (5.65)$$

where we introduced $\delta C = C(\{p\}, l) - C(\{\tilde{p}\})$. We chose a dipole-local mapping, that, for small l , acts as

$$\begin{aligned} p_1 &= \tilde{p}_1 - \frac{(\tilde{p}_2 l)}{(\tilde{p}_1 \tilde{p}_2)} \tilde{p}_1 - \frac{1}{2} l_\perp, \\ p_2 &= \tilde{p}_2 - \frac{(\tilde{p}_1 l)}{(\tilde{p}_1 \tilde{p}_2)} \tilde{p}_2 - \frac{1}{2} l_\perp, \\ p_3 &= \tilde{p}_3. \end{aligned} \quad (5.66)$$

We observe that the mapping in eq. (5.66), besides being accurate up to terms of order l_0^2 , is also accurate in the hard collinear region, up to terms of order l_t^2 . It fully satisfies the momentum conservation, as well as the on-shell conditions for p_1 and p_2 , up to terms of order l_t^2 . Now let us define

$$\begin{aligned} x_i &= \frac{2(\tilde{p}_i q)}{q^2}, \\ r_3 &= \frac{|\tilde{p}_{3,\perp}|}{\sqrt{q^2}} = \sqrt{\frac{(1-x_1)(1-x_2)}{1-x_3}}, \\ l &= l_t \frac{\tilde{p}_1}{\sqrt{s}} \alpha + l_t \frac{\tilde{p}_2}{\sqrt{s}} \beta + l_\perp, \end{aligned}$$

with $\alpha = \exp(\eta)$, $\beta = \exp(-\eta)$ and $s = 2(\tilde{p}_1\tilde{p}_2)$; a straightforward but long computation leads to the following expression for δC :

$$\begin{aligned} \delta C &= \frac{l_t}{q} h_C(\eta, \varphi), \\ h_C(\eta, \varphi) &= \frac{6}{x_3 x_1^2 x_2^2} \left\{ -2r_3^2 \frac{(1-x_3)^{\frac{5}{2}}(x_1+x_2-x_1x_2)\cos^2\varphi}{\beta x_2 + \alpha x_1 + 2\cos\varphi r_3\sqrt{1-x_3}} \right. \\ &\quad + r_3 \frac{(x_1-x_2)(1-x_3)^2(\beta x_2 - \alpha x_1)\cos\varphi}{\beta x_2 + \alpha x_1 + 2\cos\varphi r_3\sqrt{1-x_3}} \\ &\quad \left. + \frac{x_1x_2(1-x_3)^{\frac{3}{2}}(x_1+x_2-2x_1x_2)}{\beta x_2 + \alpha x_1 + 2\cos\varphi\sqrt{1-x_3}} \right\}, \end{aligned} \quad (5.67)$$

that has the same form as eq. (5.58). The first and the third term in the curly bracket decay exponentially for large $|\eta|$, but this does not hold for the second term. Nevertheless $h_C(\eta, \varphi) + h_C(\eta, \pi - \varphi)$ is suppressed for large η , such that our convergence requirements are fully satisfied, and eq. (5.67) can safely be inserted in eq. (5.59), yielding a finite integral, that can be performed with numeric techniques.

It is also interesting to evaluate separately the recoil contribution to h_C . i.e. the contribution coming from the first two terms of eq. (5.65). It reads

$$\begin{aligned} h_C^{\text{rec}}(\eta, \varphi) &= \frac{3}{x_1^2 x_2^2 x_3} \left\{ 2r_3(1-x_1)(1-x_2)[3x_1x_2 - x_1(1-x_1) - x_2(1-x_2)]\cos\varphi \right. \\ &\quad \left. + \frac{x_1x_2}{\sqrt{1-x_3}[\beta x_1(1-x_1)^2 + \alpha x_2(1-x_2)^2 + x_3(1-x_3)^2(\alpha + \beta)]} \right\}. \end{aligned} \quad (5.68)$$

Even though this contribution does not give linear power corrections, it is actually not suppressed in the hard collinear region, at large rapidities. Thus, if we neglect recoil terms when computing shape variable modifications, we will have $h_C^{\text{norec}} = h_C - h_C^{\text{rec}}$ that is ill-behaved at large η . Nevertheless, the terms proportional to $\cos\varphi$ in eq. (5.68) are removed by an azimuthal integration, and we can get rid of the terms growing with η recurring to eq. (5.63), with the coefficients A and B tuned to exactly cancel the large η behaviour. Alternatively, we can also regulate the rapidity integral by introducing an analytic regulator

$$d\eta \rightarrow d\eta e^{-\epsilon|\eta-\eta_q|}, \quad (5.69)$$

being η_q the rapidity of q in the emitting-dipole rest frame. It is easy to check that with the use of this regulator, the contribution of the recoil in eq. (5.68) vanishes.

5.6 Connection with the Milan Factor approach

Now we analyse in detail the connection between our approach and the one exposed in refs. [76, 77], namely the Milan Factor approach.

In the past years it was a common thought that, in order to estimate the linear power corrections affecting shape variables, it was sufficient to consider the corrections due to the

emission of a massive gluon, neglecting its further splitting into a $q\bar{q}$ pair [68, 70, 96, 97]. This approach has been proven to be incorrect in [51], and in [76] it was shown how to properly include the effects of gluon splitting. The result was expressed in a factorised form, with the correction factor, dubbed *Milan factor*, to be applied to previous calculations where the splitting was ignored. This procedure was also proven to be universal [77], and an analytic form of the Milan factor has been extracted from explicit computations of the C -parameter in the two-jet limit in refs. [93, 94]. Until recently, the Milan factor approach has only been used to perform non-perturbative corrections near the two-jet limit. In a recent work [84] the authors applied it to investigate non-perturbative corrections affecting the C -parameter in the symmetric three-jet region $c = 3/4$.

In order to make a connection between the Milan factor approach and our formalism, now we briefly summarise the main points of the former. Following refs. [76, 77], linear power corrections to the cumulative distribution of an observable V can be obtained by first computing its modifications due to the emission of a soft massless gluon, dubbed “gluer”,

$$\delta\Sigma = - \int d\sigma^b \delta(V(\Phi_b) - v) \int \frac{dl_t}{l_t} \left[4 \frac{\alpha_s(l_t) C_F}{2\pi} \right] \frac{l_t}{q} \int d\eta \frac{d\varphi}{2\pi} h_V(\eta, \varphi), \quad (5.70)$$

where l_t is the transverse momentum of the gluer in the emitting-dipole rest frame.³ If one considers the splitting of the gluon, one then applies a “correction” factor to eq. (5.70), by multiplying it by the Milan factor \mathcal{M} that in the large- n_f limit takes the form [93, 94]

$$\mathcal{M} = \frac{15\pi^2}{128}. \quad (5.71)$$

In [76, 77] it was argued that this method is sufficient to compute linear power corrections in phase space regions where the recoil effects are strongly suppressed, i.e. where different recoil prescriptions only lead to modifications of the observable that are at least quadratic in the gluer momentum. The consequence of this argument is that the Milan factor approach cannot be applied in a generic three-jet configuration, as in the non-degenerate three-jet region the recoil effects induce a linear dependence on the gluer momentum.

At this point we can compare the Milan factor formalism to our technique for obtaining linear power corrections. Taking an observable that satisfies the requirements listed in section 5.4, the expression for linear power corrections is reported in eq. (5.61), that can be written as

$$\mathcal{T}_\lambda[\Sigma(v; \lambda)] = - \int d\sigma^b \delta(V(\Phi_b) - v) \left[\mathcal{M} \times 4 \frac{\alpha_s C_F}{2\pi} \frac{\lambda}{q} \int d\eta \frac{d\varphi}{2\pi} h_V(\eta, \varphi) \right]. \quad (5.72)$$

We note that, in the context of the large- n_f formalism, we can obtain the same result as in eq. (5.72) by replacing λ with the integral of an effective coupling (see eq. (3.83) in ref. [24]). Also in the Milan factor approach the non-perturbative correction is expressed in terms of an integral over an effective coupling, and then we see that, in the two-jet and in the symmetric three-jet limit our result is formally equivalent to the one of the Milan factor approach.

³The same arguments follow if there is more than one emitting dipole. Indeed in that case the contributions are summed up.

Nevertheless, our approach is valid in the full three-jet region, at least in the large- n_f limit and for observables of the species described in section 5.4. Thus it follows that our large- n_f derivation both confirms and generalises the Milan factor formalism.

However, we would like to emphasize that the formulation of our result is quite different from the one of refs. [76, 77]. First, we observe that the consolidated view on the Milan-factor approach was to interpret it as a correction to a naive soft gluon result. This argument, though justified from an historical perspective, is slightly misleading, and did cause misunderstanding in the past. In fact, although it is clear from ref. [77] that the Milan factor needs to be applied to the computation of the non-perturbative effect caused by the emission of a massless gluon, it has been sometimes interpreted as the correction factor to be attached to the computation performed using a massive gluon. From our computation, it is apparent that there are no contributions to power corrections arising from the emission of a massive gluon. Furthermore, the effect induced by a massive gluon emission also depends on ambiguities arising when extending the definition of the shape variable to the case of a massive partons in the final state, see footnote 2. The power correction is only determined by the behaviour of the shape variable under the emission of a soft massless parton. This happens because for the shape variable of the kind described in section 5.4, the variation of the observable under the emission of two soft massless partons splits into two contributions, one for each emission, that can be computed in terms of a differential distribution of just one of the two partons arising from gluon splitting. This distribution is invariant (in the radiating dipole rest frame) under boosts along the dipole direction, and even under the azimuthal angle of the emitted parton. This is enough to guarantee that the result needs to have the same form *as if* the parton was just a soft massless gluon emitting by the radiating dipole. Therefore, working with our approach, there is no specific reason to express the result as a correction factor to be applied to the effect computed with the emission of a massless gluon.

Chapter 6

Applications of the factorised approach

In this chapter we will compute linear power corrections to observables other than the C -parameter in the three-jet region, exploiting the formalism we described in chapter 5. Specifically, in section 6.1 we will study the thrust distribution in the three-jet region, due to its great phenomenological interest.

6.1 Linear power corrections to thrust in the three-jet region

Let us consider linear power corrections affecting thrust distribution. Considering all final-state particles as massless, we can define the thrust shape variable T as

$$T = \max_{\vec{n}} \sum_i \frac{|\vec{n} \cdot \vec{p}_i|}{q} \quad (6.1)$$

where \vec{n} is a unit vector, i runs over all final-state particles, and p_i is the momentum of the i -th particle. For ease of notation we will use \vec{n}_m to denote the vector that maximises eq. (6.1), namely the *thrust axis*. Following eq. (6.1) it follows that in the two-jet limit $T = 1$. Since we are not interested in the two-jet region, it is more convenient to define $\bar{T} = 1 - T$, and studying its distribution. Then we consider the cumulant

$$\Sigma(\bar{t}; \lambda) = \sum_F \int d\sigma_F \theta(\bar{T}(\Phi_F) - \bar{t}), \quad (6.2)$$

along the lines of eq. (4.44).

It is easy to demonstrate that the thrust satisfies all the requirements listed in section 5.4. Following eq. (5.61), we can write the linear power corrections affecting the cumulative distribution of the thrust as

$$\mathcal{T}_\lambda[\Sigma(\bar{t}; \lambda)] = \int d\sigma^b \delta(\bar{T}(\tilde{\Phi}_b) - \bar{t}) \frac{\lambda}{q} \left[\frac{15}{8} \alpha_s C_F \pi^3 q W_T \right], \quad (6.3)$$

where

$$W_T = \frac{1}{q} \int \frac{d\eta d\varphi}{2(2\pi)^3} \left| \vec{n}_m \cdot \vec{l} \right|, \quad (6.4)$$

As done in section 5.4, l denotes the momentum of a massless soft parton, whilst η, φ, l_t denote its rapidity, azimuthal angle and absolute value of transverse momentum in the emitting dipole rest frame. We also have $\tilde{l} = l/l_t$. We observe the absence of an overall minus sign in front of eq. (6.3); this is because we are considering the distribution $\bar{T} = 1 - T$. In eq. (6.4) it is implicitly assumed the presence of the analytic regulator of eq. (5.69).

To make easier the evaluation of eq. (6.4) we use a Sudakov parameterisation for the four-vector $n_m = (0, \vec{n}_m)$, writing

$$n_m = \alpha p_1 + \beta p_2 + n_{m,\perp}, \quad (6.5)$$

where $(p_{1,2} n_{m,\perp}) = 0$. As n_m is a space-like vector in the rest frame of q , in an arbitrary frame we have $n^2 = -1$. This leads to

$$n_{m,t} = |n_{m,\perp}| = \sqrt{1 + \frac{(2p_1 t)(2p_2 t)}{(2p_1 p_2)}}. \quad (6.6)$$

The scalar product between n_m and \tilde{l} can be written in terms of the Sudakov variables α and β as follows

$$-2(\vec{n}_m \cdot \vec{l}) = 2(n_m \tilde{l}) = \sqrt{s} e^{-\eta} \left(\alpha + \beta e^{2\eta} - \frac{2n_{m,t}}{\sqrt{s}} e^\eta \cos \varphi_{ln} \right), \quad (6.7)$$

where $s = 2(p_1 p_2)$ and $\varphi_{ln} = \varphi - \varphi_{n_m}$. Replacing $\omega = e^\eta$, we can rewrite eq. (6.7) as

$$2(n_m \tilde{l}) = \frac{\sqrt{s}}{\omega} P(\omega), \quad \text{with} \quad P(\omega) = \beta(\omega - \omega_+)(\omega - \omega_-), \quad (6.8)$$

and

$$\omega_\pm = \frac{n_{m,t} \cos \varphi_{ln} \pm \sqrt{1 - n_{m,t}^2 \sin^2 \varphi_{ln}}}{\sqrt{s} \beta}, \quad (6.9)$$

where we have used the mass-shell relation $n_m^2 = \alpha\beta s - n_{m,t}^2 = -1$ in deriving this expression.

To proceed further we observe that the analytically-regulated integration volume, introduced in eq. (5.69), can be rewritten in terms of ω as

$$d\eta e^{-\epsilon|\eta - \eta_q|} = \frac{d\omega_{\text{reg}}}{\omega}, \quad d\omega_{\text{reg}} = d\omega \left[\left(\frac{\omega}{\omega_q} \right)^{-\epsilon} \theta(\omega - \omega_q) + \left(\frac{\omega}{\omega_q} \right)^\epsilon \theta(\omega_q - \omega) \right], \quad (6.10)$$

being $\omega_q = e^{\eta_q}$. Using eqs. (6.7, 6.8, 6.10), we get the following result for W_T , defined in eq. (6.4)

$$W_T = \frac{\sqrt{s}}{32\pi^3 q} \int d\omega_{\text{reg}} d\varphi \omega^{-2} |P(\omega)|. \quad (6.11)$$

Looking at eq. (6.9), it is clear that, in order to explicitly write $|P(\omega)|$, we need to consider two different cases: case A, when $n_{m,t} < 1$ and case B when $n_{m,t} > 1$. In case A, the roots of $P(\omega)$ are real-valued for all values of φ_{ln} . Furthermore, in this case it holds

$$\sqrt{1 - n_{m,t}^2 \sin^2 \varphi_{ln}} > |n_{m,t} \cos \varphi_{ln}|, \quad (6.12)$$

such that $\omega_+ > 0$ and $\omega_- < 0$ for generic values of φ_{ln} . On the other hand, when case B holds, the two roots assume real values only for $|\sin \varphi_{ln}| < 1/n_{m,t}$. Also

$$\sqrt{1 - n_{m,t}^2 \sin^2 \varphi_{ln}} < |n_{m,t} \cos \varphi_{ln}|, \quad (6.13)$$

as far as a real-valued root exists. Eq. (6.13) implies that, if $\cos \varphi_{ln}$ is negative, both roots ω_{\pm} are negative and if $\cos \varphi_{ln}$ is positive, both roots are positive.

At this point we can write eq. (6.11) as

$$W_T = \frac{\sqrt{s}}{32\pi^3 q} \int d\varphi X_T, \quad \text{with} \quad X_T = \int_0^{\infty} d\omega_{\text{reg}} \omega^{-2} |P(\omega)|, \quad (6.14)$$

and then study cases A and B separately.

For case A we write

$$X_T^A = \int_{\omega_+}^{\infty} d\omega_{\text{reg}} \omega^{-2} P(\omega) - \int_0^{\omega_+} d\omega_{\text{reg}}^{-2} P(\omega), \quad (6.15)$$

or, equivalently,

$$\begin{aligned} X_T^A &= 2 \int_{\omega_+}^{\infty} d\omega_{\text{reg}} \omega^{-2} P(\omega) - \int_0^{\infty} d\omega_{\text{reg}}^{-2} P(\omega) \\ &= -2 \int_0^{\omega_+} d\omega_{\text{reg}} \omega^{-2} P(\omega) + \int_0^{\infty} d\omega_{\text{reg}} \omega^{-2} P(\omega). \end{aligned} \quad (6.16)$$

For case B instead we obtain

$$\begin{aligned} X_T^B &= \int_0^{\infty} d\omega_{\text{reg}} \omega^{-2} P(\omega), & \cos \varphi_{ln} < 0, \\ X_T^B &= -2 \int_{\omega_-}^{\omega_+} d\omega_{\text{reg}} \omega^{-2} P(\omega) + \int_0^{\infty} d\omega_{\text{reg}} \omega^{-2} P(\omega) & \cos \varphi_{ln} > 0 \end{aligned} \quad (6.17)$$

A straightforward computation leads to

$$\int_0^{\infty} d\omega_{\text{reg}} \omega^{-2} P(\omega) = -\frac{2\beta(\omega_+ + \omega_-)}{\epsilon} + \mathcal{O}(\epsilon), \quad (6.18)$$

where the $\mathcal{O}(\epsilon)$ term vanishes upon azimuthal integration, as $\omega_+ - \omega_- \propto \cos \varphi_{ln}$. Hence we can drop all the terms from eqs. (6.16,6.17), where the ω integration is unrestricted. Consequently, for case B we only need no consider the condition $\cos \varphi_{ln} > 0$.

For what concerns case A, we need to distinguish the case $\omega_q < \omega_+$ from the $\omega_q > \omega_+$ one. In the former case we can use the representation in the first line of eq. (6.16), whilst, in the latter we can use instead the second line. Therefore, in either case, after integrating over ω and expanding in ϵ , we get

$$X_T^A = -2\beta \left[\omega_+ - \omega_- \pm \frac{\omega_+ + \omega_-}{\epsilon} - (\omega_+ + \omega_-) \ln \frac{\omega_+}{\omega_q} \right], \quad (6.19)$$

where \pm refers to $\omega_q < \omega_+$ and $\omega_q > \omega_+$, respectively. Dropping out the terms that vanish upon azimuthal integration, we can readjust eq. (6.19) as

$$X_T^A \rightarrow -2\beta [\omega_+ - \omega_- - (\omega_+ + \omega_-) \ln \omega_+] \rightarrow -\frac{4}{\sqrt{s}} \left[\sqrt{1 - n_{m,t}^2 \sin^2 \varphi_{ln}} - n_{m,t} \cos \varphi_{ln} \ln \left(n_{m,t} \cos \varphi_{ln} + \sqrt{1 - n_{m,t}^2 \sin^2 \varphi_{ln}} \right) \right]. \quad (6.20)$$

Inserting eq. (6.20) into eq. (6.14), changing variables from φ to φ_{ln} and performing an azimuthal integration, we arrive at this expression for W_T in the case A

$$W_T|_{\text{case A}} = \frac{\sqrt{s}}{32\pi^3 q} \int_0^{2\pi} d\varphi_{ln} X_T^A = -\frac{1}{2\pi^3 q} [2E(n_{m,t}^2) - K(n_{m,t}^2)]. \quad (6.21)$$

To proceed with case B we only need to study the situation with $\cos \varphi_{ln} > 0$, i.e. the second line of eq. (6.17). As for case A, we drop the terms that vanish after azimuthal integration, and note that the integral is convergent in the $\epsilon \rightarrow 0$ limit. Thus, after performing the ω integration, we obtain

$$X_T^B = -2\beta \left[2(\omega_+ - \omega_-) - (\omega_+ + \omega_-) \ln \frac{\omega_+}{\omega_-} \right] = -\frac{4}{\sqrt{s}} \left[2\sqrt{1 - n_{m,t}^2 \sin^2 \varphi_{ln}} - n_{m,t} \cos \varphi_{ln} \ln \frac{n_{m,t} \cos \varphi_{ln} + \sqrt{1 - n_{m,t}^2 \sin^2 \varphi_{ln}}}{n_{m,t} \cos \varphi_{ln} + \sqrt{1 - n_{m,t}^2 \sin^2 \varphi_{ln}}} \right] \quad (6.22)$$

Inserting X_T^B into eq. (6.14), changing variable $\varphi \rightarrow \varphi_{ln}$ and using the reality condition $|\sin \varphi_{ln}| < 1/n_{m,t}$, we obtain

$$W_T|_{\text{case B}} = \frac{\sqrt{s}}{32\pi^3 q} \int_{\varphi_{\max}}^{\varphi_{\max}} d\varphi_{ln} X_T^B = \frac{\sqrt{s}}{16\pi^3 q} \int_0^{\varphi_{\max}} d\varphi_{ln} X_T^B, \quad (6.23)$$

where $\varphi_{\max} = \arcsin(1/n_{m,t})$. Performing an azimuthal integration we get

$$W_T|_{\text{case B}} = -\frac{n_{m,t}}{\pi^3 q} \left[E\left(\frac{1}{n_{m,t}^2}\right) - \frac{2n_{m,t}^2 - 1}{2n_{m,t}^2} K\left(\frac{1}{n_{m,t}^2}\right) \right]. \quad (6.24)$$

In order to understand whether the results obtained for cases A and B are actually applicable, we observe that, in a three-jet event, the thrust axis in the q rest frame is aligned with the

three-momentum of the most energetic particle. If n_m is aligned with the momentum of either p_1 or p_2 , then $\min(z_1, z_2, z_3) \neq z_3$, being z_i the variables defined as

$$qp_i = \frac{q^2}{2}(1 - z_i), \quad i = 1, 2, 3 \quad (6.25)$$

such that $\sum_{i=1}^3 z_i = 1$, and thus

$$n_{m,t}^2 = \frac{z_1 z_2}{z_3} < \max(z_1, z_2) < 1. \quad (6.26)$$

This result implies that, if $\vec{n}_m \propto \vec{p}_1$, or $\vec{n}_m \propto \vec{p}_2$, then case A applies. On the other hand, if $\vec{n}_m \propto \vec{p}_3$, then $\min(z_1, z_2, z_3) = z_3$ and

$$n_{m,t}^2 = \frac{z_1 z_2 (1 + z_3)^2}{z_3 (1 - z_3)^2} > \frac{z_3^2 (1 + z_3)^2}{z_3 (1 - z_3)^2} > 1, \quad (6.27)$$

so case B applies.

Furthermore we observe that in the three-jet case $n_{m,t} \neq 1$. Indeed, $n_{m,t} = 1$ only if $\vec{n}_{m,t}$ is orthogonal to either $vecp_1$ or \vec{p}_2 , as can be seen in eq. (6.6). Therefore, as in the three-jet case the thrust axis is aligned with the direction of the most energetic particle, from momentum conservation it follows that none of the two remaining particles can be orthogonal to it. Thus, summarising our results, we write

$$\begin{aligned} \mathcal{T}[\Sigma(\bar{t}; \lambda)] &= \int d\sigma^b \delta(\bar{T}(\Phi_b) - \bar{t}) \times \\ &\alpha_s C_F \lambda \frac{15\pi^3}{8} \times \begin{cases} W_T|_{\text{case A}}, & \text{if } \min(z_1, z_2, z_3) \neq z_3 \\ W_T|_{\text{case B}}, & \text{if } \min(z_1, z_2, z_3) = z_3. \end{cases} \end{aligned} \quad (6.28)$$

Now we can check the correctness of our results by studying the two limiting regions $\bar{t} = 0, 1/3$, corresponding to the two-jet limit and the three-jet symmetric point. In the two-jet limit we have $\min(z_1, z_2, z_3) = z_1 = 0$ and $z_2 + z_3 = 1$. This yields to the well-known result

$$\frac{\mathcal{T}[\Sigma(0; \lambda)]}{d\sigma/d\bar{T}|_{\bar{t}=0}} = -\frac{5\pi}{8} \left(\frac{\lambda}{q}\right) \alpha_s. \quad (6.29)$$

In the three-jet symmetric point one has $z_1 = z_2 = z_3 = 1/3$, such that the thrust axis is not unambiguously defined. In this configuration the result is obtained by averaging over the three possible alignments of the thrust axis, i.e.

$$\begin{aligned} \frac{\mathcal{T}[\Sigma(1/3; \lambda)]}{d\sigma/d\bar{T}|_{\bar{t}=1/3}} &= \alpha_s C_F \lambda \frac{15\pi^3}{8} \times \left(\frac{2}{3} W_T|_{\text{case A}} + \frac{1}{3} W_T|_{\text{case B}} \right) \\ &= \left[\frac{5}{6} K\left(\frac{1}{3}\right) - \frac{5}{3} E\left(\frac{1}{3}\right) + \frac{25}{24\sqrt{3}} K\left(\frac{3}{4}\right) - \frac{5}{3\sqrt{3}} E\left(\frac{3}{4}\right) \right] \left(\frac{\lambda}{q}\right) \alpha_s. \end{aligned} \quad (6.30)$$

Chapter 7

Phenomenological predictions in the three-jet region

In this chapter we will apply the formalism developed in the previous sections in order to study linear power corrections affecting the cumulant distribution of the C -parameter and the Thrust, in a generic three-jet configuration.

We start by extracting the leading power corrections that affect the differential distributions of C -parameter and Thrust in the three-jet region, recurring to a simplified semi-analytical method, and comparing the results with the full Large- n_f computation, described in details in appendix C.

In the final part of the chapter we compared the results obtained with a fully analytic computation of the non-perturbative corrections affecting C -parameter and Thrust cumulative distributions, with the ones obtained with the method described in section 7.1.

7.1 A semi-analytic method for extracting leading power corrections

In this section we will expose a simple procedure to determine $\mathcal{O}(\lambda)$ terms only. Indeed in order to do so, all that is needed is the amplitude of the Born process ($\gamma^* \rightarrow q\bar{q}\gamma$ in our case), the eikonal current for the emission of an off-shell massive gluon, and the matrix element for its splitting into a quark-antiquark pair.

First of all we observe that, as done in the previous sections, the 5-body phase space for the final state $q\bar{q}\gamma(g^* \rightarrow q\bar{q})$ can be factorized into the product of a 4-body phase space for the production of a virtual gluon associated with a $q\bar{q}\gamma$ final state times the 2-body phase space for its decay into a $q\bar{q}$ pair. For sake of simplicity, in this section we will use the following notation

$$d\Phi_{3+2}\delta(\lambda^2 - (l + \bar{l})^2) = \frac{1}{2\pi} d\tilde{\Phi}_3 \times d\Phi_{g^*} \times d\Phi_{\text{split}}, \quad (7.1)$$

where $\tilde{\Phi}_3$ is the underlying Born phase space for the final state $q\bar{q}\gamma$, Φ_{g^*} is the radiation phase space for the emitted gluon, and Φ_{split} is the phase space for the $q\bar{q}$ pair arising from

the gluon splitting.¹

Thus, given a generic IR-safe observable O , its expectation value at $\mathcal{O}(\alpha_s)$, due to the emission or exchange of a gluon with mass λ , can be written as

$$\langle O \rangle_\lambda^{(1)} = T_V(\lambda) + T_R(\lambda) + T_R^\Delta(\lambda), \quad (7.2)$$

with, as shown in section 1.3 and reported in ref. [40]

$$T_V(\lambda) = \mathcal{N} \int d\Phi_3 V^{(\lambda)}(\Phi_3) O_3, \quad (7.3)$$

$$T_R(\lambda) = \mathcal{N} \int d\Phi_{3+1} R_{g^*}^{(\lambda)}(\Phi_{3+1}) O_{3+1}, \quad (7.4)$$

$$T_R^\Delta(\lambda) = \mathcal{N} \frac{3\pi}{\alpha_s T_F} \lambda^2 \int d\Phi_{3+2} \delta(\lambda^2 - (l + \bar{l})^2) R_{q\bar{q}}(\Phi_{3+2}) [O_{3+2} - O_{3+(2)}], \quad (7.5)$$

where \mathcal{N} is a normalization constant, Φ_{3+1} is the real emission phase space and Φ_{3+2} is the phase space for the $q\bar{q}\gamma$ ($g^* \rightarrow q\bar{q}$) final state, with $R_{q\bar{q}}$ the associated squared amplitude

$$R_{q\bar{q}}(\Phi_{3+2}) = |\mathcal{M}(p_1, p_2, p_3, l, \bar{l})|^2. \quad (7.6)$$

Furthermore, O_{3+2} denotes the observable computed with the momenta of the $q\bar{q}\gamma q\bar{q}$ final state, while $O_{3+(2)}$ is the observable evaluated with the kinematic of the real configuration, with the final $q\bar{q}$ pair clustered together. In particular, in our example we have $O_{3+2} = \theta[C(p_1, p_2, p_3, l, \bar{l}) - c]$ and $O_{3+(2)} = \theta[C(p_1, p_2, p_3, l + \bar{l}) - c]$. However, in general O can be any (infrared-safe) function of the final-state kinematics. We only require that it vanishes in the two-jet limit, where the three-jet calculation diverges.

Using the notation introduced above and putting $\tilde{\Phi}_b = \tilde{\Phi}_3$, we can write $\langle O \rangle_\lambda^{(1)}$ in eq. (7.2) as follows

$$\langle O \rangle_\lambda^{(1)} = \frac{1}{\sigma} \int d\tilde{\Phi}_b \left\{ V_\lambda O_3 + \int d\Phi_{g^*} M_{\mu\nu}(k, \lambda) \int d\Phi_{\text{split}} P_{\text{split}}^{\mu\nu} O_{3+2} \right\}, \quad (7.7)$$

where $M^{\mu\nu}$ is the squared amplitude for the production of the $q\bar{q}\gamma g^*$ final state, where the polarization vectors of the virtual gluon g^* have been stripped off. Thus we have

$$\sum_\lambda M^{\mu\nu} \epsilon_\mu^{*,\lambda} \epsilon_\nu^\lambda = -M^{\mu\nu} g_{\mu\nu} = R_{g^*}^{(\lambda)}(\Phi_{3+1}). \quad (7.8)$$

The factor $P_{\text{split}}^{\mu\nu}$ in eq. (7.7) is proportional to the squared matrix element for the decay of the virtual gluon with mass λ into a light $q\bar{q}$ pair carrying momenta l and \bar{l} , respectively. To be more precise, we define

$$P_{\text{split}}^{\mu\nu} = \frac{6\pi}{\lambda^2} \text{Tr}(l \gamma^\mu \bar{l} \gamma^\nu), \quad (7.9)$$

¹As explained in section 4.1, in order to factorize the phase space for the final state $q\bar{q}\gamma g^*$ into the product of an underlying Born phase space, times the radiation phase space, we implemented a smooth mapping in the gluon momentum k in the small k limit, that is also soft and collinear safe.

such that the following normalisation holds

$$\int d\Phi_{\text{split}} P_{\text{split}}^{\mu\nu} = -g^{\mu\nu} + \frac{k^\mu k^\nu}{\lambda^2}. \quad (7.10)$$

Furthermore, as we have

$$\frac{4\pi\alpha_s T_F}{\lambda^4} M_{\mu\nu} \text{Tr}(\not{l}\gamma^\mu \not{l}\gamma^\nu) = R_{q\bar{q}}^{(\lambda)}, \quad (7.11)$$

it also follows that

$$\frac{3\pi\lambda^2}{\alpha_s T_F} R_{q\bar{q}}^{(\lambda)} = (2\pi) M_{\mu\nu} P_{\text{split}}^{\mu\nu}. \quad (7.12)$$

Combining this equation with the normalization condition of $P_{\text{split}}^{\mu\nu}$ defined in eq. (7.10), it gets clear that the terms proportional to O_{3+1} and $O_{3+(2)}$ in eqs (7.4) and (7.5) cancel out, and disappear from eq. (7.7).

To proceed further we can manipulate eq. (7.7) as

$$\begin{aligned} \langle O \rangle_\lambda^{(1)} &= \frac{1}{\sigma} \int d\Phi_3 \left\{ \int d\Phi_{\text{rad}} M_{\mu\nu}(k, \lambda) \left[\int d\Phi_{\text{split}} P_{\text{split}}^{\mu\nu} O_{3+2} + O_3 g^{\mu\nu} \right] \right\} \\ &\quad + \frac{1}{\sigma} \int d\Phi_3 \left\{ d\Phi_{\text{rad}} M_{\mu\nu}(k, \lambda) (-g^{\mu\nu}) + V_\lambda \right\} O_3. \end{aligned} \quad (7.13)$$

From the previous arguments it is clear that no linear power corrections can arise from the second line of the above equation, as this involves the virtual corrections and the real emission contribution integrated over the radiation phase space. Therefore only the first line of eq. (7.13) can contribute to $\mathcal{O}(\lambda)$ contributions. Thus we can write

$$\mathcal{T}_\lambda \langle O \rangle_\lambda^{(1)} = \mathcal{T}_\lambda \sigma^{-1} \int d\Phi_3 \left\{ \int d\Phi_{\text{rad}} M_{\mu\nu}(k, \lambda) \left[\int d\Phi_{\text{split}} P_{\text{split}}^{\mu\nu} O_{3+2} + O_3 g^{\mu\nu} \right] \right\} \quad (7.14)$$

where \mathcal{T}_λ is the operator defined in section 4.2, that extracts $\mathcal{O}(\lambda)$ terms from the expression it acts upon. We can immediately observe that the second line in eq. (7.13) has a finite $\lambda \rightarrow 0$ limit, as virtual and integrated real cross sections are combined there. Thus, since the result is infrared finite, the first line in eq. (7.13) also must have a finite $\lambda \rightarrow 0$ limit. This implies that \mathcal{T}_λ in eq. (7.14) acts upon a quantity that starts at $\mathcal{O}(\lambda^0)$ and contains higher-order terms in the λ -expansion.

We can further simplify the expression in eq. (7.14) by observing that the term in the square brackets vanishes when the gluon momentum k gets collinear to the primary quarks, as long as the observable O is infrared and collinear safe. In fact, in this limit O_{3+2} goes into O_3 , and the integral of $P_{\text{split}}^{\mu\nu}$ becomes equal to $-g^{\mu\nu}$. Furthermore, it is reasonable to assume that in the hard collinear limit the left-over of the collinear cancellation does not contribute terms linear in λ . This can be easily verified for the thrust, where a hard collinear splitting changes the momentum of the splitting parton by an amount proportional to the square of the splitting angle, and the sum of the projections of the momenta of the pair onto the thrust axis is equal to the projection of the total. On the other hand we should be worry that this

behaviour does not hold for all the shape variables. Indeed, a generic shape variable may give rise to terms

$$\int \frac{d^2 \vec{k}_\perp}{\vec{k}_\perp^2 + \lambda^2} |\vec{k}_\perp| f(\varphi), \quad (7.15)$$

where \vec{k}_\perp is the transverse momentum of the splitting, φ is its azimuthal angle, and $f(\varphi)$ is a function that does not vanish under azimuthal integration. As we mentioned in section 5.4, in this case hard collinear regions may produce $\mathcal{O}(\lambda)$ terms. In our treatment we assume that the shape variable is such that it cannot give rise to these contributions, i.e. that if any term linear in the absolute value of the transverse momentum does arise, it vanishes upon azimuthal integration.

Thus, after these clarifications about admissible shape variables, we can conclude that for them linear power corrections can only arise if a soft massive gluon is emitted. Therefore, as we said previously, the expression in the square bracket in eq. (7.14) vanishes in the soft limit so that the full integral does not yield $\mathcal{O}(\ln \lambda)$ terms. It follows then that linear terms can only arise from the leading soft-singular part of the real squared amplitude $M^{\mu\nu}$. Thus we can safely substitute

$$M_{\mu\nu}(k, \lambda) \rightarrow B(\Phi_3) P_{\mu\nu}^{\text{soft}}(\Phi_{3+1}), \quad (7.16)$$

where B stands for the Born matrix element, and $P_{\mu\nu}^{\text{soft}}$ is the soft factor that arises from the product of the eikonal currents describing the emission of a soft *massive* gluon in the above process. Thus eq. (7.14) can be rewritten as

$$\begin{aligned} \mathcal{T}_\lambda \langle O \rangle_\lambda^{(1)} &= \mathcal{T}_\lambda \sigma^{-1} \int d\Phi_3 B(\Phi_3) \\ &\times \int d\Phi_{\text{rad}} P_{\mu\nu}^{(\text{soft})}(\Phi_{3+1}) \left[\int d\Phi_{\text{split}} P_{\text{split}}^{\mu\nu} O_{3+2} + g^{\mu\nu} O_3 \right]. \end{aligned} \quad (7.17)$$

As the term in the square bracket does not contribute in the soft limit, in principle it is not necessary to use an exact phase space to compute $\mathcal{O}(\lambda)$ terms in eq. (7.17). Nevertheless, performing a numeric computation, it may be convenient to integrate over the exact phase space, even though, in this case, unwanted singularities may develop from the soft factor $P_{\text{soft}}^{\mu\nu}$, as we now explain. Indeed, we can express $P_{\text{soft}}^{\mu\nu}$ in terms of the momenta of the real kinematics

$$P_{\text{soft}}^{\mu\nu}(k) = 4g_s^2 C_F \left(\frac{p_1^\mu}{(p_1 + k)^2} - \frac{p_2^\mu}{(p_2 + k)^2} \right) \left(\frac{p_1^\nu}{(p_1 + k)^2} - \frac{p_2^\nu}{(p_2 + k)^2} \right) \quad (7.18)$$

or in terms of the underlying Born momenta

$$\tilde{P}_{\text{soft}}^{\mu\nu}(k) = 4g_s^2 C_F \left(\frac{\tilde{p}_1^\mu}{(\tilde{p}_1 k)} - \frac{\tilde{p}_2^\mu}{(\tilde{p}_2 k)} \right) \left(\frac{\tilde{p}_1^\nu}{(\tilde{p}_1 k)} - \frac{\tilde{p}_2^\nu}{(\tilde{p}_2 k)} \right). \quad (7.19)$$

The two equations are equivalent, as long as one performs the integration over k in the region where momenta are soft. On the other hand, if one uses the soft approximation outside its range of validity, spurious divergences may arise. For instance, let us consider the case where

p_1 becomes soft so that in the rest frame of $\tilde{p}_1 + \tilde{p}_2$ (i.e. of the $p_1 + p_2 + k$) the gluon recoils against p_2 and gets collinear to \tilde{p}_1 . Although this is not a singular configuration of the full process, eq. (7.19) develops a collinear $\tilde{p}_1 \parallel k$ divergence, even if the original p_1 and k are not collinear to each other. This kind of singularity in eq. (7.19) is spurious, and would be removed by considering next-to-leading soft terms in the mapping, that we are neglecting. In order to avoid this situation, we can simply restrict the integration over the radiation phase space, to exclude the regions where either p_1 or p_2 are soft. We can do this by introducing a proper θ -function attached to $d\Phi_{\text{rad}}$ in eq. (7.17)

$$d\Phi_{\text{rad}} \rightarrow d\Phi_{\text{rad}} \theta\left(\eta - \frac{(\tilde{p}_1 k) + (\tilde{p}_2 k)}{(\tilde{p}_1 \tilde{p}_2)}\right), \quad (7.20)$$

with $0 < \eta < 1$.² In what follows we will not show this θ -function, but it is always assumed to be present in $d\Phi_{\text{rad}}$.

Similarly, we also need to take care of the kinematic regions where emitted photon is either soft or collinear to one of the primary quarks, associated with a hard gluon. This region contributes to the three-jet region as well, and gives a divergent contribution. Nevertheless, as in this case the gluon must be hard, no linear terms in λ can arise from this kinematic configuration.³ Thus we chose to suppress this region multiplying the amplitude by the factor

$$\frac{1}{(\tilde{p}_1 + k)^2 (\tilde{p}_2 + k)^2} \times \left[\frac{1}{(\tilde{p}_1 + \tilde{p}_3)^2 (\tilde{p}_2 + \tilde{p}_3)^2} + \frac{1}{(\tilde{p}_1 + k)^2 (\tilde{p}_2 + k)^2} \right]^{-1}, \quad (7.21)$$

that dampens the photon-(anti)quark collinear singularity and approaches one if the gluon is unresolved, so that it does not affect $\mathcal{O}(\lambda)$ terms.

Finally, as the integration over k in eq. (7.17) is not restricted to the soft region, we can, in principle, observe the arising of terms associated with hard gluons, and contributing at $\mathcal{O}(\lambda^0)$. Thus, in order to remove them, we consider

$$\begin{aligned} \mathcal{T}_\lambda \langle O \rangle_\lambda^{(1)} &= \mathcal{T}_\lambda \sigma^{-1} \int d\Phi_3 B(\Phi_3) \left\{ \left[\int d\Phi_{\text{rad}} P_{\mu\nu}^{(\text{soft})} \left[\int d\Phi_{\text{split}} P_{\text{split}}^{\mu\nu} O_{3+2} + g^{\mu\nu} O_3 \right] \right] \right. \\ &\quad \left. - \left[\int d\Phi_{\text{rad}} P_{\mu\nu}^{(\text{soft})} \left[\int d\Phi_{\text{split}} P_{\text{split}}^{\mu\nu} O_{3+2} + g^{\mu\nu} O_3 \right] \right]^{\lambda=0} \right\}. \end{aligned} \quad (7.22)$$

Eq. (7.22) allows us to extract the leading power corrections affecting a shape variable, by only considering the matrix element of the Born process and eikonal factors describing the soft emission of a massive gluon and its further splitting into a $q\bar{q}$ pair.

After evaluating eq. (7.22) recurring to numerical techniques, we are able to compare the results with the ones obtaining from a full large- n_f computation, described in appendix C, also comparing the two alternative formulae for the soft eikonal factors eqs. (7.18), (7.19), finding no significant differences.

²In our numerical implementation we chose $\eta = 1/2$.

³Of course this divergence can be cancelled by also considering virtual QED corrections. But again, this would involve a hard gluon, without leading to $\mathcal{O}(\lambda)$ corrections.

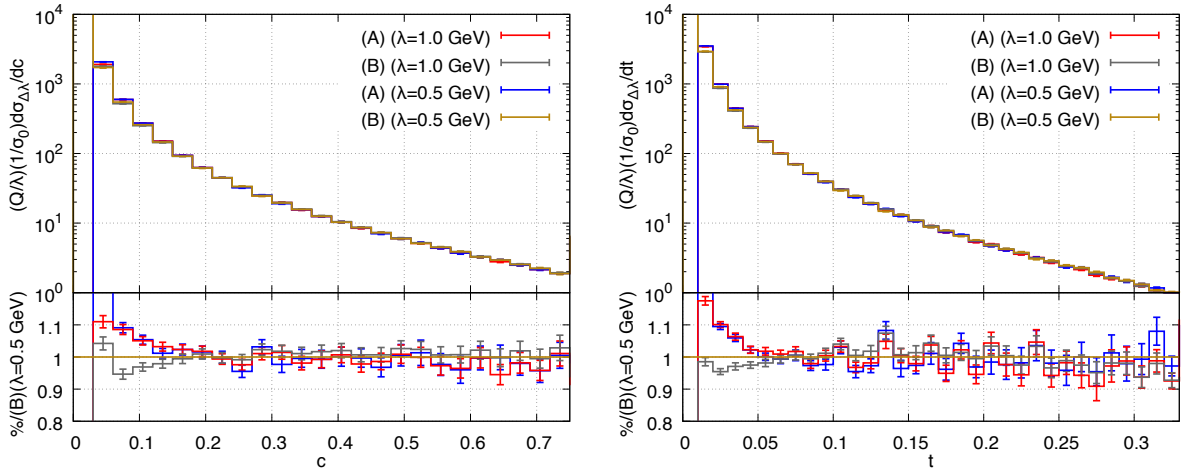


Figure 7.1: Non-perturbative shift in the differential distributions for the C -parameter (left) and the thrust (right), obtained from eq. (7.22) (A), and from a full calculation in the large- n_f limit (B). Results are shown for the process $\gamma^* \rightarrow d\bar{d}\gamma$, with $Q = 100$ GeV and $\lambda = 0.5$ GeV, $\lambda = 1$ GeV.

7.1.1 Comparison with the full large- n_f computation

As a preliminary test of our approach, we compute $\mathcal{O}(\lambda)$ terms for various observables, recurring to eq. (7.22) and compare them with the results of a full numerical calculation performed in the large- n_f approximation. This comparison is reported in figure 7.1 for the differential distributions of the C -parameter and the thrust. For both cases we perform the computation for $\lambda = 0.5$ GeV and $\lambda = 1$ GeV. Furthermore, for the numerical approach based on eq. (7.22) we use eq. (7.19) for the soft amplitude. Further details of the full large- n_f calculation can be found in appendix C.

As the results shown in figure 7.1 are divided by the gluon mass λ , the agreement between the two curves for $\lambda = 0.5$ GeV and $\lambda = 1$ GeV cases indicates that the dependence of the observable on λ is indeed linear and that eq. (7.22) captures the correct λ -dependence. We can also observe that for values of the C -parameter $c \lesssim 0.15$ and the thrust $t \lesssim 0.07$, the results of the exact calculation performed for two values of λ deviate from each other and from the result obtained through the use of eq. (7.22). This suggests that in these regions higher powers of λ get important and, in order to enable the extraction of λ terms from the large- n_f computation smaller values of the gluon mass λ are needed. However, apart of this caveat, figure 7.1 gives a strong evidence that eq. (7.22) can be used to compute linear power corrections affecting generic shape variables.

7.2 Non-perturbative correction as a shift in the shape variable

Before showing the results obtained evaluating non-perturbative corrections affecting the C -parameter and the Thrust in the three-jet region, we will briefly summarise the history of such computations.

Non-perturbative corrections to shape variables in the two-jet limit have been extensively considered in refs. [51, 69–72, 74–77, 96] (see ref. [24] for a review). These non-perturbative corrections are usually employed in conjunction with the perturbative ones, as well as with resummations, in order to extract reliable values of the strong coupling constant α_s from data on e^+e^- annihilation into hadrons [64, 65, 67, 98, 99]. Non-perturbative corrections are usually fitted in the two-jet region and then extrapolated to the three-jet region, where the α_s fits are performed. This approach relies upon the assumption that the non-perturbative corrections in the two- and the three-jet regions are equal.

Nevertheless, in a recent paper [84], the authors tried to deeply investigate the behaviour of these power corrections away from the two-jet limit, studying the C -parameter distribution that, besides the Sudakov region at $c = 0$, has a second Sudakov region in correspondence of the symmetric three-jets configuration, $c = 3/4$. The presence of this second region allows for a calculation of non-perturbative corrections with exactly the same techniques as the ones used for the two-jet region. It was found actually [84] that there is a significant difference between power corrections in the two Sudakov regions. Furthermore, the authors of ref. [84] also showed that power corrections in the region where α_s is fitted strongly depend on the model chosen in order to interpolate between the two Sudakov regions. Clearly these results require to deeply investigate the dependence of non-perturbative corrections in a generic three-jet kinematic configuration.

In the previous sections we have shown how to compute linear power corrections in the three-jet region with a fully analytic approach. Now we are able to compare the results obtained with this approach with the ones obtained with the numeric techniques described in section 7.1. Furthermore we are also in the position to compare our findings with the approximated results of ref. [84]. Conversely, we should be able to reproduce the ratio of non-perturbative corrections in the three-jet symmetric point to the non-perturbative corrections in the two-jet limit obtained in ref. [84].

Non-perturbative corrections are often presented as a shift with respect to the perturbative result [75]. More precisely, one can write the full, “hadronic” cumulant for a generic shape variable V as [75]

$$\tilde{\Sigma}^{\text{had}}(v) = \tilde{\Sigma}(v - \delta_{\text{NP}}(v)) \approx \tilde{\Sigma}(v) - \frac{1}{\sigma} \frac{d\sigma}{dV} \delta_{\text{NP}}(v), \quad (7.23)$$

where we define the perturbative cumulant as

$$\tilde{\Sigma}(v) = \frac{1}{\sigma} \int_0^c dV \frac{d\sigma}{dV}. \quad (7.24)$$

Recalling the definition of Σ given in eq. (4.44), and the fact that the total cross section σ is

free from linear power corrections, we get

$$\delta_{\text{NP}}(v) = \frac{\mathcal{T}_\lambda[\Sigma(v; \lambda)]}{d\sigma/dV}. \quad (7.25)$$

As we are mostly interested in studying the dependence of non-perturbative corrections on kinematics, we need to parameterise δ_{NP} as

$$\delta_{\text{NP}}(v) = h\zeta(v), \quad h \equiv \delta_{\text{NP}}(0), \quad (7.26)$$

from that it follows that $\zeta(0) = 1$. In what follows we will only discuss the behaviour of the function $\zeta(v)$.

We start by considering the process $\gamma^*(q) \rightarrow q(p_1) + \bar{q}(p_2) + \gamma(p_3)$, with only the $q\bar{q}$ emitting dipole. Thus we write

$$\delta_{\text{NP}}^{q\bar{q}\gamma} = h\zeta_{q\bar{q}}(v), \quad (7.27)$$

with $\zeta_{q\bar{q}}(0) = 1$. We observe that, since for $v = 0$ the $q\bar{q}\gamma$ configuration approaches a two-parton $q\bar{q}$ configuration, h must correspond to the non-perturbative shift computed in the literature for the two-jet case. Thus, for the C -parameter we have $h = -(\lambda/q)\alpha_s \times 15\pi^2/16$, while for the thrust $h = -(\lambda/q)\alpha_s \times 5\pi/8$, as can be seen in eqs. (5.22) and (6.29).

In fig. 7.2 we show the analytic results compared to the ones obtained through the method described in section 7.1, for $\zeta_{q\bar{q}}$, for both the C -parameter and the thrust, taking $q = 100$ GeV. For the numerical results we consider three different values of the gluon mass $\lambda = 1, 0.5, 0.1$ GeV, and observe that the numerical results converge to the analytic one, to a good approximation. Nevertheless, it is evident from fig. 7.2 that the agreement is not actually perfect, and that even smaller values of λ should be chosen in order to improve the situation. Unfortunately, as the numerical results involve extra quadratic terms in λ (eventually enhanced by powers of $\ln \lambda$), it is not trivial to involve very small values of λ . We also note that the analytic and numerical results tend to depart from each other at small v , for both the C -parameter and the thrust. This happens because, in this region, the effective hard scale is reduced and then the expansion parameter for power corrections is no longer λ/q , but rather λ divided by the reduced scale. On the other hand, the analytic calculation only contains linear power corrections, and it is not affected by these numerical issues.

Furthermore, looking at fig. 7.2 we observe that, for small values of V , $\zeta_{q\bar{q}}$ approaches unity. This can be easily explained by the fact that soft emissions factorize independently. So, in the dominant region where both the photon and the gluon are soft, the gluon behaves as if it was radiated by a $q\bar{q}$ dipole (see appendix D).

7.3 Including radiation from the quark-gluon dipole

The results shown in fig. 7.2 have been obtained considering the simplified process $\gamma^* \rightarrow q + \bar{q} + \gamma$ and not the much more interesting case of $\gamma^* \rightarrow q + \bar{q} + g$. As we explained in the introduction, this is a very well-known limitation of the large- n_f formalism, as processes containing gluons at the Born level have never been computed using this approach.

Nevertheless, even though we do not currently know how to overcome this limitation from a theoretical point of view, the structure of the results that we obtained allows us to

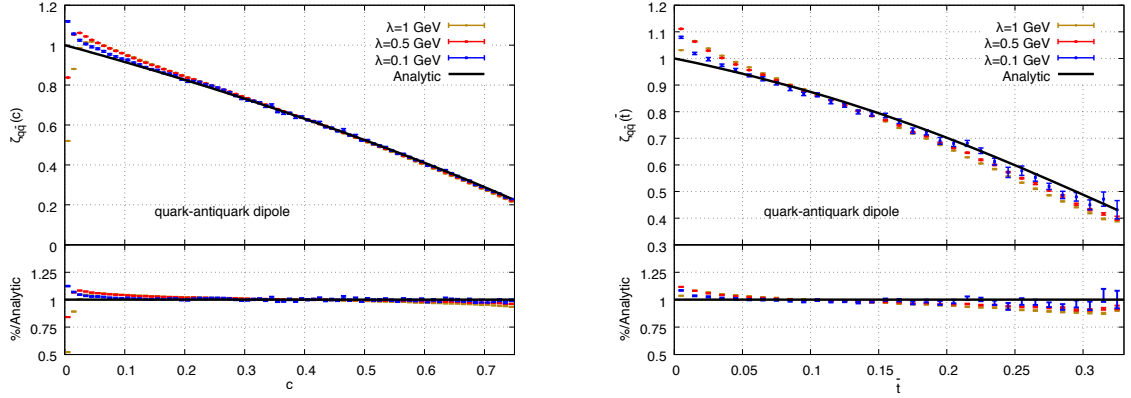


Figure 7.2: The function $\zeta_{q\bar{q}}(v)$ for the C -parameter (left panel) and the thrust $\bar{T} = 1 - T$ (right panel), evaluated numerically using $q = 100$ GeV and $\lambda = 0.1, 0.5, 1$ GeV, compared to the analytic computation (solid line). In the lower panels we reported the ratio plot of each numerical curve with respect to the analytic one.

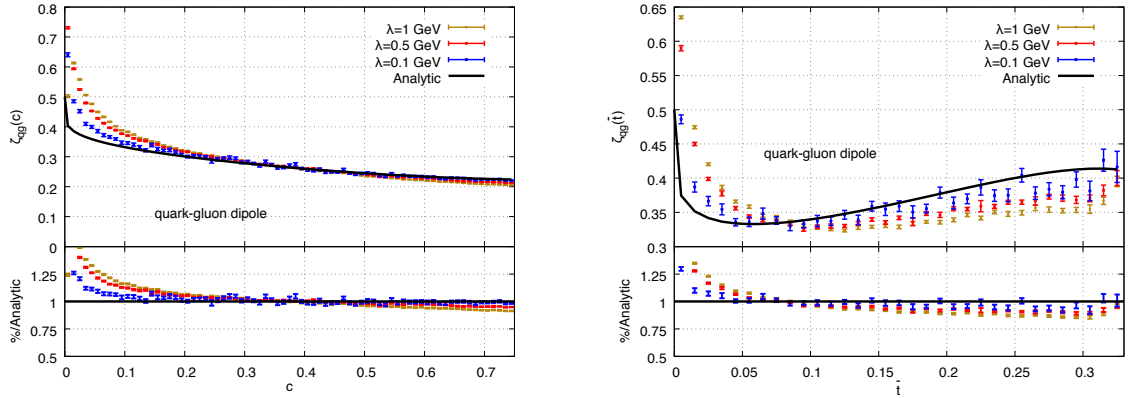


Figure 7.3: Same as fig. 7.2 but for the qg dipole.

speculate that it could be straightforward to do so. Our result, indeed, shows that linear power corrections affecting shape variables are entirely captured by the leading soft limit of the squared amplitude of the $\gamma^* \rightarrow q + \bar{q} + \gamma + g$ process. For the cases considered so far, the soft approximation originates from a color dipole formed by the $q\bar{q}$ pair. Thus it is tempting to speculate that, for the real three-jet production process $\gamma^* \rightarrow q + \bar{q} + g$, one can probe the presence of linear power corrections by simply considering the emission of an additional soft massive gluon off *all* the QCD dipoles, namely $q\bar{q}$, qg , $\bar{q}g$, that are present in this case, accounting for the relevant color factors. Once again, we stress that we are not in the condition of justifying this statement with a solid theoretical argument, but we are confident that this provides a reasonable conjecture.

Since the contributions of the three dipoles are additive, we can write

$$\zeta(v) = \zeta_{q\bar{q}}(v) \frac{C_F - C_A/2}{C_F} + \zeta_{qg}(v) \frac{C_A}{C_F}, \quad (7.28)$$

where we have exploited the fact that the qg and $\bar{q}g$ dipoles contribute equally. The function $\zeta_{qg}(v)$ is defined in the same way as $\zeta_{q\bar{q}}(v)$, except that we now are assuming that the radiating dipole is qg (or $\bar{q}g$). However, we keep the same color factor and the same normalization h used for the $q\bar{q}$ case; hence the $1/C_F$ factor in eq. (7.28).

We immediately observe that in both cases the ζ_{qg} function must approach the value $1/2$ in the two-jet limit. This can be easily explained observing that in this limit ζ in eq. (7.28) must be one by angular ordering arguments and, since $\zeta_{q\bar{q}}$ approaches one, it follows that ζ_{qg} approaches $1/2$ (see appendix D). Furthermore, in the three-jet limit, ζ_{qg} approaches the same value as $\zeta_{q\bar{q}}$. This stands because, in the symmetric limit the $q\bar{q}$ and qg dipoles are geometrically equivalent and, once color factors are removed, they must give the same results.

In order to obtain a more realistic prediction, the value of the constant h should be corrected to include also the effects due to the gluon splitting into two gluons, as it is commonly done in the dispersive model [76, 77, 94], but this is irrelevant for us, since we only report results for the ζ function.

In fig. 7.3 we compare analytic and numeric results, as done in fig. 7.2 for the $q\bar{q}$ dipole only. We observe that also in this case the numerical result converges towards the analytic one and that all the features discussed in connection with fig. 7.2 are also present for the case of a qg ($\bar{q}g$) dipole. From figure 7.3 we also note the numerical results for the qg dipole is less stable than the results for the $q\bar{q}$ one (and it is worse for the thrust than for the C -parameter), making in this way highly useful the availability of an analytic computation.

The inferior stability of the numerical result for the qg dipole with respect to the $q\bar{q}$ case may be related to the fact that the hard emitting gluon is generally softer than the emitting quarks. Thus the effective Q of the emission is smaller in the qg case, leading to larger non-perturbative effects, being they proportional to λ/Q . For what concerns the thrust, we recall that it vanishes in the symmetric three-jet configuration at Born level. This is different for the C -parameter, that approaches a constant there.

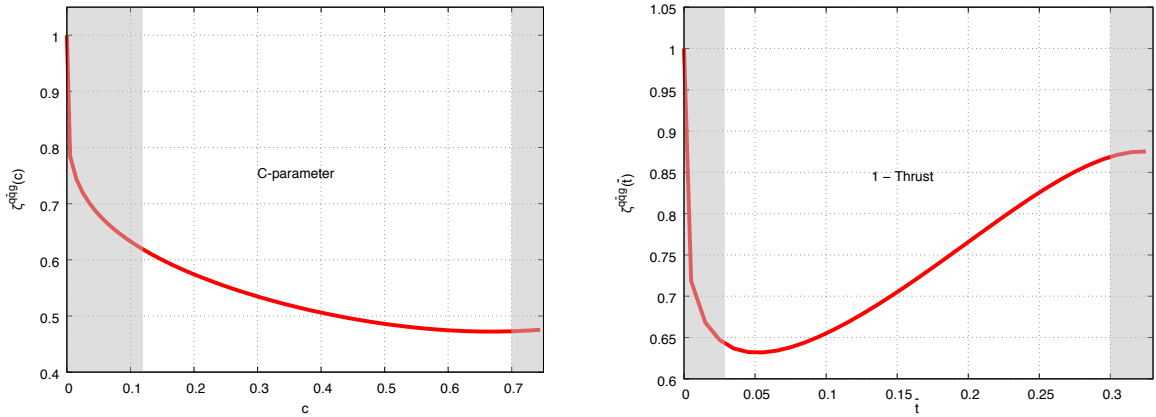


Figure 7.4: Same as fig. 7.2, but for the sum of all the QCD dipoles, with each contribution supplemented with its own color factor, according to eq. (7.28). The grey shading areas show the regions that are usually excluded from the α_s fits [84].

7.4 Results for the C -parameter and the thrust in the three-jet region and comparison with existing literature

After validating the analytic results against the numerical ones obtained thanks to the method described in section 7.1, we can compare our predictions to the results in the literature. In figure 7.4 we show our prediction for the function $\zeta^{q\bar{q}g}$ for both the C -parameter (left) and the thrust (right) cumulative distributions, according to eq. (7.28). In those plots the grey shaded areas represent the kinematic regions that are usually neglected from high precision α_s fits [84]. We also observe that for both the C -parameter and the thrust the shape of the non-perturbative corrections in the bulk of the three-jet region is non-trivial. Now we want to compare our results for the C -parameter with the predictions of ref. [84]. Exploiting eqs. (5.22, 5.23) it is straightforward to check the agreement between our results and the ones of ref. [84] for the endpoints $c = 0, 3/4$.⁴ Nevertheless, the formalism of ref. [84] does not allow to give an unambiguous prediction in the bulk of the three-jet region. Instead, the authors of ref. [84] recurred an agnostic approach, obtaining different results, depending on the assumption they made in treating the recoil momentum due to the emission of a soft massless gluon (see their fig. 3). Furthermore it is interesting to note that most of the recoil schemes adopted in ref. [84] (Catani-Seymour [95], PanLocal (antenna variant) and PanGlobal [100]) give the same result. It turns out that this result is also compatible with our prediction based on eq. (7.28).⁵ On the other hand, the FHP (Forshaw-Holguin-Plätzer) scheme of ref. [101] leads to a quite different prediction.

We can provide a clear explanation of why this is the case, recurring to our formalism. Indeed, the Catani-Seymour, PanLocal and PanGlobal schemes all satisfy the smoothness

⁴We subtle that our definition of $\zeta^{q\bar{q}g}$ and ζ in ref. [84] differ for a factor of 3π .

⁵We kindly acknowledge the authors of ref. [84] for providing us the input data of their fig. 3.

requirement in the soft limit in order not to obtain linear power corrections arising from recoil terms. Thus, if one uses these schemes, then a naive soft analysis leads to the correct result for the estimate of linear power corrections affecting the C -parameter, without additional contributions. Adopting the FHP scheme this does not hold anymore, as this recoil scheme does not satisfy our smoothness requirements.⁶ In the follows we will elaborate further on this point.

Let us first consider the PanLocal (antenna) mapping. This is dipole-local, that means that it preserves the four-momentum of the radiating dipole. It is defined as

$$p_1 = \alpha_1 \tilde{p}_1 + \beta_1 \tilde{p}_2 - f l_\perp, \quad p_2 = \alpha_2 \tilde{p}_1 + \beta_2 \tilde{p}_2 - (1 - f) l_\perp, \quad (7.29)$$

being l the momentum of the radiated soft gluon and α_i and β_i ($i = 1, 2$) specified by the momentum conservation and on-shell requirements

$$p_1 + p_2 + l = \tilde{p}_1 + \tilde{p}_2, \quad p_{1/2}^2 = 2\alpha_i \beta_i (p_1 p_2) + \mathcal{O}(l_\perp^2) = 0. \quad (7.30)$$

Eqs. (7.30) can be satisfied only if either $\beta_1 = \alpha_2 = 0$ or $\beta_2 = \alpha_1 = 0$, up to terms of order l_\perp^2 . Assuming the first assignment holds, eq. (7.29) yields

$$\alpha_1 = 1 - \frac{(l\tilde{p}_2)}{(\tilde{p}_1\tilde{p}_2)}, \quad \beta_2 = 1 - \frac{(l\tilde{p}_1)}{(\tilde{p}_1\tilde{p}_2)}, \quad (7.31)$$

such that, in the soft limit, the PanLocal scheme takes the form

$$p_1 = \left(1 - \frac{(l\tilde{p}_2)}{(\tilde{p}_1\tilde{p}_2)}\right) \tilde{p}_1 - f l_\perp, \quad p_2 = \left(1 - \frac{(l\tilde{p}_1)}{(\tilde{p}_1\tilde{p}_2)}\right) \tilde{p}_2 - (1 - f) l_\perp. \quad (7.32)$$

The PanLocal choice for f is

$$f = \frac{e^{2\bar{\eta}_k}}{1 + e^{2\bar{\eta}_k}}, \quad (7.33)$$

where $\bar{\eta}_k$ is a rapidity-like variable, defined as

$$\bar{\eta}_l = \frac{1}{2} \ln \frac{(l\tilde{p}_1)(\tilde{p}_1 q)}{(l\tilde{p}_1)(\tilde{p}_2 q)}. \quad (7.34)$$

Thus the PanLocal mapping is clearly non-linear in the soft limit. Nevertheless, the non linear term is proportional to l_\perp^μ , with an azimuthally-independent coefficient. Thus, when evaluating recoil effects using this mapping, the non-linear term always cancels after azimuthal integration, and the PanLocal mapping satisfies the smoothness criteria. Similarly, the Catani-Seymour mapping is also non-linear, but, again, the non-linear term vanishes after azimuthal integration.

The PanGlobal mapping, instead, is defined by first introducing the following intermediate variables

$$\bar{p}_1 = \left(1 - \frac{(l\tilde{p}_2)}{(\tilde{p}_1\tilde{p}_2)}\right) \tilde{p}_1, \quad \bar{p}_2 = \left(1 - \frac{(l\tilde{p}_1)}{(\tilde{p}_1\tilde{p}_2)}\right) \tilde{p}_2. \quad (7.35)$$

⁶However we stress that this feature does not affect the logarithmic accuracy of the dipole showers based upon such a recoil scheme.

Then one needs to find a boost B followed by a rescaling R , to be applied to \bar{p}_1 , \bar{p}_2 and p_3 , such that

$$p_{1/2} = RB\bar{p}_{1/2}, \quad p_3 = RB\tilde{p}_3, \quad l' = RB\tilde{l}. \quad (7.36)$$

It is quite easy to check that, in the small- l limit, this yields the mapping

$$\begin{aligned} p_1 &\approx \tilde{p}_1 - \frac{(\tilde{p}_2 l)}{(\tilde{p}_1 \tilde{p}_2)} \tilde{p}_1 - \frac{(\tilde{p}_1 q)}{q^2} l_\perp - \frac{(l_\perp q)}{q^2} \tilde{p}_1, \\ p_2 &\approx \tilde{p}_2 - \frac{(\tilde{p}_1 l)}{(\tilde{p}_1 \tilde{p}_2)} \tilde{p}_2 - \frac{(\tilde{p}_2 q)}{q^2} l_\perp - \frac{(l_\perp q)}{q^2} \tilde{p}_2, \\ p_3 &\approx \tilde{p}_3 - \frac{(\tilde{p}_3 l)}{q^2} l_\perp + \frac{(\tilde{p}_3 l_\perp)}{q^2} q - \frac{(l_\perp q)}{q^2} \tilde{p}_3. \end{aligned} \quad (7.37)$$

This mapping is fully linear, and satisfies the smoothness requirements of section 4.1. As we have mentioned previously, this implies that with these recoil schemes, linear power corrections are completely captured by a naive soft analysis.

The FHP mapping is very similar to the PanGlobal one, with the difference that only one side of the dipole gets rescaled. From a practical point of view, one parameterises the intermediate barred momenta

$$\bar{p}_1 = \left(1 - \frac{(l\tilde{p}_2)}{(\tilde{p}_1\tilde{p}_2)}\right) \tilde{p}_1, \quad \bar{p}_2 = \tilde{p}_2, \quad (7.38)$$

with probability $f(\bar{\eta}_l)$, where f and $\bar{\eta}_l$ are given in eqs. (7.33) and (7.34) and coincide with the PanLocal/PanGlobal ones. The parameterisation

$$\bar{p}_1 = \tilde{p}_1, \quad \bar{p}_2 = \left(1 - \frac{(l\tilde{p}_1)}{(\tilde{p}_1\tilde{p}_2)}\right) \tilde{p}_2, \quad (7.39)$$

is instead selected with probability $1 - f(\bar{\eta}_l)$. Then the kinematic reconstruction proceeds as in PanGlobal, where all the momenta are rescaled in order to preserve the mass of the total system, and then boosted in the original event frame. Thus it is clear that the soft limit is non-linear in the longitudinal components of the radiated parton and, therefore, it does not satisfy the smoothness conditions of section 4.1. As a consequence, an analysis of soft emissions is not sufficient to evaluate linear power corrections recurring to this recoil scheme. This is exactly what is reported in fig. 3 of ref. [84]. We conclude this section by stressing the fact that, in correspondence of the endpoints $c = 0$, $c = 3/4$, all the recoil schemes yield the same result. This is expected, as in these regions the sensitivity of the shape variable to recoil effects is strongly suppressed [84].

Chapter 8

Conclusions

In the second part of this work we performed an explicit and analytic computation of linear power corrections affecting the C -parameter and the thrust distributions, showing that our arguments also apply to a larger class of shape variables.

The main result of our work can be summarised in a simple statement: for a shape observable that is sensitive to the presence of colored particles in the final state, linear power corrections affecting the cumulant distribution in the three-jet region can be written as the product of a universal, constant factor times the behaviour of the shape variable under the emission of a single soft massless parton. Our findings also apply to the two-jet region, where an equivalent result has been formulated long ago [77].

We performed the computation working within the large- n_f model of QCD, considering a $q\bar{q}\gamma$ final state, rather than a $q\bar{q}g$. In this framework we are perfectly able to estimate the linear renormalon contribution affecting the shape observable, associated with the power corrections arising from the emission of a soft virtual gluon which can either eventually fluctuate into virtual $q\bar{q}$ pairs or, eventually, decay into one of them.

Furthermore, since renormalons can be studied considering soft emissions, we can elaborate that, when considering the realistic case of a $q\bar{q}g$ final state, linear power corrections can be obtained by summing up the soft emissions off all the three colour dipoles, namely $q\bar{q}$, qg and $\bar{q}g$, each weighted for its own color factor. In such a way we obtain a theoretical prediction that can be confronted with data.

Our assumptions are essentially the same that underly the so called *dispersive model* of power corrections [76, 77]. This model is indeed fully consistent with the large- n_f limit of QCD, and it has been recently applied for computing power corrections to the C -parameter in the three-jet symmetric point [84].

At this point it is convenient to summarise the motivations that allow for a computation of power corrections in the two-jet region, in the three-jet symmetric point [84], and in the generic three-jet configuration, as done in this work. Let us start by considering the cumulant of a generic shape variable V

$$\Sigma(v) = \int d\sigma(\{\tilde{p}\})\theta(V(\{\tilde{p}\}) - v) + \int d\sigma(\{p, k\})\theta(V(\{p, k\}) - v), \quad (8.1)$$

where with $\{\tilde{p}\}$ we denote the hard final state momenta with no soft particles emitted, $\{p\}$

denote the hard final state momenta of the kinematic configuration in that a soft gluon has been emitted, and with k we label generically the sum of the momenta of the final state particles arising from the radiated soft gluon. Furthermore, we assume that $\sigma(\{\tilde{p}\})$ also contains the virtual soft gluon corrections, such that the left-hand side of eq. (8.1) contains all the relevant corrections to the cumulant. As in the previous sections, $V(\{\tilde{p}\})$ and $V(\{p\}, l)$ stand for the values of the shape variable computed with the hard final state partons (without soft gluon emission) and for the final state including the gluon emission and its decay products.

In the two-jet region $v \rightarrow 0$, we have a final state with two back-to-back partons. Thus $V(\{\tilde{p}\})$ takes a constant value, and we can rewrite eq. (8.1) as follows

$$\begin{aligned} \Sigma(v) &= \left[\int d\sigma(\{\tilde{p}\}) + \int d\sigma(\{p, k\}) \right] \theta(V(\{\tilde{p}\}) - v) \\ &+ \int d\sigma(\{p, k\}) \left[\theta(V(\{p, k\}) - v) - \theta(V(\{\tilde{p}\}) - v) \right]. \end{aligned} \quad (8.2)$$

The first line of eq. (8.2) is proportional to the total cross section, and then it is free from infrared linear renormalons. For what concerns the second term, we observe that the term in the square bracket vanishes in the soft limit, and then we only need to work within the soft approximation to $d\sigma(\{p, k\})$, along the lines of [76, 77].

Not let us move to the C -parameter near the three-jet symmetric point, where the contribution to the observable from the hard partons is given by [84]

$$C_{\text{hard}} = \frac{3}{4} - \frac{81}{16}(\epsilon_q^2 + \epsilon_q \epsilon_{\bar{q}} + \epsilon_{\bar{q}}^2) + \mathcal{O}(\epsilon^3), \quad (8.3)$$

where $\epsilon_{q(\bar{q})} = 2E_{q(\bar{q})} - 2/3$. Applying eq. (8.1) for c close to $3/4$, the momenta $\{\tilde{p}\}$ will be forced to approach the symmetric limit, where $C(\{\tilde{p}\})$ takes a constant value. Thus we can act as for eq. (8.2), taking $V = C$. Also in this case the first term is proportional to a cross section that is inclusive in the radiation of a soft gluon and thus will not provide linear renormalons. Because of eq. (8.3) we can replace $C(\{p(\tilde{p}, k)\}) - c \rightarrow C(\{\tilde{p}, k\}) - c$ in the square bracket, and, because of the ensuing soft suppression, we can again resort to the leading soft approximation in order to perform the computation, as it was done in ref. [84]. Thus the computation in both the two-jet and the three-jet symmetric point relies on the fact that recoil effects are strongly suppressed. Thus it does not seem straightforward how to generalise these arguments to a generic three-jet configuration.

In this work we provide a method to solve this issue as generally as possible. For sake of simplicity, we assume that the soft emission originates from a single dipole, and thus we introduce a mapping $p(\tilde{p}, k)$ that, for small k is linear in k and that is collinear-safe as the gluon gets collinear to the partons that form the emitting dipole. Then, for a generic shape variable and for a generic kinematic configuration we can write eq. (8.3) as

$$\begin{aligned} \Sigma(v) &= \int [d\sigma(\{\tilde{p}\}) + d\sigma(\{p(\tilde{p}, k), k\})] \theta(V(\{\tilde{p}\}) - v) \\ &+ \int d\sigma(\{p(\tilde{p}, k), k\}) [\theta(V(\{p(\tilde{p}, k), k\}) - v) - \theta(V(\{\tilde{p}\}) - v)]. \end{aligned} \quad (8.4)$$

We observe that the first term involves an inclusive integration of the cross section at fixed underlying Born momenta, with the underlying Born defined by a mapping that is linear in k for small k . In appendix B we demonstrate that these species of integrals cannot yield linear power corrections. Hence we can neglect the first line of eq. (8.4), considering only the second one, that again can be evaluated in the soft approximation.

Conclusions

This thesis work deals with the investigation of linear power corrections, associated with IR linear renormalons, in observables relevant to collider physics. As there is not a solid theoretical background for a complete formulation of non-perturbative effects when considering processes which do not admit an OPE, we need to resort to assumptions and approximations in order to get an insight into the problem. A valuable method for performing renormalon calculations is the large- b_0 approximation, that consists in performing the full computation in the Abelian limit of QCD, with a large and negative number of light flavors n_f , replacing the Abelian beta function with the non-Abelian one at the end of the computation. For processes that do not involve gluons at leading order, an all-order large- n_f computation can be related to the calculation of a NLO correction to the process, due to the emission and exchange of a gluon with non vanishing mass. A linear dependence on the gluon mass for small masses is related to the presence of a linear renormalon.

The large- b_0 approximation has been widely used in literature [24]. In ref. [25], it was shown that the Drell-Yan total cross section does not contain linear renormalons. This conclusion has been used to argue that, contrary to previous claims, soft gluons resummation does not give a solid evidence of the presence of linear renormalons in the Drell-Yan cross section. Furthermore, in ref. [56] it was shown that, under certain assumptions, the rapidity distribution of Drell-Yan pairs is free from linear power corrections. This result leads to conclude that also in the large- b_0 approximation there are no linear renormalons affecting the rapidity distribution of Drell-Yan pairs.

In the first part of this work we make use of the large- n_f limit to probe the presence of infrared linear renormalons in the transverse momentum distribution of a Z boson produced in hadronic collisions. This work was motivated by the fact that this distribution has been measured with high precision by the experimental collaborations and the presence of a linear renormalon would affect in a sensible way the theoretical error in the corresponding calculation. Our approach for this study is semi numeric and it is analogous to the calculation performed in ref. [40]. The results obtained from this study are reported in section 2.1, and do not show any numerical evidence of an infrared linear renormalon affecting the transverse momentum distribution of the Z boson.

In the second part of the thesis we look for (and find) a solid theoretical explanation about the presence or absence of linear power corrections associated with infrared linear renormalons for generic collider processes. Our main finding can be summarized as follows: for observables that are fully inclusive in the soft gluon radiation, no linear power corrections can arise. This assessment can be easily applied to the results obtained in the part I, concerning the absence

of infrared linear renormalons in the transverse momentum distribution of the Z boson, as this observable is actually inclusive in the soft gluon distribution in the final state. This result also applies to the Drell-Yan total cross section and rapidity distribution, thus confirming the conclusions of [25, 56].

We considered the implications of our main finding for the study of shape variables in e^+e^- collisions in the three-jet region. Traditionally these studies have been used to test perturbative QCD and to measure the strong coupling constant α_s . In the past it was common practice to estimate NP corrections affecting shape variables in the two-jet limit (two back-to-back jets) and then extrapolate them in the full three-jet region, where α_s fits are usually performed. This approach relies upon the assumption that the NP corrections are equal in the whole phase space. In a recent work [84] it is demonstrated that this is not the case, showing that the NP correction affecting the C -parameter in the three-jet symmetric limit is lower than the one evaluated in the two-jet limit, thus hinting at a possible explanation of the disagreement between the α_s estimates from shape variables distributions and the nominal PDG value [102, 103].

As a consequence of our main finding (that for observables that are fully inclusive in the soft gluon radiation no linear power correction can arise) we were able to show that recoil effects, under certain conditions, do not give rise to linear renormalons since they affect the radiation in an inclusive way. Thanks to this finding we were able to perform a fully analytic computation of the leading NP corrections affecting the C -parameter and thrust in the generic three-jet region for the first time, obtaining agreement with the literature in the limit of the two-jet region [93, 94] and of the three-jet symmetric point [84].

We also found that for a certain class of shape variables it is possible to cast the leading NP correction in a fully factorised form, with one factor depending upon the change of the observable due to the emission of a soft massless parton, and a constant universal factor, only depending on the kinematic of the emission, strictly connected to the Milan factor [76, 77].

These results open new prospects to the study of shape variables in e^+e^- annihilation.

Appendix A

Renormalons structure

In sec. 1.3 we stated that the presence of a linear renormalon in the cross section of a generic process which does not involve a gluon at LO is strictly related to the function $T(\lambda)$ in eq. (1.16). If this function is analytic in λ , a non vanishing linear term $T'(0)$ leads to the arising of a linear renormalon.

As long as one considers the region $\lambda < \mu_C$, which is relevant for IR renormalons, a linear term in $T(\lambda)$ leads to the contribution (see eq. (1.16))

$$-\frac{1}{b_0\alpha_s} \frac{dT(\lambda)}{d\lambda} \Big|_{\lambda=0} \int_0^{\mu_C} \frac{d\lambda}{\pi} \arctan \frac{\pi b_0\alpha_s}{1 + b_0\alpha_s \log \frac{\lambda^2}{\mu_C^2}}. \quad (\text{A.1})$$

In order to ease the notation we define

$$a \equiv b_0\alpha_s, \quad (\text{A.2})$$

such that the integral in eq. (A.1) leads to the following expression

$$\int_0^1 \frac{dl}{\pi a} \arctan \frac{\pi a}{1 + a \log l^2} = \frac{1}{\pi a} \arctan(\pi a) + \int_0^1 dz \frac{\pi a z \cos(\pi z/2) - \sin \pi z/2}{1 + (\pi z a)^2} + \frac{1}{\pi a} \text{P} \int_0^\infty dt \frac{\exp(-\frac{t}{2a})}{1-t} - \frac{1}{a} \exp\left(-\frac{1}{2a}\right), \quad (\text{A.3})$$

where with P we mean that the integral must be taken with the principal value prescription. Furthermore we observe that the first two terms in eq. (A.3) are analytic in a neighbourhood of $a = 0$. The third term looks like a Borel representation of a fixed sign power expansion with factorially growing coefficients, resummed with a principal value prescription for handling the pole on the real axis. If we handled instead the pole by moving the integration path by a tiny amount above or below the real axis, then the absolute value of the imaginary part of the resulting integral would be equal to the last term in the equation. At the end of the computation, replacing $a = b_0\alpha_s = 1/\log(\mu_C^2/\Lambda^2)$ it leads to a power correction

$$\exp\left(-\frac{1}{2a}\right) = \frac{\Lambda}{\mu_C}. \quad (\text{A.4})$$

Thus the presence of a linear behaviour in the function $T(\lambda)$ of eq. (1.16) is related to the arising of IR linear renormalon, which, due to the asymptotic freedom of QCD, shows up as linear power corrections.

Furthermore we observe that the integral on the left-hand side of eq. (A.1) cannot be cast in the form of a Borel sum with a principal value prescription, because of the last term, whose presence is due to the discontinuity of the arctangent in the left-hand side integral, arising when $\lambda = \lambda_L$, with

$$\lambda_L = \mu_C \exp\left(-\frac{1}{2a}\right). \quad (\text{A.5})$$

In ref. [104] it is shown an alternative method in order to make the arctangent continuous, when one is interested to the resummed expansion with a principal value prescription.

Appendix B

Soft integrals

In this appendix we are going to give a discussion around the soft integrals arising from the integration of the real squared amplitude for the final emission of massive gluon with mass λ off a QCD dipole, introduced in section 4.1. Thus we consider integrals of the form

$$\vec{I}(v, \tilde{p}_{1,2}) = \int [dk] \theta[(k-q)^2] \frac{\tilde{p}_1 \tilde{p}_2}{(\tilde{p}_1 k)(\tilde{p}_2 k)} \left\{ 1, \frac{kv}{q^2}, \frac{\lambda^2}{(kp_{1,2})} \right\}, \quad (\text{B.1})$$

with $[dk] = d^4k \delta_+(k^2 - \lambda^2)/(2\pi)^3$ and v is a generic vector, $q = \tilde{p}_1 + \tilde{p}_2$ and $\tilde{p}_i^2 = 0$, with $i = 1, 2$. In order to evaluate the integrals in eq. (B.1) regardless the types of dipoles involved, it is useful to introduce a Sudakov decomposition. The discussion deals with the computation of the final-final configuration, but the whole calculation can be repeated for initial-final and initial-initial ones, with the required modifications. We write

$$k = \alpha \tilde{p}_1 + \beta \tilde{p}_2 + k_\perp. \quad (\text{B.2})$$

Since $2(\tilde{p}_1 \tilde{p}_2) = q^2$ we obtain

$$d^4k \delta_+(k^2 - \lambda^2) \theta[(q-k)^2] = \frac{q^2}{2} d\alpha d\beta d^2\vec{k}_\perp \delta(q^2 \alpha \beta - \vec{k}_\perp^2 - \lambda^2) \theta[q^2 - q^2(\alpha + \beta) + \lambda^2], \quad (\text{B.3})$$

and

$$2(\tilde{p}_1 k) = q^2 \beta, \quad 2(\tilde{p}_2 k) = q^2 \alpha. \quad (\text{B.4})$$

Applying a Sudakov decomposition to all the integrals in eq. (B.1), we get

$$(vk) = (\tilde{p}_1 v) \alpha + (\tilde{p}_2 v) \beta + (vk_\perp). \quad (\text{B.5})$$

As this is the only dependence on the k_\perp -direction in the integrals, the last terms in eq. (B.5) vanishes upon azimuthal integration, and thus it is safe to apply the following replacement in eq. (B.1)

$$(vk) \rightarrow (\tilde{p}_1 k) \alpha + (\tilde{p}_2 v) \beta. \quad (\text{B.6})$$

Thus it follows that to compute eq. (B.1) we need to evaluate the following integrals

$$\frac{1}{16\pi^2} \int d\alpha d\beta \theta(q^2 \alpha \beta - \lambda^2) \theta[q^2(1 - \alpha - \beta) + \lambda^2] \frac{1}{\alpha \beta} \left\{ 1, \alpha, \frac{\lambda^2}{\alpha}, \frac{\lambda^2 \beta}{\alpha}, \frac{\lambda^2 \beta^2}{\alpha}, \frac{\lambda^4 \beta}{\alpha^2} \right\}. \quad (\text{B.7})$$

In order to proceed further, we need to know the integration boundaries, which can be found from the two θ -functions in eq. (B.7). If we first integrate over β , we have

$$\frac{\lambda^2}{q^2\alpha} < \beta < 1 - \alpha + \frac{\lambda^2}{q^2}. \quad (\text{B.8})$$

The boundaries for the subsequent α integration can be deduced from the condition

$$\frac{\lambda^2}{q^2\alpha} < 1 - \alpha + \frac{\lambda^2}{q^2}, \quad (\text{B.9})$$

which can be rewritten in the more compact form

$$(\alpha - 1)\left(\alpha - \frac{\lambda^2}{q^2}\right) < 0. \quad (\text{B.10})$$

Thus the integration range for α is

$$\frac{\lambda^2}{q^2} < \alpha < 1. \quad (\text{B.11})$$

Then it is straightforward to verify that the integrals reported in eq. (B.1) can be written in terms of the following ones

$$\int_{\lambda^2/q^2}^1 \frac{d\alpha}{\alpha} \int_{\lambda^2/(q^2\alpha)}^{1-\alpha+\lambda^2/q^2} \frac{d\beta}{\beta} \left\{ 1, \alpha, \frac{\lambda^2}{\alpha}, \frac{\lambda^2\beta}{\alpha}, \frac{\lambda^2\beta^2}{\alpha}, \frac{\lambda^4\beta}{\alpha^2} \right\}. \quad (\text{B.12})$$

From eq. (B.12) it is obvious that the integrals in eq. (B.1) are actually functions of λ^2 .

Appendix C

Full calculation of the shape variables in the large- n_f limit

In this appendix we are going to describe the computation of QCD corrections to the process $\gamma^* \rightarrow q\bar{q} + \gamma$, working in the large- n_f limit. As we have done in part I of this work, we assume that the final state photon γ only couples to the primary quarks, that, for simplicity, are assumed to be of defined flavor d . We know [40] that the exact result of a large- n_f computation can be written as in eq. (1.16).

Thus for the process of our interest we need to compute the $T(\lambda)$ function defined in eq. (1.18). All the required amplitudes have been analytically computed thanks to the symbolic manipulation software MAXIMA [53]. The scalar integrals arising from the computation of the virtual corrections have been calculated by the COLLIER library [55]. The virtual term is infrared finite as the gluon mass acts as an infrared regulator. The ultraviolet divergences have been regulated working in dimensional regularization.

The integration over the external momenta for the process $\gamma^* \rightarrow d\bar{d}\gamma$ diverges in the two-jet limit; thus in order to ensure that the numerical computations are restricted to a three-jet region, we introduced a suppression factor

$$F_{\text{supp}} = C^2, \tag{C.1}$$

where C is the C -parameter, which by construction vanishes in the two-jet limit, regulating the integral. This factor is then divided out when computing distributions and cross sections with cuts. In such a way, we are able to obtain a correct result as long as we do not consider observables which are sensitive to the two-jet region.

The real contribution to $T(\lambda)$ has been computed along the lines of sec. 1.4, adding the emission of a massive gluon in all the possible ways to the Born diagram. Integrating over its momentum, the real emission corrections are affected by collinear divergences, arising when the photon becomes collinear to one of the primary quarks. These configurations can contribute to the three-jet region, when the radiated gluon is hard and not collinear. These divergences are dealt with routinely by the POWHEG BOX framework [52], that we use for our calculation.

We also have singularities associated with soft or collinear gluons, which are regulated by the gluon mass λ , and manifest themselves as terms proportional to $\ln \lambda$ raised to first or second power. The same logarithmic contributions, but with opposite sign, arise from the virtual corrections, such that the sum of real and virtual corrections is free of $\ln \lambda$ terms.

In order to properly cancel the singularities mentioned above, a carefully-constructed importance sampling near the singular regions is needed, to reliably estimate the $\lambda \rightarrow 0$ behaviour. Thus the real contribution is divided into three regions

$$R = R^{(1)} + R^{(2)} + R^{(3)}, \quad (\text{C.2})$$

where

$$R^{(1)} = \frac{f_{d\gamma}^2 + f_{\bar{d}\gamma}^2}{f_{d\gamma}^2 + f_{\bar{d}\gamma}^2 + f_{dg}^2 + f_{\bar{d}g}^2} R, \quad (\text{C.3})$$

$$R^{(2)} = \frac{f_{dg}^2}{f_{d\gamma}^2 + f_{\bar{d}\gamma}^2 + f_{dg}^2 + f_{\bar{d}g}^2} R, \quad (\text{C.4})$$

$$R^{(3)} = \frac{f_{\bar{d}g}^2}{f_{d\gamma}^2 + f_{\bar{d}\gamma}^2 + f_{dg}^2 + f_{\bar{d}g}^2} R, \quad (\text{C.5})$$

and

$$f_{ij} = \frac{E_i + E_j}{(k_i + k_j)^2}. \quad (\text{C.6})$$

Here k_i and E_i denote the four-momentum and energy of the i -th particle, respectively, and R is a short-hand notation for the R_{g^*} function introduced in eq. (1.23). The various contributions $R^{(i)}$ in eq. (C.2) correspond to different kinematic configurations of the $d\bar{d}\gamma g$ final state. For instance $R^{(1)}$ corresponds to the region where the final state photon becomes collinear to either the d or the \bar{d} quark, whilst $R^{(2)}$ and $R^{(3)}$ project on regions where the emitted gluon is collinear to d or \bar{d} , respectively.

The contribution arising from region (1) is handled within the `POWHEG BOX` [52], which implements the required subtractions of IR singularities associated with configurations containing a soft or a collinear photon. The two other regions are finite, but still require a dedicated importance sampling of the regions that become singular in the $\lambda \rightarrow 0$ limit.

Finally, we also compute the amplitude for the process $\gamma^* \rightarrow d\bar{d}\gamma + (g^* \rightarrow q\bar{q})$. This contribution is IR finite when the $\lambda \rightarrow 0$ limit is taken, but is affected by the QED singularity associated with the final state photon. Thus we proceed as for the region (1), by evaluating it within the `POWHEG BOX` framework. Furthermore we computed the NLO corrections to the process $\gamma^* \rightarrow d\bar{d}\gamma$ with a massless gluon and subtracted its result from the λ -dependent one, in order to isolate the $\mathcal{O}(\lambda)$ term.

The shape variable distributions are obtained in a standard way, by computing each contribution to sufficient accuracy, so that after the cancellation of $\ln^2 \lambda$, $\ln \lambda$ and λ^0 terms one can extract the λ dependence with enough precision.

Appendix D

On the two-jet limit of C

In this appendix we will elaborate more on the two-jet limit of the cumulant of shape variables within our framework. For sake of simplicity we will only focus on the case of the C -parameter.

We start by considering the process $\gamma^*(q) \rightarrow q(p_1) + \bar{q}(p_2) + \gamma(p_3)$. Extending the notation introduced above, we can define the “double underlying” Born momenta \hat{p}_1 and \hat{p}_2 as follows:

- If \tilde{p}_3 becomes collinear to \tilde{p}_1 , then $\hat{p}_1 \approx \tilde{p}_1 + \tilde{p}_3$ and $\hat{p}_2 \approx \tilde{p}_2$;
- If \tilde{p}_3 becomes collinear to \tilde{p}_2 , then $\hat{p}_2 \approx \tilde{p}_2 + \tilde{p}_3$ and $\hat{p}_1 \approx \tilde{p}_1$;
- If \tilde{p}_3 becomes soft, then $\hat{p}_2 \approx \tilde{p}_2$ and $\hat{p}_1 \approx \tilde{p}_1$.

At this point we want to show that, in the two-jet limit, the non-perturbative correction to the cumulant of C becomes proportional to the non-perturbative correction to the expectation value of C in the $\gamma^* \rightarrow q\bar{q}$ process. In order to prove this we need to make three observations:

- As c approaches to zero, the Born cross section manifests two collinear-singular regions, arising when the photon becomes collinear to either primary quark; a soft singular region, when the photon is soft and two soft-collinear regions, when the photon is both collinear and soft;
- The correction to the C -parameter due to the emission of a soft gluon with momentum k can be written as

$$C_k(p_1, p_2, p_3, k; q) = -3 \sum_{i=1}^3 \frac{(kp_i)^2}{(kq)(p_iq)}; \quad (\text{D.1})$$

eq. (D.1) has a smooth limit if any pair of the 1, 2 and 3 particles becomes collinear, as well as if one of them becomes soft. In particular, if \tilde{p}_3 becomes soft or collinear to either \tilde{p}_1 or \tilde{p}_2 , we can write

$$C_k(\Phi_3, k) = -3 \sum_{i=1}^3 \frac{(k\tilde{p}_i)^2}{(kq)(\tilde{p}_iq)} \rightarrow -3 \sum_{i=1}^3 \frac{(k\hat{p}_i)^2}{(kq)(\hat{p}_iq)} = C_k(\Phi_2, k), \quad (\text{D.2})$$

where we have used the compact notation $\{\tilde{p}_1, \tilde{p}_2, \tilde{p}_3\} = \Phi_3$ and $\{\hat{p}_1, \hat{p}_2\} = \Phi_2$;

- The eikonal factor for the emission of a soft massive gluon only depends upon the direction of the radiating partons, and not upon the absolute value of their momenta.

Considering the $q\bar{q}\gamma$ final state, we only need to consider the emission from the quark-antiquark dipole. Thus our result for the non-perturbative correction can be concisely written as

$$\delta_{\text{NP}} \equiv -\frac{\mathcal{T}_\lambda \Sigma(c)}{d\sigma/dC} = -\frac{\alpha_s}{2\pi} C_F \times \frac{\int d\Phi_3 \delta(C(\Phi_3) - c) |\mathcal{M}(\Phi_3)|^2 \mathcal{T}_\lambda I_c(\Phi_3)}{\int d\Phi_3 \delta(C(\Phi_3) - c) |\mathcal{M}(\Phi_3)|^2}, \quad (\text{D.3})$$

where

$$I_c(\Phi_3; q; \lambda) = 8\pi^2 \int \frac{d^4k}{(2\pi)^3} \delta_+(k^2 - \lambda^2) \theta[(q - k)^2] \frac{2(\tilde{p}_1 \tilde{p}_2)}{(\tilde{p}_1 k)(\tilde{p}_2 k)} C_k(\Phi_3, k), \quad (\text{D.4})$$

and \mathcal{T}_λ is the operator introduced in section 4.2. For both the collinear and soft limits of the Born configuration, the integrand in eq. (D.4) takes the form

$$\frac{(\tilde{p}_1 \tilde{p}_2)}{(\tilde{p}_1 k)(\tilde{p}_2 k)} C_k(\Phi_3, k) \rightarrow \frac{(\hat{p}_1 \hat{p}_2)}{(\hat{p}_1 k)(\hat{p}_2 k)} C_k(\Phi_2, k). \quad (\text{D.5})$$

Thus, in these limits, we can also write

$$I_c(\Phi_3; q; \lambda) \rightarrow I_c(\Phi_2; q; \lambda), \quad (\text{D.6})$$

that can be taken outside the integral in eq. (D.3), yielding

$$\delta_{\text{NP}} \underset{c \rightarrow 0}{\approx} -\frac{\alpha_s}{2\pi} C_F \times \mathcal{T}_\lambda I_c(\Phi_2; q; \lambda). \quad (\text{D.7})$$

Eq. (D.7) stands for the non-perturbative correction to the average value of C in the two-jet case. We stress that the limit $c \rightarrow 0$ does not imply that \tilde{p}_3 is either soft or collinear. We could also have \tilde{p}_1 or \tilde{p}_2 soft, or collinear to each other. What is important is that for all the dominant singular contributions in the amplitude, the function I_c can be taken out of the integral.

We can now move on to consider the $\gamma^* \rightarrow q\bar{q}g$ process, and use the the conjecture on non-perturbative corrections that we described in the text. For this process we need to also consider the qg ($\bar{q}g$) dipoles, apart from the $q\bar{q}$ dipole. For the $q(p_1)g(p_3)$ dipole, the eikonal factor in eq. (D.5) becomes

$$\frac{(\tilde{p}_1 \tilde{p}_3)}{(\tilde{p}_1 k)(\tilde{p}_3 k)} C_k(\Phi_3, k). \quad (\text{D.8})$$

Furthermore, when \tilde{p}_2 gets collinear to \tilde{p}_3 , it reduces to

$$\frac{(\tilde{p}_1 \tilde{p}_3)}{(\tilde{p}_1 k)(\tilde{p}_3 k)} C_k(\Phi_3, k) \underset{p_2 \parallel p_3}{\approx} \frac{(\hat{p}_1 \hat{p}_2)}{(\hat{p}_1 k)(\hat{p}_2 k)} C_k(\Phi_2, k), \quad (\text{D.9})$$

as before. Therefore, as \tilde{p}_1 gets collinear to \tilde{p}_3 it becomes zero. Thus in this case we have

$$\delta_{\text{NP}} \underset{c \rightarrow 0}{\approx} -\frac{1}{2} \times \frac{\alpha_s}{2\pi} C_F \times \mathcal{T}_\lambda I_c(\Phi_2; q; \lambda). \quad (\text{D.10})$$

This comes from the fact that the most enhanced regions when $c \rightarrow 0$ are the soft-collinear ones, but only one of the two contributes, hence the factor of one half.

We further remark that the soft-collinear approximation is enough to take these results, that can be considered as direct consequences of angular ordering. In the quark-antiquark dipole case, the result directly follows from the full soft factorization which applies in abelian theories. In this case we expect that the limit is reached earlier. This does not hold for the (anti)quark-gluon case, since the Born level gluon and the gluon emitted by the qg ($\bar{q}g$) dipole do not factorize simultaneously in the soft limit.

Appendix E

The G_i functions

The functions $G_{1,\dots,5}$ were introduced in eq. (5.4). They read

$$\begin{aligned}
 G_1 = & \frac{(1 - \beta^2)^{-3/2}}{48\beta^6(x(y-1) + 1)^2(xy-1)^2} \left[\beta^6 \left(2x^3y(-42y^3 + 84y^2 - 421y + 379) \right. \right. \\
 & \left. \left. + 29x^4(y-1)^2y^2 + x^2(1706y^2 - 1706y - 271) + x(-948y^2 + 948y + 542) - 271 \right) \right. \\
 & \left. + \beta^4 \left(-159x^4(y-1)^2y^2 + 2x^3y(187y^3 - 374y^2 + 1203y - 1016) \right. \right. \\
 & \left. \left. + x^2(-4542y^2 + 4542y + 749) + 2x(1255y^2 - 1255y - 749) + 749 \right) \right. \\
 & \left. + 5\beta^2 \left(47x^4(y-1)^2y^2 + 2x^3y(-50y^3 + 100y^2 - 271y + 221) \right. \right. \\
 & \left. \left. + 165x^2(6y^2 - 6y - 1) + x(-548y^2 + 548y + 330) - 165 \right) \right. \\
 & \left. - 105 \left(x^4(y-1)^2y^2 - 2x^3y(y^3 - 2y^2 + 5y - 4) + 3x^2(6y^2 - 6y - 1) \right. \right. \\
 & \left. \left. + x(-10y^2 + 10y + 6) - 3 \right) \right],
 \end{aligned} \tag{E.1}$$

$$\begin{aligned}
 G_2 = & \frac{\sqrt{1 - \beta^2}(x-1) \ln^2\left(\frac{1+\beta}{1-\beta}\right)}{32\beta^8x(x(y-1) + 1)^2(xy-1)^2} \\
 & \times \left[\beta^4(x^2(-117y^2 + 117y + 34) + 83x^3(y-1)y - 53x + 19) \right. \\
 & \left. - 10\beta^2(x^2(-29y^2 + 29y + 8) + 21x^3(y-1)y - 11x + 3) \right]
 \end{aligned} \tag{E.2}$$

$$\begin{aligned}
 & + 35 \left(x^2 (-7y^2 + 7y + 2) + 5x^3(y-1)y - 3x + 1 \right) \Big], \\
 G_3 = & \frac{\ln \left(\frac{\sqrt{1-\beta^2 c_{12}^2} + \beta s_{12}}{\sqrt{1-\beta^2 c_{12}^2} - \beta s_{12}} \right)}{96\beta^7 (1-\beta^2)^{3/2} s_{12} x \sqrt{1-\beta^2 c_{12}^2} (x(y-1)+1)(xy-1)} \\
 & \times \left[\beta^8 x (29x^2(y-1)y + x(-84y^2 + 84y + 15) - 15) \right. \\
 & - 2\beta^6 (x^2(-229y^2 + 229y + 51) + 94x^3(y-1)y - 186x + 135) \\
 & + \beta^4 (x^2(-874y^2 + 874y + 232) + 394x^3(y-1)y - 758x + 526) \\
 & - 10\beta^2 (x^2(-71y^2 + 71y + 25) + 34x^3(y-1)y - 78x + 53) \\
 & \left. + 105(x-2)(x^2(y-1)y + x-1) \right], \tag{E.3}
 \end{aligned}$$

$$\begin{aligned}
 G_4 = & \frac{\ln \left(\frac{1+\beta}{1-\beta} \right)}{96\beta^7 (1-\beta^2)^{3/2} x(x(y-1)+1)^2(xy-1)^2} \left[\beta^8 x \left(3x^4(y-1)^2 y^2 \right. \right. \\
 & - 6x^3 y (2y^3 - 4y^2 + 57y - 55) + x^2 (758y^2 - 758y - 113) \\
 & \left. + x(-428y^2 + 428y + 226) - 113 \right) - 6\beta^6 \left(11x^5(y-1)^2 y^2 \right. \\
 & + x^4 y (-29y^3 + 58y^2 - 479y + 450) + x^3 (1046y^2 - 1046y - 171) \\
 & + x^2 (-596y^2 + 596y + 387) - 261x + 45 \left. \right) + 2\beta^4 \left(114x^5(y-1)^2 y^2 \right. \\
 & + x^4 y (-261y^3 + 522y^2 - 3187y + 2926) + 8x^3 (848y^2 - 848y - 139) \\
 & + x^2 (-3858y^2 + 3858y + 2487) - 1638x + 263 \left. \right) - 10\beta^2 \left(27x^5(y-1)^2 y^2 \right. \\
 & + x^4 y (-57y^3 + 114y^2 - 607y + 550) + x^3 (1278y^2 - 1278y - 211) \\
 & \left. + x^2 (-728y^2 + 728y + 475) - 317x + 53 \right) + 105 \left(x^5(y-1)^2 y^2 \right. \\
 & \left. - 2x^4 y (y^3 - 2y^2 + 10y - 9) + 7x^3 (6y^2 - 6y - 1) - 8x^2 (3y^2 - 3y - 2) - 11x + 2 \right) \Big], \tag{E.4}
 \end{aligned}$$

$$\begin{aligned}
 G_5 = & \frac{\sqrt{1-\beta^2} \ln \left(\frac{1+\beta}{1-\beta} \right) \ln \left(\frac{\sqrt{1-\beta^2 c_{12}^2} + \beta s_{12}}{\sqrt{1-\beta^2 c_{12}^2} - \beta s_{12}} \right)}{64\beta^8 s_{12} x(x(y-1)+1)(xy-1)\sqrt{1-\beta^2 c_{12}^2}} \\
 & \times \left[\beta^6 x (x^2(y-1)y + x(-4y^2 + 4y - 5) + 5) + \beta^4 \left(x^2 (54y^2 - 54y - 17) \right. \right.
 \end{aligned}$$

$$\begin{aligned} & - 21x^3(y-1)y + 55x - 38 \Big) + 5\beta^2 \left(x^2(-24y^2 + 24y + 5) \right. \\ & \left. + 11x^3(y-1)y - 17x + 12 \right) - 35(x-2)(x^2(y-1)y + x - 1) \Big]. \end{aligned} \tag{E.5}$$

List of Figures

1	Feynman diagram contributing to the transverse momentum distribution of a Z boson, represented by a zigzag line. The soft-radiation pattern is represented by the dashed line, and is associated with the color dipoles formed by the outgoing gluon (wavy line) and the initial state quarks.	9
2	Born diagram for the production of a Z boson in photon-quark collision. The green lines represent the incoming and outgoing quarks, while the photon and the Z are represented by the wavy and zig zag line, respectively. This process has an asymmetric pattern for the soft emission, and looks suitable for probing the presence of IR linear renormalons in the p_T distribution of the Z	10
1.1	Sets of Feynman diagrams to be evaluated in order to compute QCD radiative corrections to the process represented in fig. 2 in the large- b_0 limit.	13
1.2	Feynman diagrams for the $q\bar{q}$ initiated subprocesses, entering in the factorization formula for initial state collinear singularities, arising as the outgoing quark gets collinear to the initial state photon, contributing respectively to the \mathcal{D}_g and $\mathcal{D}_{q\bar{q}}$ amplitudes.	15
1.3	Relevant Feynman diagrams contributing to F_2 in the Large- n_f limit.	16
1.4	Feynman diagrams contributing to the process $d\gamma \rightarrow Zd$ at the Born level. The zigzag line represents the Z boson, while the wavy line represents the incoming photon.	19
1.5	Feynman diagram describing the collinear singularities due to the splitting of the photon into a $d\bar{d}$ pair, in the process $d\gamma \rightarrow Zdg$ process.	19
1.6	On the left (right) the Feynman diagram contributing to the collinear initial (final) state singularity, and to a soft singularity.	21
2.1	$T(\lambda)$ function (as defined in eq. (1.18)) as a function of the gluon mass λ for the cross section of a Z boson with a transverse momentum $p_{T,Z} > p_T^c$, with $p_T^c = 20$ GeV (left) and $p_T^c = 40$ GeV (right). The green points have been obtained by computing $T(\lambda)$ for different values of λ . The curves for fit 1 and 2 have been derived from the fit function in eq. (2.2), where for fit 1 we considered all the fit parameters, and in fit 2 we fixed the linear coefficient b to 0. We did not consider the point $\lambda = 5$ GeV in the fitting procedure.	25
2.2	The same as in fig. 2.1, with the further cut over the rapidity of the Z : $0 < y_Z < y_c$, where $y_c = 0.6$	26

7.1	Non-perturbative shift in the differential distributions for the C -parameter (left) and the thrust (right), obtained from eq. (7.22) (A), and from a full calculation in the large- n_f limit (B). Results are shown for the process $\gamma^* \rightarrow d\bar{d}\gamma$, with $Q = 100$ GeV and $\lambda = 0.5$ GeV, $\lambda = 1$ GeV.	72
7.2	The function $\zeta_{q\bar{q}}(v)$ for the C -parameter (left panel) and the thrust $\bar{T} = 1 - T$ (right panel), evaluated numerically using $q = 100$ GeV and $\lambda = 0.1, 0.5, 1$ GeV, compared to the analytic computation (solid line). In the lower panels we reported the ratio plot of each numerical curve with respect to the analytic one.	75
7.3	Same as fig. 7.2 but for the qg dipole.	75
7.4	Same as fig. 7.2, but for the sum of all the QCD dipoles, with each contribution supplemented with its own color factor, according to eq. (7.28). The grey shading areas show the regions that are usually excluded from the α_s fits [84].	77

Bibliography

- [1] C. Anastasiou and K. Melnikov, *Higgs boson production at hadron colliders in NNLO QCD*, *Nucl. Phys. B* **646** (2002) 220–256, [[hep-ph/0207004](#)].
- [2] C. Anastasiou, L. J. Dixon, K. Melnikov and F. Petriello, *Dilepton rapidity distribution in the Drell-Yan process at NNLO in QCD*, *Phys. Rev. Lett.* **91** (2003) 182002, [[hep-ph/0306192](#)].
- [3] S. Catani, L. Cieri, D. de Florian, G. Ferrera and M. Grazzini, *Diphoton production at hadron colliders: a fully-differential QCD calculation at NNLO*, *Phys. Rev. Lett.* **108** (2012) 072001, [[1110.2375](#)].
- [4] G. Ferrera, M. Grazzini and F. Tramontano, *Associated WH production at hadron colliders: a fully exclusive QCD calculation at NNLO*, *Phys. Rev. Lett.* **107** (2011) 152003, [[1107.1164](#)].
- [5] M. Grazzini, S. Kallweit and D. Rathlev, *ZZ production at the LHC: fiducial cross sections and distributions in NNLO QCD*, *Phys. Lett. B* **750** (2015) 407–410, [[1507.06257](#)].
- [6] M. Grazzini, S. Kallweit, D. Rathlev and M. Wiesemann, *$W^\pm Z$ production at hadron colliders in NNLO QCD*, *Phys. Lett. B* **761** (2016) 179–183, [[1604.08576](#)].
- [7] M. Czakon, D. Heymes, A. Mitov, D. Pagani, I. Tsinikos and M. Zaro, *Top-pair production at the LHC through NNLO QCD and NLO EW*, *JHEP* **10** (2017) 186, [[1705.04105](#)].
- [8] P. Bolzoni, F. Maltoni, S.-O. Moch and M. Zaro, *Higgs production via vector-boson fusion at NNLO in QCD*, *Phys. Rev. Lett.* **105** (2010) 011801, [[1003.4451](#)].
- [9] F. Cascioli, T. Gehrmann, M. Grazzini, S. Kallweit, P. Maierhöfer, A. von Manteuffel, S. Pozzorini, D. Rathlev, L. Tancredi and E. Weihs, *ZZ production at hadron colliders in NNLO QCD*, *Phys. Lett. B* **735** (2014) 311–313, [[1405.2219](#)].
- [10] S. Catani, L. Cieri, G. Ferrera, D. de Florian and M. Grazzini, *Vector boson production at hadron colliders: a fully exclusive QCD calculation at NNLO*, *Phys. Rev. Lett.* **103** (2009) 082001, [[0903.2120](#)].

-
- [11] P. Bärnreuther, M. Czakon and A. Mitov, *Percent Level Precision Physics at the Tevatron: First Genuine NNLO QCD Corrections to $q\bar{q} \rightarrow t\bar{t} + X$* , *Phys. Rev. Lett.* **109** (2012) 132001, [[1204.5201](#)].
- [12] D. de Florian and J. Mazzitelli, *Higgs Boson Pair Production at Next-to-Next-to-Leading Order in QCD*, *Phys. Rev. Lett.* **111** (2013) 201801, [[1309.6594](#)].
- [13] C. Anastasiou, C. Duhr, F. Dulat, F. Herzog and B. Mistlberger, *Higgs Boson Gluon-Fusion Production in QCD at Three Loops*, *Phys. Rev. Lett.* **114** (2015) 212001, [[1503.06056](#)].
- [14] C. Anastasiou, C. Duhr, F. Dulat, E. Furlan, T. Gehrmann, F. Herzog and B. Mistlberger, *Higgs boson gluon-fusion production at threshold in N^3LO QCD*, *Phys. Lett. B* **737** (2014) 325–328, [[1403.4616](#)].
- [15] B. Mistlberger, *Higgs boson production at hadron colliders at N^3LO in QCD*, *JHEP* **05** (2018) 028, [[1802.00833](#)].
- [16] S. Prestel, *Matching N^3LO QCD calculations to parton showers*, *JHEP* **11** (2021) 041, [[2106.03206](#)].
- [17] G. Altarelli, *Introduction to renormalons*, in *5th Hellenic School and Workshops on Elementary Particle Physics*, pp. 221–236, 1996.
- [18] D. J. Gross and A. Neveu, *Dynamical Symmetry Breaking in Asymptotically Free Field Theories*, *Phys. Rev. D* **10** (1974) 3235.
- [19] B. E. Lautrup, *On High Order Estimates in QED*, *Phys. Lett. B* **69** (1977) 109–111.
- [20] G. 't Hooft, *Can We Make Sense Out of Quantum Chromodynamics?*, *Subnucl. Ser.* **15** (1979) 943.
- [21] L. S. Brown and L. G. Yaffe, *Asymptotic behavior of perturbation theory for the electromagnetic current-current correlation function in qcd*, *Phys. Rev. D* **45** (Jan, 1992) R398–R402.
- [22] V. Zakharov, *Qcd perturbative expansions in large orders*, *Nuclear Physics B* **385** (1992) 452–480.
- [23] A. H. Mueller, *On the Structure of Infrared Renormalons in Physical Processes at High-Energies*, *Nucl. Phys. B* **250** (1985) 327–350.
- [24] M. Beneke, *Renormalons*, *Phys.Rept.* **317** (1999) 1–142, [[hep-ph/9807443](#)].
- [25] M. Beneke and V. M. Braun, *Power corrections and renormalons in Drell-Yan production*, *Nucl. Phys. B* **454** (1995) 253–290, [[hep-ph/9506452](#)].

- [26] R. Boughezal, A. Guffanti, F. Petriello and M. Ubiali, *The impact of the LHC Z-boson transverse momentum data on PDF determinations*, *JHEP* **07** (2017) 130, [[1705.00343](#)].
- [27] CMS collaboration, V. Khachatryan et al., *Measurement of the Z boson differential cross section in transverse momentum and rapidity in proton–proton collisions at 8 TeV*, *Phys. Lett. B* **749** (2015) 187–209, [[1504.03511](#)].
- [28] ATLAS collaboration, G. Aad et al., *Measurement of the transverse momentum and ϕ_η^* distributions of Drell–Yan lepton pairs in proton–proton collisions at $\sqrt{s} = 8$ TeV with the ATLAS detector*, *Eur. Phys. J. C* **76** (2016) 291, [[1512.02192](#)].
- [29] CMS collaboration, A. M. Sirunyan et al., *Measurements of differential Z boson production cross sections in proton–proton collisions at $\sqrt{s} = 13$ TeV*, *JHEP* **12** (2019) 061, [[1909.04133](#)].
- [30] ATLAS collaboration, G. Aad et al., *Measurement of the transverse momentum distribution of Drell–Yan lepton pairs in proton–proton collisions at $\sqrt{s} = 13$ TeV with the ATLAS detector*, *Eur. Phys. J. C* **80** (2020) 616, [[1912.02844](#)].
- [31] R. Boughezal, J. Campbell, R. K. Ellis, C. Focke, W. Giele, X. Liu and F. Petriello, *Z-Boson Production in Association with a Jet at Next-To-Next-To-Leading Order in Perturbative QCD*, *Physical Review Letters* **116** (2016) .
- [32] A. Gehrmann-De Ridder, T. Gehrmann, E. Glover, A. Huss and T. Morgan, *Precise QCD Predictions for the Production of a Z Boson in Association with a Hadronic Jet*, *Physical Review Letters* **117** (2016) .
- [33] A. Gehrmann-De Ridder, T. Gehrmann, E. Glover, A. Huss and D. Walker, *NNLO QCD corrections to the transverse momentum distribution of weak gauge bosons*, *Physical Review Letters* **120** (2018) .
- [34] W. Bizon, A. Gehrmann-De Ridder, T. Gehrmann, N. Glover, A. Huss, P. F. Monni, E. Re, L. Rottoli and D. M. Walker, *The transverse momentum spectrum of weak gauge bosons at $N^3LL + NNLO$* , *Eur. Phys. J. C* **79** (2019) 868, [[1905.05171](#)].
- [35] Y. L. Dokshitzer, D. Diakonov and S. I. Troian, *On the Transverse Momentum Distribution of Massive Lepton Pairs*, *Phys. Lett. B* **79** (1978) 269–272.
- [36] G. Parisi and R. Petronzio, *Small Transverse Momentum Distributions in Hard Processes*, *Nucl. Phys. B* **154** (1979) 427–440.
- [37] J. C. Collins, D. E. Soper and G. F. Sterman, *Transverse Momentum Distribution in Drell–Yan Pair and W and Z Boson Production*, *Nucl. Phys. B* **250** (1985) 199–224.
- [38] W. Bizoń, X. Chen, A. Gehrmann-De Ridder, T. Gehrmann, N. Glover, A. Huss, P. F. Monni, E. Re, L. Rottoli and P. Torrielli, *Fiducial distributions in Higgs and Drell–Yan production at $N^3LL+NNLO$* , *JHEP* **12** (2018) 132, [[1805.05916](#)].

-
- [39] G. Parisi, *On Infrared Divergences*, *Nucl. Phys. B* **150** (1979) 163–172.
- [40] S. Ferrario Ravasio, P. Nason and C. Oleari, *All-orders behaviour and renormalons in top-mass observables*, *JHEP* **01** (2019) 203, [[1810.10931](#)].
- [41] T. Becher and M. Neubert, *Drell-Yan Production at Small q_T , Transverse Parton Distributions and the Collinear Anomaly*, *Eur. Phys. J. C* **71** (2011) 1665, [[1007.4005](#)].
- [42] G. Bozzi, S. Catani, G. Ferrera, D. de Florian and M. Grazzini, *Production of Drell-Yan lepton pairs in hadron collisions: Transverse-momentum resummation at next-to-next-to-leading logarithmic accuracy*, *Phys. Lett. B* **696** (2011) 207–213, [[1007.2351](#)].
- [43] T. Becher, M. Neubert and D. Wilhelm, *Electroweak Gauge-Boson Production at Small q_T : Infrared Safety from the Collinear Anomaly*, *JHEP* **02** (2012) 124, [[1109.6027](#)].
- [44] M. G. Echevarria, A. Idilbi and I. Scimemi, *Factorization Theorem For Drell-Yan At Low q_T And Transverse Momentum Distributions On-The-Light-Cone*, *JHEP* **07** (2012) 002, [[1111.4996](#)].
- [45] T. Becher and M. Hager, *Event-Based Transverse Momentum Resummation*, *Eur. Phys. J. C* **79** (2019) 665, [[1904.08325](#)].
- [46] F. Hautmann, I. Scimemi and A. Vladimirov, *Non-perturbative contributions to vector-boson transverse momentum spectra in hadronic collisions*, *Phys. Lett. B* **806** (2020) 135478, [[2002.12810](#)].
- [47] R. Angeles-Martinez et al., *Transverse Momentum Dependent (TMD) parton distribution functions: status and prospects*, *Acta Phys. Polon.* **B46** (2015) 2501–2534, [[1507.05267](#)].
- [48] T. Becher and G. Bell, *Enhanced nonperturbative effects through the collinear anomaly*, *Phys. Rev. Lett.* **112** (2014) 182002, [[1312.5327](#)].
- [49] I. Scimemi and A. Vladimirov, *Power corrections and renormalons in Transverse Momentum Distributions*, *JHEP* **03** (2017) 002, [[1609.06047](#)].
- [50] S. Frixione, P. Nason and C. Oleari, *Matching NLO QCD computations with Parton Shower simulations: the POWHEG method*, *JHEP* **11** (2007) 070, [[0709.2092](#)].
- [51] P. Nason and M. H. Seymour, *Infrared renormalons and power suppressed effects in e^+e^- jet events*, *Nucl. Phys. B* **454** (1995) 291–312, [[hep-ph/9506317](#)].
- [52] S. Alioli, P. Nason, C. Oleari and E. Re, *A general framework for implementing NLO calculations in shower Monte Carlo programs: the POWHEG BOX*, *JHEP* **06** (2010) 043, [[1002.2581](#)].

-
- [53] Maxima, *Maxima, a Computer Algebra System. Version 5.43.2.* <http://maxima.sourceforge.net/>, 2020.
- [54] G. Passarino and M. J. G. Veltman, *One Loop Corrections for $e^+ e^-$ Annihilation Into $\mu^+ \mu^-$ in the Weinberg Model*, *Nucl. Phys. B* **160** (1979) 151–207.
- [55] A. Denner, S. Dittmaier and L. Hofer, *Collier: a fortran-based Complex One-Loop Library in Extended Regularizations*, *Comput. Phys. Commun.* **212** (2017) 220–238, [[1604.06792](#)].
- [56] M. Dasgupta, *Power corrections to the differential Drell-Yan cross-section*, *JHEP* **12** (1999) 008, [[hep-ph/9911391](#)].
- [57] PARTICLE DATA GROUP collaboration, P. A. Zyla et al., *Review of Particle Physics*, *PTEP* **2020** (2020) 083C01.
- [58] JADE collaboration, J. Schieck, S. Bethke, O. Biebel, S. Kluth, P. A. Movilla Fernandez and C. Pahl, *Measurement of the strong coupling α_s from the four-jet rate in $e^+ e^-$ annihilation using JADE data*, *Eur. Phys. J. C* **48** (2006) 3–13, [[0707.0392](#)].
- [59] G. Dissertori, A. Gehrmann-De Ridder, T. Gehrmann, E. W. N. Glover, G. Heinrich, G. Luisoni and H. Stenzel, *Determination of the strong coupling constant using matched NNLO+NLLA predictions for hadronic event shapes in e^+e^- annihilations*, *JHEP* **08** (2009) 036, [[0906.3436](#)].
- [60] A. Kardos, S. Kluth, G. Somogyi, Z. Tulipánt and A. Verbytskyi, *Precise determination of $\alpha_s(M_Z)$ from a global fit of energy–energy correlation to NNLO+NNLL predictions*, *Eur. Phys. J. C* **78** (2018) 498, [[1804.09146](#)].
- [61] R. Akhoury and V. I. Zakharov, *Leading power corrections in QCD: From renormalons to phenomenology*, *Nucl. Phys. B* **465** (1996) 295–314, [[hep-ph/9507253](#)].
- [62] G. P. Salam and D. Wicke, *Hadron masses and power corrections to event shapes*, *JHEP* **05** (2001) 061, [[hep-ph/0102343](#)].
- [63] A. H. Hoang and I. W. Stewart, *Designing gapped soft functions for jet production*, *Phys. Lett. B* **660** (2008) 483–493, [[0709.3519](#)].
- [64] R. Abbate, M. Fickinger, A. H. Hoang, V. Mateu and I. W. Stewart, *Thrust at N^3LL with Power Corrections and a Precision Global Fit for $\alpha_s(m_Z)$* , *Phys. Rev. D* **83** (2011) 074021, [[1006.3080](#)].
- [65] T. Gehrmann, G. Luisoni and P. F. Monni, *Power corrections in the dispersive model for a determination of the strong coupling constant from the thrust distribution*, *Eur. Phys. J. C* **73** (2013) 2265, [[1210.6945](#)].

-
- [66] V. Mateu, I. W. Stewart and J. Thaler, *Power Corrections to Event Shapes with Mass-Dependent Operators*, *Phys. Rev. D* **87** (2013) 014025, [[1209.3781](#)].
- [67] A. H. Hoang, D. W. Kolodrubetz, V. Mateu and I. W. Stewart, *Precise determination of α_s from the C -parameter distribution*, *Phys. Rev. D* **91** (2015) 094018, [[1501.04111](#)].
- [68] N. G. Gracia and V. Mateu, *Toward massless and massive event shapes in the large- β_0 limit*, *JHEP* **07** (2021) 229, [[2104.13942](#)].
- [69] A. V. Manohar and M. B. Wise, *Power suppressed corrections to hadronic event shapes*, *Phys. Lett. B* **344** (1995) 407–412, [[hep-ph/9406392](#)].
- [70] B. R. Webber, *Estimation of power corrections to hadronic event shapes*, *Phys. Lett. B* **339** (1994) 148–150, [[hep-ph/9408222](#)].
- [71] Y. L. Dokshitzer, G. Marchesini and B. R. Webber, *Dispersive approach to power behaved contributions in QCD hard processes*, *Nucl. Phys. B* **469** (1996) 93–142, [[hep-ph/9512336](#)].
- [72] M. Dasgupta and B. R. Webber, *Power corrections and renormalons in e^+e^- fragmentation functions*, *Nucl. Phys. B* **484** (1997) 247–264, [[hep-ph/9608394](#)].
- [73] P. Nason and B. R. Webber, *Nonperturbative corrections to heavy quark fragmentation in e^+e^- annihilation*, *Phys. Lett. B* **395** (1997) 355–363, [[hep-ph/9612353](#)].
- [74] M. Beneke, V. M. Braun and L. Magnea, *Phenomenology of power corrections in fragmentation processes in e^+e^- annihilation*, *Nucl. Phys. B* **497** (1997) 297–333, [[hep-ph/9701309](#)].
- [75] Y. L. Dokshitzer and B. R. Webber, *Power corrections to event shape distributions*, *Phys. Lett. B* **404** (1997) 321–327, [[hep-ph/9704298](#)].
- [76] Y. L. Dokshitzer, A. Lucenti, G. Marchesini and G. P. Salam, *Universality of $1/Q$ corrections to jet-shape observables rescued*, *Nucl. Phys. B* **511** (1998) 396–418, [[hep-ph/9707532](#)].
- [77] Y. L. Dokshitzer, A. Lucenti, G. Marchesini and G. P. Salam, *On the universality of the Milan factor for $1/Q$ power corrections to jet shapes*, *JHEP* **05** (1998) 003, [[hep-ph/9802381](#)].
- [78] G. P. Korchemsky and G. F. Sterman, *Power corrections to event shapes and factorization*, *Nucl. Phys. B* **555** (1999) 335–351, [[hep-ph/9902341](#)].
- [79] G. P. Korchemsky and S. Tafat, *On power corrections to the event shape distributions in QCD*, *JHEP* **10** (2000) 010, [[hep-ph/0007005](#)].
- [80] E. Gardi and J. Rathsmann, *Renormalon resummation and exponentiation of soft and collinear gluon radiation in the thrust distribution*, *Nucl. Phys. B* **609** (2001) 123–182, [[hep-ph/0103217](#)].

-
- [81] E. Gardi and L. Magnea, *The C parameter distribution in $e^+ e^-$ annihilation*, *JHEP* **08** (2003) 030, [[hep-ph/0306094](#)].
- [82] C. W. Bauer, C. Lee, A. V. Manohar and M. B. Wise, *Enhanced nonperturbative effects in Z decays to hadrons*, *Phys. Rev. D* **70** (2004) 034014, [[hep-ph/0309278](#)].
- [83] C. Lee and G. F. Sterman, *Momentum Flow Correlations from Event Shapes: Factorized Soft Gluons and Soft-Collinear Effective Theory*, *Phys. Rev. D* **75** (2007) 014022, [[hep-ph/0611061](#)].
- [84] G. Luisoni, P. F. Monni and G. P. Salam, *C -parameter hadronisation in the symmetric 3-jet limit and impact on α_s fits*, *Eur. Phys. J. C* **81** (2021) 158, [[2012.00622](#)].
- [85] S. Kluth, *Tests of Quantum Chromo Dynamics at $e^+ e^-$ Colliders*, *Rept. Prog. Phys.* **69** (2006) 1771–1846, [[hep-ex/0603011](#)].
- [86] OPAL collaboration, G. Abbiendi et al., *Measurement of the Strong Coupling $\alpha(s)$ from four-jet observables in $e^+ e^-$ annihilation*, *Eur. Phys. J. C* **47** (2006) 295–307, [[hep-ex/0601048](#)].
- [87] J. Broedel, C. Duhr, F. Dulat and L. Tancredi, *Elliptic polylogarithms and iterated integrals on elliptic curves. Part I: general formalism*, *JHEP* **05** (2018) 093, [[1712.07089](#)].
- [88] J. Broedel, C. Duhr, F. Dulat and L. Tancredi, *Elliptic polylogarithms and iterated integrals on elliptic curves II: an application to the sunrise integral*, *Phys. Rev. D* **97** (2018) 116009, [[1712.07095](#)].
- [89] J. Broedel, C. Duhr, F. Dulat, B. Penante and L. Tancredi, *Elliptic symbol calculus: from elliptic polylogarithms to iterated integrals of Eisenstein series*, *JHEP* **08** (2018) 014, [[1803.10256](#)].
- [90] J. Broedel, C. Duhr, F. Dulat, B. Penante and L. Tancredi, *Elliptic Feynman integrals and pure functions*, *JHEP* **01** (2019) 023, [[1809.10698](#)].
- [91] J. Broedel, C. Duhr, F. Dulat, B. Penante and L. Tancredi, *Elliptic polylogarithms and Feynman parameter integrals*, *JHEP* **05** (2019) 120, [[1902.09971](#)].
- [92] S. Weinzierl, *Feynman Integrals*, [2201.03593](#).
- [93] M. Dasgupta, L. Magnea and G. Smye, *Universality of $1/Q$ corrections revisited*, *JHEP* **11** (1999) 025, [[hep-ph/9911316](#)].
- [94] G. E. Smye, *On the $1/Q$ correction to the C - parameter at two loops*, *JHEP* **05** (2001) 005, [[hep-ph/0101323](#)].
- [95] S. Catani and M. H. Seymour, *A General algorithm for calculating jet cross-sections in NLO QCD*, *Nucl. Phys. B* **485** (1997) 291–419, [[hep-ph/9605323](#)].

-
- [96] Y. L. Dokshitzer and B. R. Webber, *Calculation of power corrections to hadronic event shapes*, *Phys. Lett. B* **352** (1995) 451–455, [[hep-ph/9504219](#)].
- [97] R. Akhoury and V. I. Zakharov, *On the universality of the leading, $1/Q$ power corrections in QCD*, *Phys. Lett. B* **357** (1995) 646–652, [[hep-ph/9504248](#)].
- [98] S. Catani and B. R. Webber, *Resummed C parameter distribution in $e+e-$ annihilation*, *Phys. Lett. B* **427** (1998) 377–384, [[hep-ph/9801350](#)].
- [99] R. A. Davison and B. R. Webber, *Non-Perturbative Contribution to the Thrust Distribution in $e+e-$ Annihilation*, *Eur. Phys. J. C* **59** (2009) 13–25, [[0809.3326](#)].
- [100] M. Dasgupta, F. A. Dreyer, K. Hamilton, P. F. Monni, G. P. Salam and G. Soyez, *Parton showers beyond leading logarithmic accuracy*, *Phys. Rev. Lett.* **125** (2020) 052002, [[2002.11114](#)].
- [101] J. R. Forshaw, J. Holguin and S. Plätzer, *Building a consistent parton shower*, *JHEP* **09** (2020) 014, [[2003.06400](#)].
- [102] PARTICLE DATA GROUP collaboration, M. Tanabashi, K. Hagiwara, K. Hikasa, K. Nakamura, Y. Sumino, F. Takahashi, J. Tanaka, K. Agashe, G. Aielli, C. Amsler, M. Antonelli et al., *Review of particle physics*, *Phys. Rev. D* **98** (Aug, 2018) 030001.
- [103] J. Huston, K. Rabbertz and G. Zanderighi, *2019 update to the quantum Chromodynamics review (2019)*, .
- [104] P. Ball, M. Beneke and V. M. Braun, *Resummation of $(\beta_0\alpha_s)^n$ corrections in QCD: Techniques and applications to the τ hadronic width and the heavy quark pole mass*, *Nucl. Phys. B* **452** (1995) 563–625, [[hep-ph/9502300](#)].